

University of Louisville

## ThinkIR: The University of Louisville's Institutional Repository

---

Electronic Theses and Dissertations

---

5-2019

### Exploring the role of PTN1 in *ustilago maydis*.

Lalu Murali Krishna Vijayakrishna Pillai  
*University of Louisville*

Follow this and additional works at: <https://ir.library.louisville.edu/etd>



Part of the [Cell and Developmental Biology Commons](#)

---

#### Recommended Citation

Vijayakrishna Pillai, Lalu Murali Krishna, "Exploring the role of PTN1 in *ustilago maydis*." (2019). *Electronic Theses and Dissertations*. Paper 3210.  
<https://doi.org/10.18297/etd/3210>

This Doctoral Dissertation is brought to you for free and open access by ThinkIR: The University of Louisville's Institutional Repository. It has been accepted for inclusion in Electronic Theses and Dissertations by an authorized administrator of ThinkIR: The University of Louisville's Institutional Repository. This title appears here courtesy of the author, who has retained all other copyrights. For more information, please contact [thinkir@louisville.edu](mailto:thinkir@louisville.edu).

EXPLORING THE ROLE OF PTN1 IN *USTILAGO MAYDIS*

By

Lalu Murali Krishna Vijayakrishna Pillai  
M.Sc., Biotechnology, Bangalore University, 2005

A Dissertation

Submitted to the Faculty of the  
College of Arts and Sciences of the University of Louisville in  
Partial Fulfillment of the Requirements for the Degree of

Doctor of Philosophy in Biology

Department of Biology,  
Division of Molecular, Cellular and Developmental Biology,  
College of Arts and Sciences  
University of Louisville  
Louisville, Kentucky

May 2019



EXPLORING THE ROLE OF PTN1 IN *USTILAGO MAYDIS*

By

Lalu Murali Krishna Vijayakrishna Pillai  
M.Sc., Biotechnology, Bangalore University, 2005

A Dissertation Approved on

April 15, 2019

By the following Dissertation Committee:

---

Dr. Michael H. Perlin, Principal Advisor

---

Dr. Susanna Remold

---

Dr. Mark Running

---

Dr. David Schultz

---

Dr. David Samuelson

## ACKNOWLEDGMENTS

First and foremost, I would like to express my deepest appreciation to my mentor Dr. Michael H. Perlin for helping me realize my educational goal. Dr. Perlin has been a wonderful human being and without his patience, guidance and consistent support this dissertation would not have been possible. On a personal level, Dr. Perlin, inspired me by his genuinely good nature, hardworking and passionate attitude. I am truly fortunate to have had the opportunity to work with him. I would like to thank my committee members, Dr. David Schultz, Dr. Mark Running, Dr. David Samuelson, and Dr. Susanna Remold for being friendly and helpful, with the guidance and intellectually stimulating suggestions that they offered to me throughout.

I am highly grateful to all the undergraduate students who worked with me, especially, Michael Groeschen and Jack Desmarais, for providing me with assistance during both exciting and challenging times. I would like to thank every one of the current and previous goat lab members for their invaluable assistance, support, feedback, and friendship. I am grateful to Su San Toh, Michael Cooper, and Margaret Wallen for sharing their knowledge with me during my initial days in the Goat Lab. I am thankful to Swathi Kuppireddy, Nelson Ming Tsai, and Sunita Khanal for the help and support I received from them time to time.

I am extremely indebted to my family and friends who offered me constantly with love, support, encouragement and confidence to pursue and complete this long journey.

Finally, I would like to express my gratitude to the University of Louisville for giving me the opportunity to pursue my doctoral studies at this institution and for the fellowship, funding and other valuable resources provided to me to complete my doctoral training.

## ABSTRACT

### EXPLORING THE ROLE OF PTN1 IN *USTILAGO MAYDIS*

Lalu M Vijayakrishnapillai

March 31, 2019

Signal transduction is a key aspect of biological life. PTEN (phosphatase and tensin homolog) is a widely studied signaling protein in mammalian systems, where it acts as a tumor suppressor. Numerous studies have conclusively demonstrated the anti-cancerous effect of this protein. Mutations in the *PTEN* gene have been implicated in several disorders including cancer, diabetes, and Cowden syndrome, among others. It is part of the PI3K-PTEN-AKT-mTOR signaling pathway and is responsible for various metabolic and cellular activities. This pathway is found to be conserved across several eukaryotic systems including yeast, *Drosophila melanogaster* and *Caenorhabditis elegans*. While PTEN orthologues have been characterized in ascomycete fungi, it has not been reported in any basidiomycete fungi. The initial part of the current study was aimed at the characterization of *PTEN* orthologue, *ptn1*, of *Ustilago maydis*, a basidiomycete fungus. When the *U. maydis*, *ptn1* gene was either deleted or overexpressed, it was found that the deletion of this gene lead to reduced virulence, spore production, and germination rate; effects of the overexpression were more subtle or not discernable. Previous studies have indicated that two other signaling proteins, Rho1 and Pdc1, are physical interactors of Ptn1. The goal of the latter part of the present study was to explore the functional interaction of Ptn1 with

Rho1 and Pdc1. Our experiments indicated a functional connection between these genes, especially in processes that are related to stress tolerance, cellular morphology, and virulence of the fungus, suggesting that they may be elements of the same regulatory pathway. We predict that the *pdcl* interaction with *ptn1* may be the reverse of that of *rho1* with *ptn1*. In addition, our experiments with an orthologue of S6K1, *agal*, showed that its deletion leads to some of the same phenotypes seen with that of *ptn1*, *pdcl* and/or *rho1*. The current phenotypes of these mutant strains when considered in the context of already available information about the role of these genes in other systems indicate that they may be part of a pathway that modulates cytoskeletal rearrangements.



## TABLE OF CONTENTS

	PAGE
ACKNOWLEDGEMENTS.....	iii
ABSTRACT.....	v
LIST OF TABLES.....	ix
LIST OF FIGURES.....	x
CHAPTER I	
INTRODUCTION.....	1
Functions of PTEN in non-mammalian systems.....	7
<i>Ustilago maydis</i> as a model system for signaling research.....	12
Life cycle of <i>U maydis</i> .....	13
Regulation of mating process in <i>U. maydis</i> .....	15
Regulation of dimorphism in <i>U. maydis</i> .....	16
Regulation of in planta development of <i>U. maydis</i> .....	18
Research interest .....	22
CHAPTER II	
DELETION OF PTN1, A PTEN/TEP1 ORTHOLOGUE, IN <i>USTILAGO MAYDIS</i> REDUCES PATHOGENICITY AND TELIOSPORE DEVELOPMENT...	
Summary.....	24
Introduction.....	25
Material and Methods.....	27
Results.....	32
Discussion.....	49
CHAPTER III	
INTERACTION OF PTN1 WITH RHO1 AND PDC1 IN <i>USTILAGO MAYDIS</i>	
Summary.....	66
Introduction.....	67
Material and Methods.....	83
Results.....	71
Discussion.....	91
CHAPTER IV	
DELETION OF AGA1 OF <i>USTILAGO MAYDIS</i> LEADS TO MORPHOLOGICAL DEFECTS AND REDUCED STRESS TOLERANCE.....	
	97

Summary.....	97
Introduction.....	97
Material and Methods.....	99
Results.....	100
Discussion.....	108
CHAPTER V	
DISCUSSION.....	113
REFERENCES.....	121
CURRICULUM VITAE.....	138

## LIST OF TABLES

TABLE		PAGE
2.1	Strains used in chapter 2 study.....	27
2.2	List of primers.....	29
2.3	Protein prediction analysis of Ptn1 using PredictProtein.....	65
3.1	Strains used in chapter 3 study.....	70
4.1	Strains used in chapter 4 study.....	99

## LIST OF FIGURES

FIGURE		PAGE
1.1	Schematic depiction of Ras/Raf/MAPK pathway.....	3
1.2	Generalized PKA pathway.....	4
1.3	Representative diagram of PTEN-PI3K-AKT-mTOR Signaling.....	6
1.4	Developmental stages in the <i>U. maydis</i> life cycle.....	14
1.5	Interactions between the two mating-type loci during development of <i>U. maydis</i> .....	15
1.6	Schematic overview of the interplay between PKA pathway and the pheromone response pathway during pathogenic development.....	18
1.7	Stages in <i>U. maydis</i> teliospore development.....	20
2.1	Sequence alignment of <i>U. maydis</i> Ptn1 and other PTEN proteins.....	33
2.2	Mating assay and testing for pheromone production.....	34
2.3	Mating compared between deletion strains using two different constructs and different genetic backgrounds. Formation of aerial hyphae in D132 background .....	35
2.4	Response of mutants to cell wall stress.....	39
2.5	Plant infection.....	40
2.6	Are functional copies of the <i>ptn1</i> gene in both partners required for pathogenicity?.....	42
2.7	Plant growth parameters.....	44
2.8	Chlorophyll estimation.....	45
2.9	Spore count.....	47
2.10	Spore germination assay.....	48
2.11	Spore germination tube formation.....	48
2.12	Motif scan analysis of Ptn1 using Hits.....	55

2.13	SignalP 4.1 prediction of the presence signal peptide.....	56
2.14	TargetP prediction of sub-cellular localization of Ptn1 .....	56
2.15	The charcoal assay for fuzz production performed with SG200 and SG200 $\Delta ptn1$ strains.....	57
2.16	The relative expression analysis of <i>mfa2</i> , <i>pra2</i> , and <i>prf1</i> ( <i>U. maydis</i> mating pathway genes) in wildtype and $\Delta ptn1$ under high and low ammonium conditions.....	57
2.17	Growth assay of <i>ptn1</i> .....	58
2.18	Infection of plants with $\Delta ptn1$ deletion strains in SG200 background....	58
2.19	Infection of plants with $\Delta ptn1$ deletion strains in different backgrounds and created through two different methods.....	59
2.20	Teliospores from infected maize plants.....	60
2.21	Dissection of tumors under microscope showing teliospores.....	61
2.22	Deletion of <i>ptn1</i> alters ability to produce tumors in maize cobs.....	62
2.23	Interaction Network Analysis of Ptn1 protein sequence using STRING software.....	62
3.1	Overexpressing <i>pdcl</i> in <i>ptn1</i> deleted strains showed background specific growth effects with the 2/9 $\Delta ptn1$ <i>pdcl</i> <sup>otef</sup> more affected than the 1/2 $\Delta ptn1$ <i>pdcl</i> <sup>otef</sup> strain.....	73
3.2	Calcofluor staining assay of <i>ptn1</i> and <i>pdcl</i> mutants.....	76
3.3	Deletion or overexpression of <i>pdcl</i> reduces aerial hyphal formation in the <i>ptn1</i> deletion background.....	78
3.4	Stress sensitivity of <i>pdcl</i> and <i>ptn1</i> mutant strains.....	79
3.5	Plant infection profile of <i>ptn1</i> and <i>pdcl</i> mutants.....	81
3.6	Deletion of both <i>ptn1</i> and <i>rho1</i> results in decreased mating deficiency...	82
3.7	Cell wall sensitivity assay of <i>rho1</i> and <i>ptn1</i> mutants.....	84
3.8	Testing for the virulence of <i>rho1</i> and <i>ptn1</i> mutant strains.....	86
3.9	Morphology of wild type and mutant <i>rho1</i> and <i>ptn1</i> strains.....	89
3.10	Spore count and teliospore germination rate.....	90
4.1	Charcoal assay showing defect in aerial hyphae formation 24 hours post-mating.....	101
4.2	Virulence assay and analysis of symptoms in planta.....	102

4.3	Assay comparing the growth of wildtype with $\Delta agal$ strains.....	103
4.4	Defects in cell morphology as observed through calcofluor staining of fungal cells.....	104
4.5	Osmotic and cell wall stress assays testing the effect of <i>agal</i> deletion on stress tolerance.....	105
4.6	Testing the effect of LiCl on <i>U. maydis</i> strains.....	107
4.7	Effect of low ammonium (10 $\mu$ M) on <i>agal</i> mutants.....	108
5.1	Possible mode of action of the signaling proteins.....	118

## CHAPTER 1

### GENERAL INTRODUCTION

Signal transduction is a key cellular function in almost all living systems, as organisms constantly need to respond to dynamic internal and external surroundings. The basic purpose of signaling is to exchange information between different parts of the same cell or to release information to other cells so that a certain action can be taken. Most of the cell signals are chemical in nature. Examples include growth factors, hormones, and neurotransmitters, among others. In a higher order multicellular system, *e.g.*, mammalian systems, these substances can communicate locally, or they might travel large distances. In the typical cell signaling process, the cell receives a signal at a receptor leading to its activation. The signal is then propagated through various intracellular signaling pathways, resulting in a cellular response often by a change in gene expression. The cell employs signaling for a myriad of activities such as growth and differentiation of cells, to interact with other cells or with other cellular components, to regulate the metabolic processes, for defense response, synthesis and secretion of specific proteins and to respond to environmental conditions. As cell signaling involves a series of biochemical and molecular steps that regulate the normal cellular functions, any disruption at any of these steps is likely to have substantial impacts on cell physiology. Most of the signaling pathways are not linear but are part of extensive networks. There are several signaling pathways and

some of them could be very specific to a certain type of cell. The occurrence of variations of the pathways among different systems shows that they might have been specialized to achieve a specific response based on the cell type. The cells achieve this by having unique or specialized cell-surface receptors (cell-specific proteins or markers), thus preserving the specificity of the incoming signal. However, some of those signaling pathways are universal to organisms especially among the eukaryotes, examples of these include the PKA-cAMP pathway and MAPK and PTEN-PI3K-mTOR signaling pathways among others.

The classic MAPK (Mitogen activate protein kinase) cascade begins at the cell membrane where the MAPKKKs (MAP3K or Mitogen activated protein kinase kinase kinases) are activated by small GTPases and other kinases (G-protein coupled receptors, tyrosine receptor kinases, p21 activated kinases). The MAPK cascade consists of a series of enzymes that are activated in the order, MAPK kinase kinase (MAPKKK), MAPK kinase (MAPKK) and MAP kinase (MAPK). In mammalian systems, MAPK pathways respond to a diverse set of stimuli (cytokines, growth factors, mitogens, osmotic stress, etc.) and cause an appropriate physiological response such as cell proliferation, differentiation, inflammatory responses and apoptosis (W. Zhang & Liu, 2002). One of the best characterized MAPK pathways is the Ras/Raf/MAPK Pathway (Figure 1.1). For instance, the binding of a signal such as EGF (epidermal growth factor) to an EGFR receptor (protein tyrosine kinase receptor) activates the pathway. This results in the recruitment of guanine nucleotide exchange factors (GEFs) by adaptor proteins to the cell membrane. The GEF activates the Ras proteins, which recruits RAF proteins to the cell membrane. RAF phosphorylates MEK (a protein kinase) which in turn phosphorylates



ERK, an activator of several transcriptional factors that control the expression of genes encoding proteins that regulate cell proliferation and survival (Molina & Adjei, 2006).

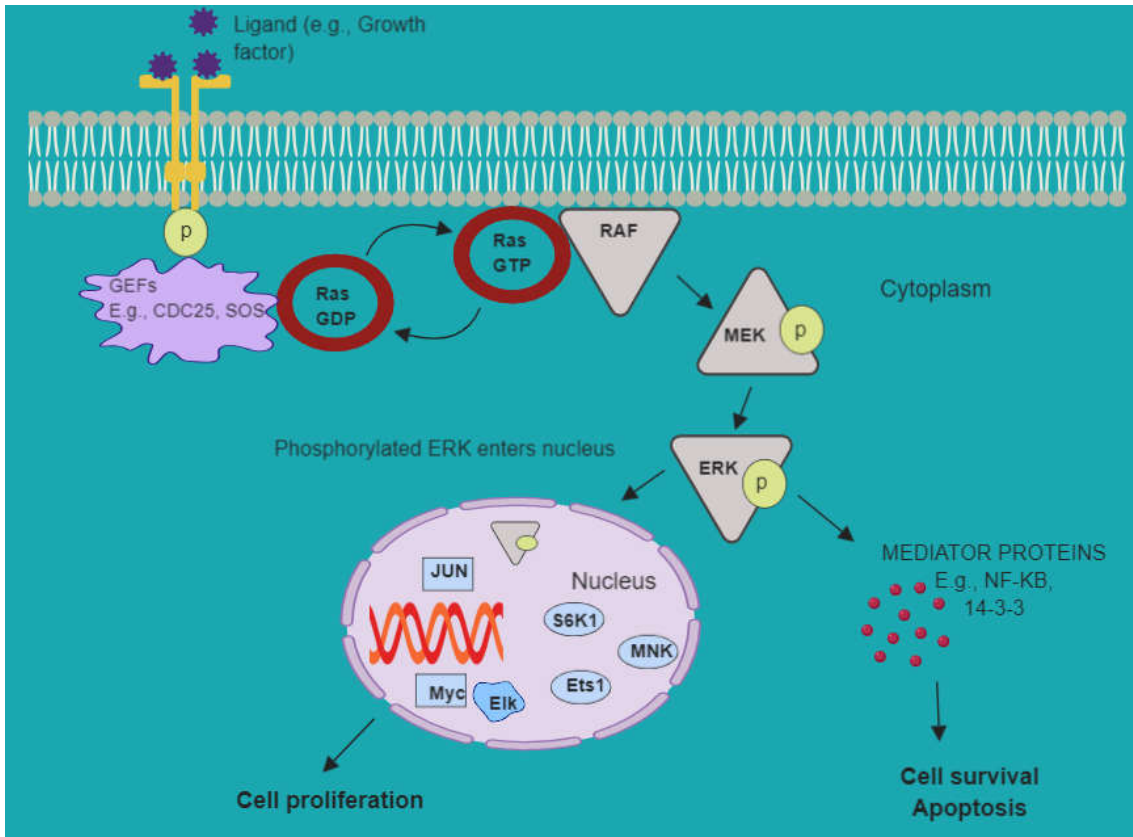


**Figure 1.1.** Schematic depiction of Ras/Raf/MAPK pathway.

The PKA-cAMP (cAMP dependent protein kinase A) pathway (Figure 1.2) employs the service of a key secondary messenger called cAMP (adenosine 3',5'-cyclic monophosphate). The levels of cAMP in the cell are regulated by the coordinated activities between two enzymes, adenylyl cyclase (AC) and cyclic nucleotide phosphodiesterase (PDE). PKA is an important effector of cAMP. The binding of cAMP to the two regulatory (R) subunits of PKA, causes the dissociation of its catalytic (C) subunits and the subsequent activation of PKA (Yan, Gao, Cui, Zhang, & Zhou, 2016). Numerous substrates have been identified for PKA which include several metabolic enzymes (in the glycogen synthesis

and glycogen breakdown process), acetyl CoA carboxylase (blocks lipid synthesis), among others (Sassone-Corsi, 2012). There is cross talk between PKA and other pathways; for example, PKA activates MAP kinases through the phosphorylation of inhibitory tyrosine phosphatases (Sassone-Corsi, 2012). Also, PKA can negatively regulate Rho1 and Raf functions thereby regulating ion permeability. Thus, PKA regulates several physiological and cellular processes through the PKA pathway and also by influencing other signaling proteins and metabolic pathways.

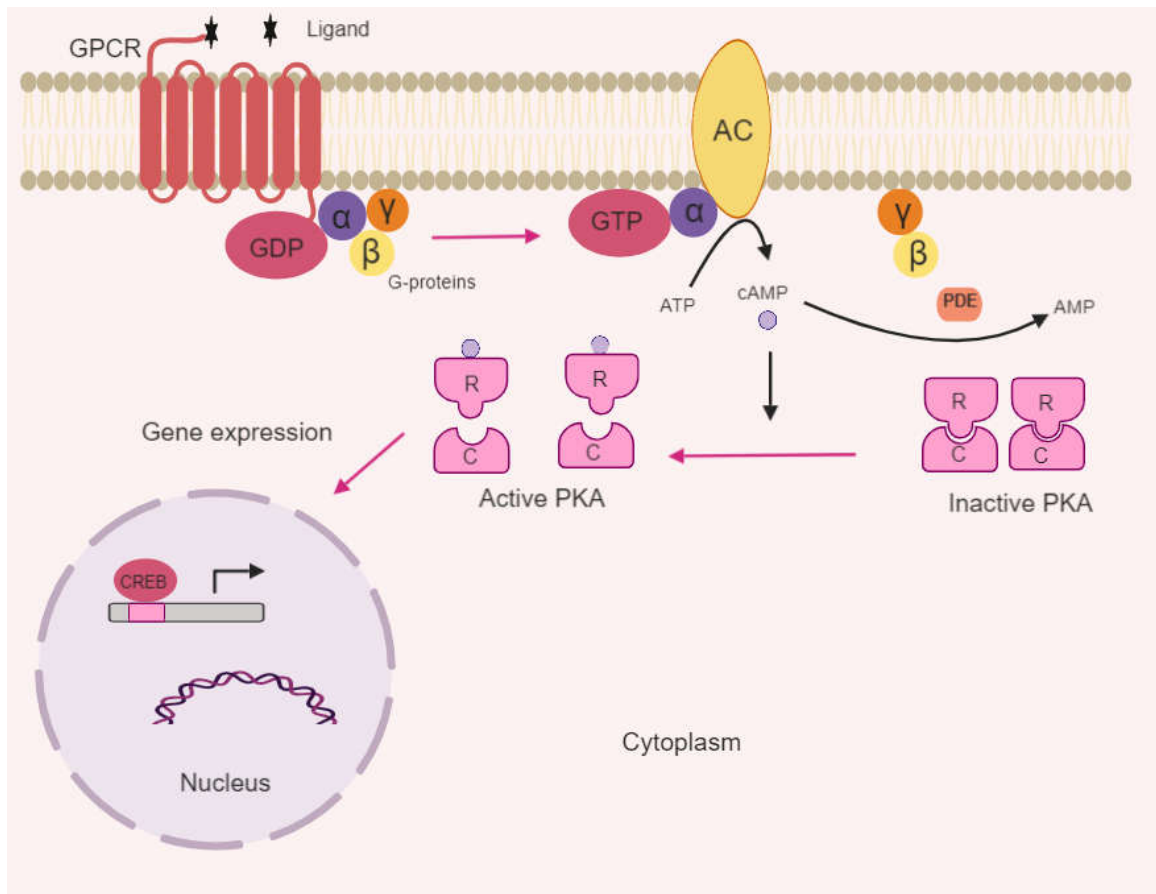


**Figure 1.2.** Generalized PKA pathway

Another key signaling cascade that is conserved among eukaryotic organisms is the PTEN/PI3K/mTOR pathway. The key components of the pathway involve a dual specificity phosphatase protein PTEN, a serine threonine kinase protein AKT, both of

which are found upstream of mTOR, another serine threonine kinase protein (Backman, Stambolic, & Mak, 2002). While PI3K is a positive regulator of the pathway, PTEN acts as an antagonist suppressing the pathway. Consequently, the coordinated positive and negative regulation of this pathway play a vital role in controlling the metabolic and physiological functions in the cell.

*PTEN* was initially discovered as a tumor suppressor gene that is frequently mutated in several human cancers (Chalhoub & Baker, 2009). It is a dual phosphatase that can act both on protein and phosphoinositide substrates, with a preference toward phosphoinositide substrates, dephosphorylating the lipid second messenger, phosphatidylinositol (3,4,5)-trisphosphate (PIP3) to phosphatidylinositol (4,5)-bisphosphate (PIP2) (Maehama & Dixon, 1998). The human PTEN is a 403 amino acid protein with five functional domains, an N-terminal PIP2-binding domain, a phosphatase domain, a C2 domain, a C-terminal tail, and a PDZ (Postsynaptic-density protein of 95 kDa, discs large, zona occludens-1) -interaction domain (Chalhoub & Baker, 2009; Song, Salmena, & Pandolfi, 2012). PTEN is a negative regulator of the PTEN-PI3K-AKT-mTOR signaling pathway; an active and unmutated PTEN maintains the levels of PIP3 low in the cell, thereby suppressing the activation of other proteins downstream in the pathway (Figure 1.3), which play crucial roles in cell survival, cell proliferation, and anabolic metabolism (Song et al., 2012). The formation of PIP3s at the plasma membrane is important for the control of cell growth and survival in mammals (Cantley, 2002). The catalytic subunit of PI3-kinase, p110, is recruited to RTKS (receptor tyrosine kinases) or GPCRs (G-protein coupled receptors) to respond to extracellular stimuli (insulin, growth factors, chemokines), catalyzing the phosphorylation of PIP2 to PIP3 (Chalhoub & Baker,

2009). The PIP3 acts as a secondary messenger for several downstream targets including the serine-threonine kinase, AKT (or PKB). This results in the recruitment of AKT to the membrane and its subsequent full activation by mTORC, PDK1, or other kinases, which in turn have a variety of substrates that are either inhibited or activated, but result in cellular growth, survival, and proliferation through various mechanisms (Chalhoub & Baker, 2009).

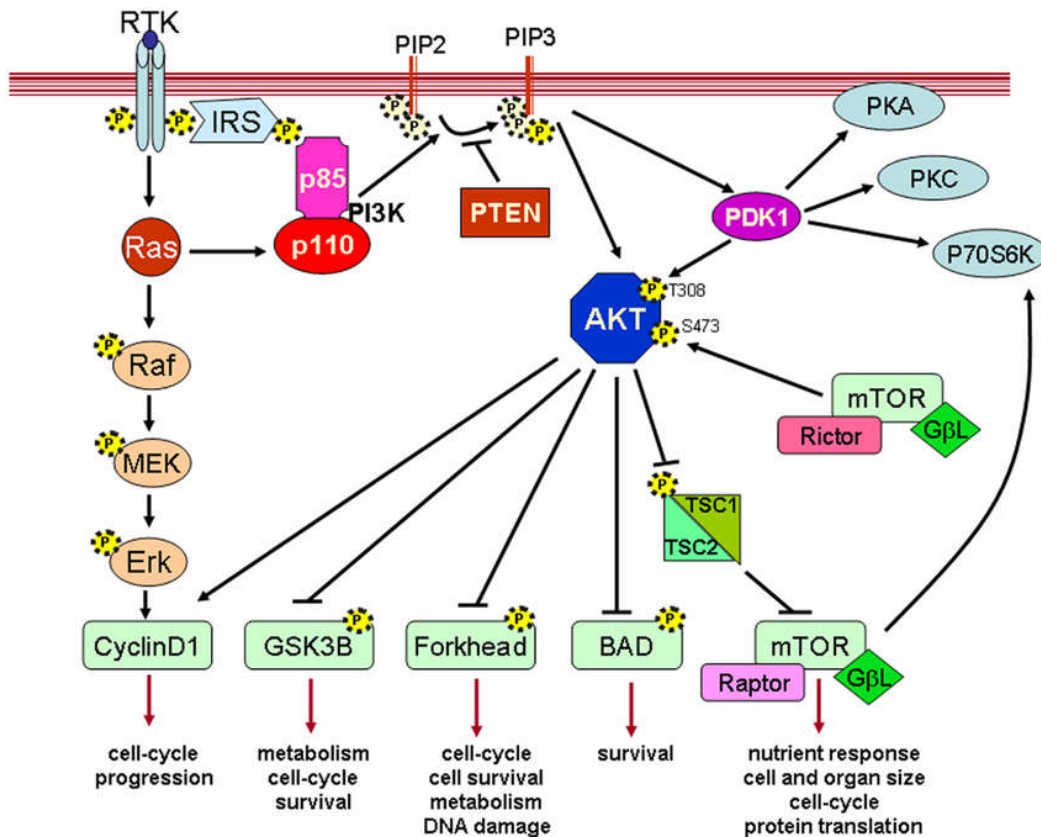


**Figure 1.3** Representative diagram of PTEN-PI3K-AKT-mTOR signaling. Reused with permission from the open access journal ‘Frontiers in Oncology’ (Carnero & Paramio, 2014)

The loss of PTEN function can happen due to various mutations, including deletions, transcriptional silencing, or protein instability (Ali, Schriml, & Dean, 1999; Chalhoub & Baker, 2009). A majority of the mutations occur in the phosphatase domain of PTEN and affect its catalytic activity (Eng, 2003). Studies conducted in glioblastoma

cells when *PTEN* is overexpressed resulted in the inhibition of cell cycle progression (Cheney et al., 1998). Even a small change in the level of PTEN or its activity results in cancer susceptibility and favors tumor development. The level of PTEN in a cell may be maintained through mechanisms such as post translational modification (phosphorylation, acetylation, oxidation, and ubiquitination), and subcellular localization (Tamguney & Stokoe, 2007). The C-terminal tail of PTEN contains several sites for phosphorylation, which may control its stability and recruitment to the membrane (Vazquez & Devreotes, 2006). Most of the studies show PTEN as a cytosolic protein which gets recruited to the membrane, however, there are others which show that PTEN can be present in other locations. There have been reports of PTEN being able to interact with organelles such as mitochondria, endoplasmic reticulum, or indicating its presence in the nucleus while other studies point out that it may also be secreted and exported outside the cell (Bononi & Pinton, 2015). In addition to PTEN being an active area of study in the field of cancer research, it has been implicated in the case of Alzheimer's disease (a neurodegenerative disease), Bannayan-Riley-Ruvalcaba syndrome, Cowden syndrome, Proteus syndrome, and autism among others. Orthologues of *PTEN* have been identified in several organisms such as *Schizosaccharomyces pompe*, *Fusarium graminearum*, *Saccharomyces cerevisiae*, *Arabidopsis thaliana*, *Drosophila melanogaster*, *Caenorhabditis elegans*, among others. A brief overview of the functions of PTEN in some of these systems is given below.

### **Functions of PTEN in non-mammalian systems**

***Epinephelus coioides*.** *Epinephelus coioides* or orange-spotted grouper is a marine fish of economic importance commonly found in the tropical and subtropical ecosystems. The *PTEN* orthologue of *E. coioides*, *EcPTEN*, codes for a polypeptide of length 422 amino

comprised of conserved residues and the characteristic domains that are critical for the functionality of PTEN (Luo et al., 2016). While the *EcPTEN* mRNA is broadly expressed in all of the fish tissues examined, the highest expression level was observed in immune tissues, particularly in liver. The overexpression of EcPTEN in HeLa cells resulted in a stimulation of apoptotic signaling pathway with alterations in the activity of Myc (a family of regulatory genes coding for transcriptional factors) promoters among others in HeLa cells, indicating a close sequence similarity of EcPTEN to that of its mammalian counterpart.

***Drosophila melanogaster.*** One of the most important genetic model organisms, *Drosophila melanogaster*, commonly known as fruit fly, has *DPTEN*, an orthologue of human tumor suppressor gene *PTEN*. In *D. melanogaster*, *DPTEN* is found to have both protein phosphatase and lipid phosphatase activities (Goberdhan, Paricio, Goodman, Mlodzik, & Wilson, 1999). Studies conducted using cell culture revealed its lipid phosphatase activity, where it is involved in controlling cell proliferation and survival. *In vivo* studies where *DPTEN* gene was deleted resulted in reduced hyperplastic growth in flies by both cell size and number (Goberdhan et al., 1999). Screening for *Drosophila* tumor suppressor mutations *in vitro* cell culture conditions also demonstrated its role in cell proliferation. When primary cells were generated, wildtype cells emerged on average at 37 days, while *DPTEN* mutated cells appeared on average at 11 days and the cultures became confluent in about 3 weeks (Justiniano, Mathew, Mitra, Manivannan, & Simcox, 2012). The characterization of *DPTEN* showed that both its inactivation and overexpression affect cell size in *D. melanogaster*. The overexpression of *DPTEN* resulted in the inhibition cell cycle progression during the early phase of mitosis and showed an

increase in cell death during eye development (Huang et al., 1999). Epistasis experiments aimed at identifying the canonical PTEN-PI3K-AKT pathway showed that it exists in *D. melanogaster*. When *Dakt1*, the *Drosophila* Akt was expressed using the *eyeless* promoter to make *Dakt1* homozygous mutant eyes, resulting flies had smaller eyes when compared to wildtype flies (Scanga et al., 2000). Similarly, when the activity of *Dp110* (*Drosophila* PI3K catalytic subunit) was repressed it resulted in a similar phenotype.

***Caenorhabditis elegans.*** *Caenorhabditis elegans* is a widely used model organism for lifespan studies due to the availability of its full genome sequence and a short lifespan of 19 days. *C. elegans* shows the presence of the human *PTEN* orthologue named *daf-18*. DAF-18 regulates the level of PIP3, thereby limiting the activation of AKT-1 and AKT-2 (*C. elegans* AKT equivalent) (Ogg & Ruvkun, 1998). Furthermore, the deletion of the catalytic portion of DAF-18, dramatically shortened the lifespan of the worms (Mihaylova, Borland, Manjarrez, Stern, & Sun, 1999). Studies have shown that human *PTEN* can substitute for DAF-18 and rescue the longevity defects caused due to DAF-18 mutation (J. Liu & Chin-Sang, 2015; Solari et al., 2005). Homozygous deletion of *daf-18* in *C. elegans* results in a shorter life span but results in viable and fertile worms. Moreover, the role of DAF-18 with other aging related signaling components of *C. elegans* further supports a potential role of *PTEN* in mammalian aging (J. Liu & Chin-Sang, 2015; Solari et al., 2005).

***Arabidopsis thaliana.*** While the role of *PTEN* signal transduction is widely studied in animal cells, very little is known about the role of *PTEN* in plants. It appears that *Arabidopsis thaliana*, the most well studied plant model system, has a *PTEN* orthologue, *AtPTEN1*. When *AtPTEN1* is expressed as a recombinant protein glutathione S-transferase–*AtPTEN1* fusion protein and its Tyr phosphatase activity assayed by using a

<sup>32</sup>P-labeled synthetic peptide as a substrate, it was found to function as an active phosphatase that dephosphorylates phosphatidylinositol substrates (Gupta, Ting, Sokolov, Johnson, & Luan, 2002). The examination of the expression pattern of *AtPTEN1* in transgenic *A. thaliana* plants showed that the gene is expressed exclusively in pollen grains during the late stage of development. When *AtPTEN1* gene expression was suppressed through RNA interference, death of pollen grains resulted. When *AtPTEN1* was overexpressed in tobacco plants, it resulted in the accumulation of autophagic bodies in pollen tubes while causing gametophytic male sterility in *Arabidopsis* plants (Y. Zhang et al., 2011) indicating its role in controlling autophagy.

***Schizosaccharomyces pombe*.** Genetic and molecular biology research have benefited greatly from *Schizosaccharomyces pombe* (fission yeast), an ascomycete fungus, as a model system. In *S. pombe*, the *PTEN* orthologue, *ptn1*, appears to perform the traditional role of converting PIP3 to PIP2, as is the case with mammalian *PTEN*. Cells lacking *ptn1* showed a significant increase in the levels of PI(3,4)P2 (phosphatidylinositol-(3,4)-diphosphate) and PI(3,4,5)P3 (phosphatidylinositol-(3,4,5)-trisphosphate). However, on the introduction of a recombinant *ptn1p* vector that dephosphorylates PI (3,4,5) P3, the PI (3,4) P2 and PI (3,4,5) P3 levels were restored close to wild type levels, showing that *ptn1* regulates the levels of PI(3,4)P2 and PI(3,4,5)P3. Thus, *ptn1* may have a role in maintaining vacuole morphology as the *ptn1* deletion mutants showed irregularly shaped vacuoles and an increased sensitivity to osmotic agents (Mitra et al., 2004).

***Saccharomyces cerevisiae*.** The budding yeast, *Saccharomyces cerevisiae*, is an ascomycete fungus and is one of the most commonly used eukaryotic model systems. *S. cerevisiae* has an orthologue of *PTEN*, known as *TEP1* (Heymont et al., 2000). The



deletion of *TEPI* in haploid strains did not produce any phenotypes, indicating that it is probably not an essential gene in *S. cerevisiae*. However, the homozygous deletion diploids exhibited resistance to wortmannin, a PI3K (a phosphatidylinositol 3-kinase) inhibitor and to lithium ions both of which are known to affect the phosphatidylinositol pathway (Kitagishi, Kobayashi, Kikuta, & Matsuda, 2012; Sinha et al., 2005). The experiments performed to measure the average lifespan of the yeast strains showed that the null *TEPI* haploid cells and double deletion *TEPI* strains had an average lifespan of 18.27 and 17.85 divisions compared to the 18.25 and 17.43 for haploid and diploid wildtype yeast strains respectively; thus, it appears that neither haploid *TEPI* nor diploid mutants displayed any effect on the lifespan of yeast strains. A previous transcriptional profile study on the yeast sporulation process (Chu et al., 1998) indicates that *TEPI* is one of the genes significantly upregulated during the sporulation stage. Also, an alteration was observed in the cell wall of *TEPI* mutants as they exhibited a reduced deposition of dityrosine a fluorescent compound synthesized by yeast cells during aacus maturation (Briza, Winkler, Kalchhauser, & Breitenbach, 1986). The results are consistent with a role of *TEPI* in the developmental process of sporulation.

***Fusarium graminearum.*** *Fusarium graminearum* is the pathogenic agent of Fusarium head blight (FHB or Head Scab), a serious disease affecting wheat and barley causing significant yield loss and reduced grain quality. These are filamentous fungi with a cosmopolitan distribution and belong to the phylum Ascomycota (Ascomycetes) (Sharma & Marques, 2018). A study conducted in *F. graminearum* focusing on its pathogenesis indicated the presence of a *PTEN* orthologue, *FgTEPI*. *FgTEPI* of *F. graminearum* is the functional homologue of *TEPI* gene of *S. cerevisiae* (D. Zhang et al., 2010). The functional

similarity of *FgTEPI* to that of yeast *TEPI* was demonstrated mainly through the wortmannin resistant phenotype and a specific phenotype that is connected to treatment with lithium ions. *FgTEPI* deletion strains are more resistant to wortmannin, a PI3K inhibitor, which connects *FgTEPI* to the phosphatidylinositol signaling pathway. Wortmannin sensitive yeast cells lacking *TEPI* when complemented with *FgTEPI* were able to regain the wortmannin sensitivity of the wildtype cells. The *FgTEPI* deletion mutants showed a decreased production in conidia, especially in the presence of lithium ions. *FgTEPI* mutants exhibited a reduced mycelial growth, sensitivity to lithium and a reduction in virulence on wheat coleoptiles. It appears that while *FgTEPI* is not normally required for the growth of mycelium or conidia, the mycelial growth and conidial germination of *FgTEPI* mutants were reduced in the presence of wortmannin and lithium, respectively. As the authors point out, it is possible that the lack of *FgTEPI* might be disruptive to the PI3K signaling of *F. graminearum* during the infection process.

### ***Ustilago maydis* as a model system for signaling research**

Knowing how cells respond to internal and external stimuli is important as it is key to our understanding of fundamental processes such as cell growth, cell survival or even cell death. We have seen how the studies aimed at understanding the molecular mechanism of the complex signaling networks in several of the model systems has tremendously contributed to our understanding of cellular signaling, particularly that of higher order eukaryotes. One such model system is *Ustilago maydis*. *U. maydis* is a basidiomycete fungus and is a known pathogen of *Zea mays* (maize or corn). It is a biotrophic fungus and has a high degree of host specificity, specialized to infect corn plants (*Zea mays*) and its progenitor, teosinte (*Zea mays* subsp. *parviglumis*) (Basse & Steinberg, 2004). In the past

few decades *U. maydis* has become an excellent model system for cell signaling studies. The establishment of a variety of techniques that can characterize the molecular, cellular and functional aspects of the organism allows studies of the crucial cellular processes in this fungus (Bolker, 2001). *Ustilago maydis* being a pathogenic fungus allows the study of host pathogen interaction and the mechanisms contributing to it (Basse & Steinberg, 2004). The short generation time and the presence of yeast-like haploid form allows for the easy maintenance on culture plates under laboratory conditions, while relatively short reproduction time in planta means the complete investigation of the biotrophic phase of the fungus takes less than a month. Genetic manipulation is relatively easy since *U. maydis* has a very efficient homologous recombination system (Kamper et al., 2006). A unique advantage that makes *U. maydis* or for that matter any fungi, a good model system for cell signaling studies, is that they are unicellular eukaryotes, making it easier to explore the mechanisms of cell growth, differentiation, proliferation and reproduction. These processes are controlled by environmental and nutritional signals, and many of the responses to such signals for these fundamental mechanisms and pathways are conserved across organisms.

### **Life cycle of *Ustilago maydis***

*U. maydis* has a complex lifecycle that requires a living host to complete sexual reproduction (*i.e.* it is a biotrophic fungus). The life cycle of *U. maydis* involves mainly two different morphological forms, the saprophytic yeast like haploid sporidia and the pathogenic dikaryotic hyphal form (Snetselaar, Bolker, & Kahmann, 1996). The life cycle involving the yeast form and the dikaryotic hyphal form is shown in Figure 1.4. The dikaryotic form, upon reaching a plant surface, forms an appressorium, a penetrating structure; once inside the plant hyphae develop, multiply and spread to adjacent tissues.

The infection with *U. maydis* results in the induction of tumors/galls on the green aerial parts of the plant, including stems, leaves, tassels and ears (Bolker, 2001). The tumors can be small or big and usually have a smutty appearance upon rupture, due to the presence of black fungal teliospores within. As the tumor matures, plant cells are replaced with fungal cells. Teliospores on maturity are released. Such spores later germinate on suitable surfaces or when nutrients are present. They then undergo meiosis to yield haploid sporidia. Compatible haploid sporidia can fuse together to form the dikaryon and continue the life cycle.

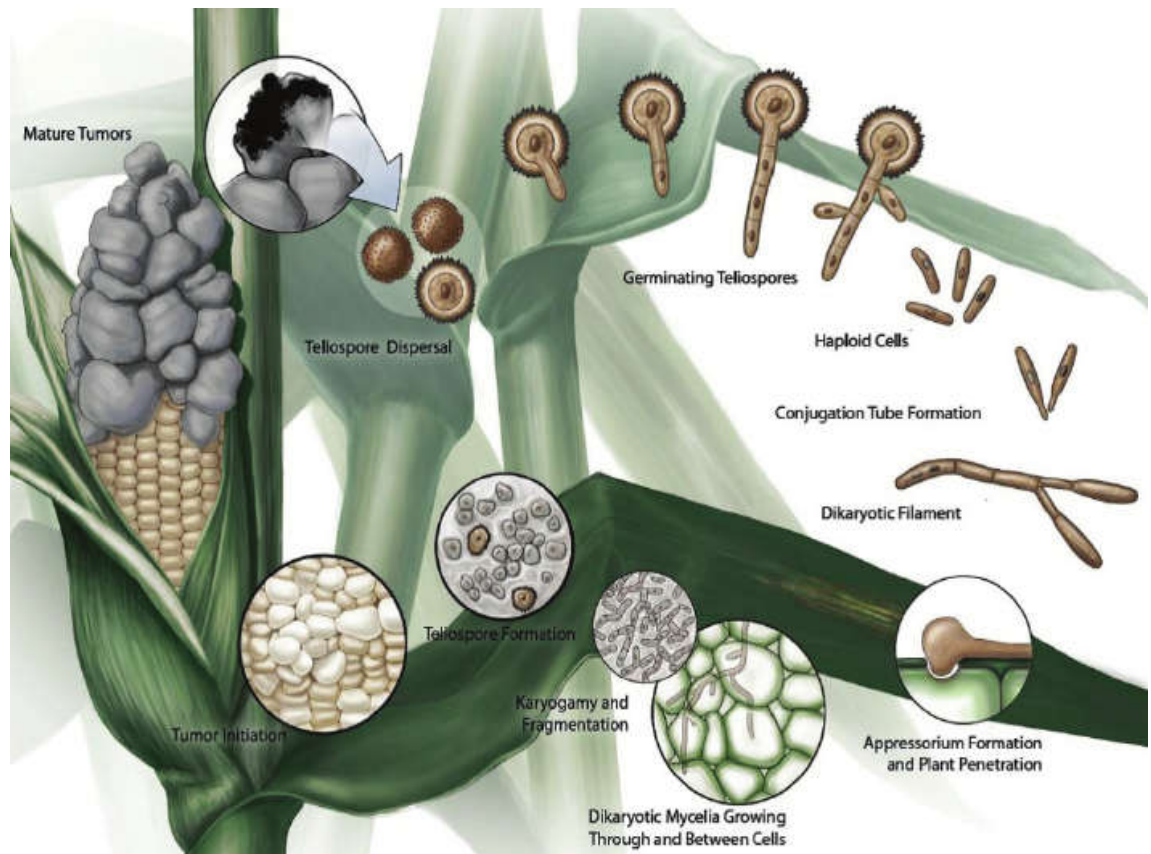


**Figure 1.4.** Developmental stages in the *U. maydis* life cycle. Reused from the book ‘Molecular Mechanisms and Cytogenetic Diversity’ by open access publisher IntechOpen (Saville, Donaldson, & Doyle, 2012)

## Regulation of the mating process in *U. maydis*

The haploid yeast cells (sporidia) multiply by budding whereas the dikaryotic hyphae is formed by the fusion of two sexually compatible sporidia, which is mediated by the two mating type loci *a* and *b* (Kahmann, Romeis, Bölker, & Kämper, 1995). The two haploid sporidia of opposite mating types (*a1b1/a2b2*) come together and recognize each other by the lipopeptide pheromone (*mfa1/2*) - pheromone receptor (*pra1/2*) mechanism which happens usually on the plant surface (Bolker, Urban, & Kahmann, 1992).

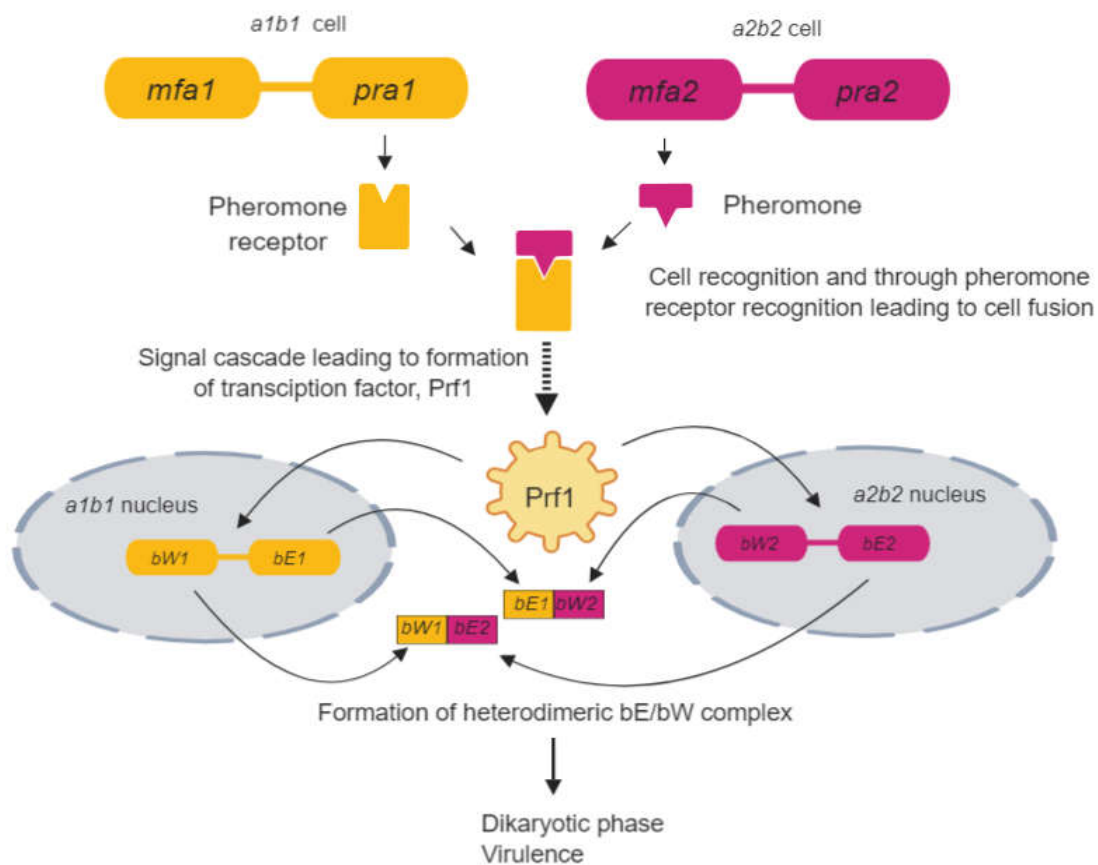


**Figure 1.5.** Interactions between the two mating-type loci during development of *U. maydis*. The biallelic *a* locus encodes a pheromone-based cell recognition system, which triggers cell fusion. After fusion, different alleles at the multiallelic *b* locus induce sexual and pathogenic development by formation of an active heterodimeric transcription factor (Bölker, 2001)

The pheromone receptor system is encoded by the biallelic *a* locus which regulates the cell-cell (external) recognition, whereas the multiallelic *b* locus encodes two unrelated homeodomain proteins bE and bW which facilitates an internal self/non-self-recognition (Müller, Weinzierl, Brachmann, Feldbrügge, & Kahmann, 2003) (Figure 1.5). In order to form the heterodimer, each bE protein should physically interact with a bW protein product from a different allele in order to form that functional heterodimer (Steven J. Klosterman, Perlin, Garcia-Pedrajas, Covert, & Gold, 2007). The heterodimer acts as a transcription factor for genes that are involved in the establishment of the pathogenic dikaryotic form (Kronstad & Leong, 1989b). The transmission of signals from the pheromone receptor to other components and the following cascade altering the gene expression in the *a* and *b* loci leading to the formation of heterodimer is part of a MAPK signaling pathway. (Feldbrugge, Kamper, Steinberg, & Kahmann, 2004; Steven J. Klosterman et al., 2007).

### **Regulation of dimorphism in *U. maydis***

In fungi, the regulation of dimorphic switch is tightly controlled as it requires considerable degree of coordination between cell cycle, cytoskeletal elements, cell wall enzymes, and other cellular components to accomplish the dimorphic transition. We know that the life cycle of *U. maydis* involves mainly two different morphological forms, the saprophytic yeast-like form and the pathogenic dikaryotic hyphal form. This dimorphic switch is induced by both detection of pheromone from the opposite mating type by the G-protein coupled pheromone receptor or by environmental or nutrient signals such as low ammonium, acidic pH, and lipids (Smith, Garcia-Pedrajas, Gold, & Perlin, 2003). The activation of the pheromone receptor causes the heterotrimeric G protein to dissociate into

G $\alpha$  and G $\beta\gamma$  subunits. The released G $\beta\gamma$  subunit in turn activates the MAP kinase signaling pathway, a pathway that is conserved from yeast to humans. In *U. maydis*, it consists of a series of MAP kinases belonging to a family of serine/threonine protein kinases, (Figure 1.6), each of which (MAPKKK (Kpp4 or Ubc4), MAPKK (Fuz7 or Ubc5) and MAPK (Kpp2 or Ubc3 and Kpp6)) is activated by the phosphorylation of the previous kinase. The signal, upon reaching MAPK, leads to the activation of a transcription factor Prf1 which, in turn, will activate the *a* and *b* locus genes, eventually leading to the formation of the bE/bW heterodimer. Heterozygosity (any combination of different *b* alleles) at the *b* locus initiates the dimorphic switch to the filamentous dikaryotic form (Schulz et al., 1990).

In addition to the MAPK pathway, the cAMP dependent PKA pathway also plays a major role in mating and hyphal development, especially in response to environmental signals, causing morphogenic transition (Figure 1.6). The major elements of the PKA pathway include the G $\alpha$  subunit, adenylate cyclase (Uac1) and dimeric PKA protein module (Ubc1/Adr1). Among the four G $\alpha$  subunits (Gpa1 through Gpa4) identified in *U. maydis*, only Gpa3 is important in the mating response (Steven J. Klosterman et al., 2007). Gpa3, on activation by the perception of environmental signals, leads to the activation of the adenylate cyclase (Uac1) and thereby leads to increased cAMP levels (N. Lee, D'Souza, & Kronstad, 2003). cAMP causes the dissociation of the PKA module into regulatory subunit Ubc1 and catalytic subunit Adr1 (Durrenberger, Wong, & Kronstad, 1998). The unbound catalytic subunit can now activate the Pheromone-Responsive transcription Factor, Prf1, which is necessary for the up-regulation of the *a* and *b* genes leading to mating and filamentation response (Kaffarnik, Muller, Leibundgut, Kahmann, & Feldbrugge, 2003).

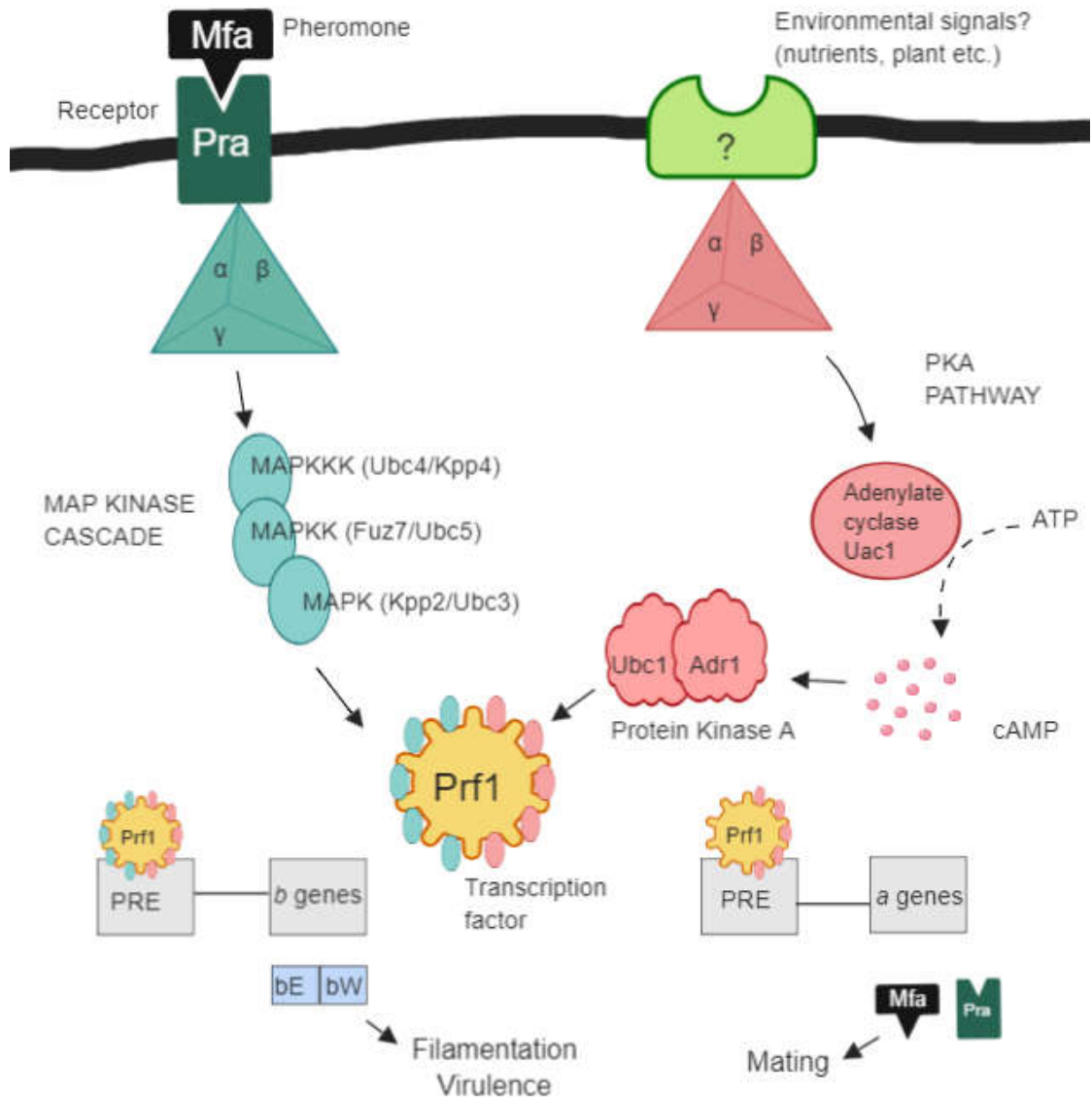


**Figure 1.6.** Schematic overview of the interplay between PKA pathway and the pheromone response pathway during pathogenic development (Bölker, 2001; Nadal, Garcia-Pedrajas, & Gold, 2008).

### Regulation of in planta development of *U. maydis*

The establishment of a biotrophic relationship with the host is necessary for *U. maydis* to complete its life cycle (Brefort et al., 2009). Only the dikaryotic filamentous



form can infect the plant. However, the dikaryon would be a dead-end cell type due to cell-cycle arrest unless an unknown plant-host signal releases the cell-cycle arrest (Nadal et al., 2008). The dikaryon formed by the fusion of haploid sporidia produces specialized infection structures called appressoria and grows through the host epidermal layer (Krüger et al., 2000). The entry and colonization into the plant may require the production of lytic and other enzymes (S. J. Klosterman, Perlin, Garcia-Pedrajas, Covert, & Gold, 2007). However, not much is known regarding the role of lytic enzymes in the infection process in *U. maydis*. The filamentous dikaryon grows through the plant tissues without evoking a plant defense response (S. J. Klosterman et al., 2007). For instance, when the gene *gas1*, which codes for the catalytic subunit of a glucosidase II enzyme was deleted, the deletion strains were able to penetrate the plant but were stopped at the epidermal layer (Schirawski et al., 2005). The infection with *U. maydis* causes hypertrophy and hyperplasia of the plant cells of the infected tissue (Banuett & Herskowitz, 1996). Increased levels of plant hormones such as auxins in the infected tissue leads to the speculation that they are responsible for the growth of tumors (S. J. Klosterman et al., 2007; Moulton, 1942). Studies have shown that *U. maydis* can synthesize auxin (indole-3-acetic acid), however, it is still uncertain whether the auxin produced by *U. maydis* is responsible for tumor formation (Guevara-Lara, Valverde, & Paredes-López, 2000). The growth and proliferation of the dikaryotic fungal mycelium within the plant, leads to the formation of characteristic tumors or galls. In the tumors, the fungal cells undergo karyogamy to form diploid hyphae, which proliferate and undergo sporogenesis (Brefort et al., 2009). The sporogenic hyphae that have proliferated in the plant tumors produce diploid teliospores. Signal molecules from the host are speculated to be responsible for teliospore production (Ruiz-Herrera, León-

Ramírez, Cabrera-Ponce, Martínez-Espinoza, & Herrera-Estrella, 1999). The various stages that result in the formation of teliospores include proliferation of hyphae to form a large fungal mass, development of a mucilaginous matrix around this fungal mass, fragmentation of the fungal hyphae, development of the fragmented cells into round echinulate structures, and development of melanized walls around these structures, resulting in the formation of teliospores. The Figure 1.7 depicts the various stages involved in the teliospore development and the genes responsible for each of those events.

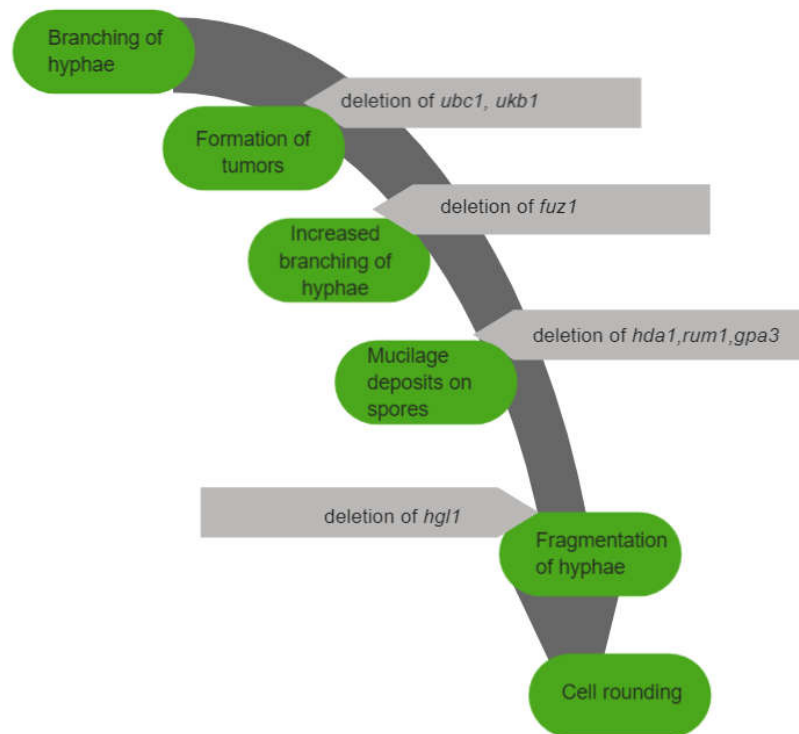


**Figure 1.7** Stages in *U. maydis* teliospore development. The developmental stages blocked due to the deletion of specific gene in mutants are indicated with arrows (Steven J. Klosterman et al., 2007).

Some of the signal transduction proteins involved in facilitating these events include Ubc1 (regulatory subunit of PKA) or Ukb1 (a protein kinase B-related enzyme) which are required for inducing tumor formation and the accumulation of the hyphal masses in the tumors, which leads to the idea that these proteins are connected to the *U.*

*maydis* cAMP pathway (Abramovitch, Yang, & Kronstad, 2002; Gold, Brogdon, Mayorga, & Kronstad, 1997). The deletion of *Gpa3* resulted in no tumor formation while its overexpression led to decreased teliospore formation (Krüger et al., 2000). The Krüger et al., (2000) study indicates that tight regulation of the cAMP pathway is important for the development of fungus within the plant but does not play a significant role with the tumor induction process. While the *fuz1* mutants showed no defect in hyphal development, they did not produce the mucilage matrix found in the tumors of normally infected tissues (Banuett & Herskowitz, 1996). Proteins such as Hda1 (a histone deacetylase) and Rum1 control the expression of specific genes, functioning more like a repressor of genes that are activated by bE/bW heterodimer (Reichmann et al., 2002). While the *hda1* deletion mutants did not produce teliospores, *rum1* mutants failed to develop in the later stages of teliospore formation, especially after the mucilage matrix formation stage (Quadbeck-Seeger, Wanner, Huber, Kahmann, & Kamper, 2000). The presence of a DNA-binding domain and a histone deacetylase-interaction domain indicates that Rum1 possibly forms a complex with Hda1 (Quadbeck-Seeger et al., 2000). The partial deletion of the *hgl1* gene resulted in normal initial fungal hyphal development in planta, but they did not make rounded cells or mature teliospores (Durrenberger, Laidlaw, & Kronstad, 2001). Ust1, an APSES domain transcription factor, is known to be a master repressor of teliospore formation since the deletion of *ust1* resulted in the production of numerous, pigmented teliospore-like cells in *in vitro* cultures (García-Pedrajas, Baeza-Montañez, & Gold, 2010). Interestingly, Unh1, an Ndt80-like DNA binding protein, when deleted, led to the production of unpigmented teliospores, while its constitutive expression resulted in haploid cells with abnormal pigmentation indicating that the gene has a potential role in coloration of the teliospores

(Doyle, Kitty Cheung, Spence, & Saville, 2016). A recent study indicates that the WOPR family Protein, Ros1, is another master regulator of teliospore formation in *U. maydis*. It was found that *ros1* expression was induced only during late infection playing a role in massive fungal proliferation and spore formation. Transcriptional profiling and ChIP-seq analyses performed in this study indicated that Ros1 remodels expression of about 30% of all *U. maydis* genes with 40% of these being direct targets. Another recent study indicated that RGS (regulators of G-protein signaling) proteins such as Rgs1, Rgs2 and Rgs3 in *U. maydis* play distinct roles in virulence, tumorigenesis and sporogenesis, possibly through the direct modulation of the G $\alpha$  subunit-activated signaling pathways, since elevated cAMP levels were observed in *rgs2* and *rgs3* mutants (Moretti et al., 2017). It showed that *rgs1* deletion had a minor role in virulence, *rgs2* mutants had defective cell morphology, growth, mating and did not show disease symptoms in plants, and *rgs3* mutants had defect in mating, virulence and teliospore maturation. The proteins required for filamentation (proteins of MAPK and cAMP pathways) are required for *U. maydis* proliferation in planta and for subsequent tumor formation, indicating a cross talk between various pathways. While we have some data about the molecular pathways and a few noteworthy players in teliospore formation and development in *U. maydis*, overall the details of processes governing teliospore maturation and pigmentation are poorly characterized and demands further exploration.

### **Research Interest**

The role of the *PTEN* gene has been characterized in a variety of organisms. While we know that this gene plays a vital role in most of the eukaryotic systems, including some ascomycete fungal systems, it is not characterized in any of the basidiomycete fungal

systems, such as *Ustilago maydis*. The goal of the current study was to characterize *ptn1*, the *PTEN* orthologue, in *U. maydis* and to explore the role of this gene in the growth and pathogenicity aspects of the fungal life cycle. The subsequent chapters aim to investigate the role of *ptn1* in causing plant infection and teliospore formation and later focuses on the connection of *ptn1* with other elements of the signal transduction pathways controlling growth, morphology and pathogenicity of *U. maydis*.

## CHAPTER II

### DELETION OF PTN1, A PTEN/TEP1 ORTHOLOGUE, IN *USTILAGO MAYDIS* REDUCES PATHOGENICITY AND TELIOSPORE DEVELOPMENT

#### SUMMARY

The PTEN/PI3K/mTOR signal transduction pathway is involved in the regulation of biological processes such as metabolism, cell growth, cell proliferation and apoptosis. This pathway has been extensively studied in mammals, leading to the conclusion that *PTEN* is a major tumor suppressor gene. *PTEN* orthologues have been characterized in a variety of organisms, both vertebrates and non-vertebrates, and the studies of the associated PTEN/PI3K/mTOR pathway indicate that it is widely conserved. Studies in some fungal systems indicated a role of *PTEN* in the developmental process of sporulation as in *Saccharomyces cerevisiae*. The present study was aimed at investigating the role of the *PTEN* ortholog, *ptn1*, in *Ustilago maydis*, the pathogen of maize. *U. maydis ptn1* mutant strains where *ptn1* gene is deleted or overexpressed were examined for phenotypes associate with mating, virulence and spore formation. While overexpression of *ptn1* had no substantial effects on virulence, *ptn1* deletion strains showed slight reduction in mating efficiency and significant reduction in virulence; tumor formation on stem and/or leaves were severely reduced. Moreover, tumors, when present, had significantly lower levels of

mature teliospores and the percent germination of such spores was similarly reduced. Thus, *ptn1* is required for these important aspects of virulence in this fungus.

## INTRODUCTION

*Ustilago maydis*, is a plant pathogen responsible for smut disease in *Zea mays* (Brefort et al., 2009). In the past few decades, *U. maydis* has developed into a model system for a variety of research areas including, but not limited to, cellular transport processes, plant-pathogen interaction and DNA repair mechanisms (Steinberg & Perez-Martin, 2008). Due to the great level of genetic similarity shared between *U. maydis* and metazoans, it may serve as a viable model for the study of essential cellular processes of higher eukaryotes (Perez-Nadales et al., 2014; Steinberg & Perez-Martin, 2008). Several homologues of human proteins involved in DNA repair and genomic stability are present in *U. maydis*, e.g. the BRCA2 orthologue, Brh2 (Vollmeister et al., 2012).

*PTEN* (phosphatase deleted on chromosome ten; also known as *MMAC1* or *TEP1* (tensin-like phosphatase)) is a human tumor suppressor gene mapping on chromosome 10 at 10q23.3 (Steck et al., 1997). The *PTEN* gene is either deleted or inactivated in several tumors including those associated with breast, endometrial, brain, and prostate cancers (Jing Li et al., 1997). The sequence of the phosphatase domain of *PTEN* is most similar to those of dual specificity protein phosphatases such as cell division cycle 14 (CDC14), baculovirus phosphatase (BVP), DUSP3, and DUSP4. However, the amino-terminal region of *PTEN* containing the phosphatase catalytic domain, also has homology to proteins such as actin-binding protein, tensin-1 (TNS1) and auxilin, the cofactor of ATPase heat shock protein HSC70, though such proteins are unrelated to *PTEN* catalytic functions (Song et al., 2012). The *PTEN* gene codes for a protein which is a major phosphatase

enzyme that dephosphorylates PtdIns(3,4,5)P3 (PIP3) to PtdIns(4,5)P2 (PIP2), thereby counteracting the signaling by Phosphatidylinositol-4,5-bisphosphate 3-kinase (PI3Ks) and playing a major role in the regulation of the PTEN/AKT/mTOR signaling pathway (Leslie & Downes, 2004). Studies conducted in mouse models and humans suggest that *PTEN* is highly regulated and very critical for cellular functions. It is evident from mouse model studies that a 20% reduction in *PTEN* expression level is sufficient to develop a range of tumors (Alimonti et al., 2010).

*PTEN* is mostly known for its tumor suppressor activity. However, it has also been shown to be involved in a variety of other functions, including regulation of cell size, metabolism, aging and development of neurons (J. Liu & Chin-Sang, 2015). Orthologs of *PTEN* have been identified in *Drosophila melanogaster* (Huang et al., 1999b), *Caenorhabditis elegans* (Gil, Malone Link, Liu, Johnson, & Lees, 1999; Solari et al., 2005), and budding yeast (Heymont et al., 2000). *PTEN* is essential for *Drosophila* where it regulates cell size, cell proliferation and apoptosis (Huang et al., 1999b). In *C. elegans*, mutations in *PTEN* may cause disruptions in the developmental process, characterized by constitutive dauer (larval morphology) formation (Gil et al., 1999; Solari et al., 2005). The deletion of the *PTEN* orthologue, *TEP1*, in the budding yeast, *S. cerevisiae*, revealed that it has a role in sporulation. *TEP1* mutants had defects in the trafficking or deposition of dityrosine, a major component of yeast spore walls (Heymont et al., 2000).

In this study, we have begun the functional characterization of the sole *PTEN* ortholog, *ptn1* (UMAG\_03760), in *U. maydis*. We examined the phenotypes of *U. maydis* cells overexpressing or deleted for *ptn1*. In the absence of a functional *ptn1* gene, *U. maydis*



haploid cells grow normally in axenic culture, but displayed a reduced capability to tolerate cell wall stress. More strikingly, such mutants, when mixed with compatible mating partners, were defective in tumor formation, teliospore development, and the rate of teliospore germination.

## MATERIALS AND METHODS

**Strains and growth conditions.** The *U. maydis* strains used in this study are listed in Table 1. *Escherichia coli* strains TOP10 and DH5 $\alpha$  (Invitrogen/Thermo Fisher) were used for all cloning and plasmid maintenance. *U. maydis* strains were grown at 26 °C in solid or liquid YEPS, PDA, HSS media (Brachmann, König, Julius, & Feldbrügge, 2004) or Holliday Salt media as described previously (Holliday, 1974). Strains grown in liquid media were shaken overnight at 250 rpm. Mating media was made with solid PDA and 1% activated charcoal, while stress media was made with solid YEPS and either Congo red (Fisher Scientific, Fairlawn, NJ, 15  $\mu$ g/ml), sodium chloride (1M), calcofluor white (50  $\mu$ M; Sigma-Aldrich, St. Louis, MO) or sorbitol (1M) as described in (Cervantes-Chávez, Ali, & Bakkeren, 2011).

**Table 2.1 Strains used in this study.**

List of strains		
<i>Ustilago</i> Strain	Genotype	References
1/2	<i>alb1</i>	(Gold et al., 1997)
2/9	<i>a2b2</i>	(Gold et al., 1997)
1/2 $\Delta$ <i>ptn1</i>	<i>alb1 ptn1::cbx<sup>R</sup></i>	This study
1/2 $\Delta$ <i>ptn1J</i>	<i>alb1 ptn1::hyg<sup>R</sup></i>	This study
2/9 $\Delta$ <i>ptn1</i>	<i>a2b2 ptn1::cbx<sup>R</sup></i>	This study
2/9 $\Delta$ <i>ptn1J</i>	<i>a2b2 ptn1::hyg<sup>R</sup></i>	This study
FB1 $\Delta$ <i>ptn1J</i>	<i>alb2 ptn1::hyg<sup>R</sup></i>	This study
1/2 <i>ptn1</i> <sup>otef</sup>	<i>alb1 P<sub>otef</sub>-ump2, cbx<sup>R</sup></i>	This study
2/9 <i>ptn1</i> <sup>otef</sup>	<i>a2b2 P<sub>otef</sub>-ump2, cbx<sup>R</sup></i>	This study

SG200	<i>almfa2 bE1bW2</i>	(Muller, Aichinger, Feldbrugge, & Kahmann, 1999)
SG200 $\Delta$ <i>ptn1</i>	<i>almfa2 bE1bW2 ptn1::hyg<sup>R</sup></i>	This study
d132	<i>ala2b1b2</i>	(Kronstad & Leong, 1989a)
d132 $\Delta$ <i>ptn1</i>	<i>ala2b1b2 ptn1 ptn1::hyg<sup>R</sup></i>	This study
1/2 $\Delta$ <i>ptn1c</i>	<i>alb1 ptn1::cbx<sup>R</sup> P<sub>otef</sub>-ptn1, hyg<sup>R</sup></i>	This study
2/9 $\Delta$ <i>ptn1c</i>	<i>a2b2 ptn1::cbx<sup>R</sup> P<sub>otef</sub>-ptn1, hyg<sup>R</sup></i>	This study
FBD11-7	<i>ala1 b1b2</i>	(Brachmann et al., 2004)
FBD12-17	<i>a2a2 b1b2</i>	(Brachmann et al., 2004)
Plasmids	<b>Genotype</b>	<b>References</b>
DelsGate <i>ptn1</i>	<i>kan<sup>R</sup> ptn1::cbx<sup>R</sup></i>	(Garcia-Pedrajas et al., 2008)
Otef- <i>ptn1</i> - <i>cbx</i>	<i>bla(amp<sup>R</sup>) P<sub>otef</sub>-ptn1 cbx<sup>R</sup></i>	This study
Otef- <i>ptn1</i> - <i>hyg</i>	<i>bla(amp<sup>R</sup>) P<sub>otef</sub>-ptn1 hyg<sup>R</sup></i>	This study

**Vector construction and nucleic acid manipulations.** The *ptn1* deletion strains in *U. maydis* were made using homologous recombination by the DelsGate protocol as described previously (Garcia-Pedrajas et al., 2008) using primers (Table 2.2) designated UPTN-K1-K4 to amplify the flanks of *ptn1*. These strains 1/2  $\Delta$ *ptn1* and 2/9  $\Delta$ *ptn1* were created by replacing the *ptn1* ORF with the DelsGate deletion construct plasmid containing a carboxin resistance marker. Confirmed  $\Delta$ *ptn1* mutants were complemented with a plasmid containing a hygromycin resistance gene and wild type copy of the gene under the control of the constitutive *otef* promoter (*P<sub>otef</sub>*) to yield 1/2  $\Delta$ *ptn1c* and 2/9  $\Delta$ *ptn1c* complemented strains. The overexpression strains of *ptn1* were generated by expressing the *ptn1* ORF under the control of *P<sub>otef</sub>*, using a derivative of p123 bearing a carboxin resistance marker (Pham et al., 2009). *P<sub>otef</sub>*-based vectors were linearized using *SspI* digestion prior to transforming *U. maydis* protoplasts (Pham et al., 2009). Additional *ptn1* deletion strains 1/2  $\Delta$ *ptn1J*, 2/9  $\Delta$ *ptn1J*, FB1  $\Delta$ *ptn1J*, SG200  $\Delta$ *ptn1*, and d132  $\Delta$ *ptn1* were generated via replacing the *ptn1* ORF with a hygromycin resistance cassette. The hygromycin replacement construct was prepared through overlap-PCR (Harrison, Cavinder, Townsend,

& Trail, 2013; Kamper, 2004) using primers PTENUPLT, PTENUPRT, PTENDNLT, CPDNRT, HYGPTENLT, HYGPTENRT (Table 2.2) as described previously (Harrison et al., 2013) with minor modifications.

Transformed *U. maydis* strains were selected on YEPS agar plates containing either 3 µg carboxin per ml (Santa Cruz Biotechnology, Dallas, TX) or 150 µg/ml hygromycin B (Gold Biotech). Transformation was confirmed using PCR with primers that would be diagnostic for true transformants and distinct for wild type. For  $\Delta ptn1$  derivatives, qPCR was used to confirm loss of gene expression relative to wild type. Primers were designed using the Primer3 software (<http://bioinfo.ut.ee/primer3/>) based on the genome sequence available at JGI (<http://genome.jgi.doe.gov/Ustma1/Ustma1.home.html>). PCR was carried out in a T100 Thermal Cycler (Bio-Rad Laboratories, Hercules, CA). For PCR amplification reactions either Hot Start ExTaq DNA Polymerase, PrimeSTAR HS DNA Polymerase (Takara Bio, USA), Platinum Taq Green Hot Start DNA Polymerase (Life Technologies Corporation) or EconoTaq DNA Polymerase (Lucigen Corporation) were used.

**Table 2.2 List of primers**

<b>Primers</b>	<b>Sequence</b>
UPTN-K1	TAGGGATAACAGGGTAATCAACAAAATGACGCAACCAC
UPTN-K3	GGGACAAGTTTGTACAAAAAAGCAGGCTAAGAACGATGTTT GCGTGTCAG
UPTN-K4	GGGGACCACTTTGTACAAGAAAGCTGGGTACGTTAGACAAA GCGCAATCA
UPTN-K2	GGAAGGTGATCGTGAAGGAA
PTENUPLT	GCAACAAAATGACGCAACC
PTENUPRT	GTAGTTACCACGTTCCGGCCATAAGGTGGTGGGACTGCTTT
PTENDNLT	GCTTTGCTCTTTGCTCTTCTG
CPDNRT	GCCTTAATTAATATACGCCCGATTGCTTACC
HYGPTENLT	AAAGCAGTCCCACCACCTTATGGCCGAACGTGGTAACTAC
HYGPTENRT	AGAAGAGCAAAGAGCAAAGCCTCAGGCCTCATGTTTGACA
PTEN5	TGAGGCCTGAGTGGCCTATATACCCCTGCCCTGT

PTEN3           CGAATTCTTGCGCTTTGTCTAACGAAC  
HYGSPH1RT    TTTGCATGCCTCAGGCCTCATGTTTGACA  
NEW  
HYGMFE1       TTTCAATTGTGGCCGAACGTGGTAACTAC

**RNA isolation and expression analysis.** RNA isolation from *U. maydis* strains and quantitative real-time PCR were carried out as described in (Paul, Wallen, Zhao, Shi, & Perlin, 2018). The RNA expression data were analyzed in GraphPad Prism using unpaired T-test after normalization to wild type expression under high ammonium conditions; a probability value of  $P < 0.05$  was considered as a significant difference.

**Cell growth, mating, and plant infection.** For cell growth rate and mating assays, liquid cultures of the strains grown overnight in 4 ml YEPS liquid media shaken at 260 rpm were used at an absorbance at 600 nm ( $OD_{600}$ ) of 0.6-0.8. To determine growth rates, cells grown overnight to reach exponential growth phase were collected, washed, and resuspended in fresh YEPS liquid media. Subsequently,  $4 \times 10^6$  cells were transferred into 10 ml of fresh YEPS liquid media, and optical density was determined every 2 hours for the first 12 h and every 6 h afterwards up to 30 h (Ho, Cahill, & Saville, 2007; Pham et al., 2009). Data were analyzed using Graphpad Prism. Mating assays were performed using *U. maydis* cells grown overnight in YEPS broth to an  $OD_{600}$  of 0.8 and were resuspended in water to an  $OD_{600}$  of 1.6 prior to spotting. Opposite mating-type strains was co-spotted (10  $\mu$ l) onto PDA charcoal plates and the mating reaction was observed after incubation at 26 °C for 24-48 h (Gold et al., 1997).

For plant infection assay, 4 ml overnight cultures were diluted using 50 ml fresh YEPS liquid media and grown overnight to an  $OD_{600}$  of 1.0, harvested and resuspended in water to an  $OD_{600}$  of 3.0 prior to infection (Muller et al., 1999). Plant infection was performed by

inoculating 7-9 days old maize seedlings [Golden Bantam seeds, Bunton Seed Co., Louisville, KY and W. Atlee Burpee & Co., 62 Warminster, PA]. Haploid strains of opposite mating types were mixed prior to plant infection, while diploid d132 and the solopathogenic SG200 strain were used directly as previously described (Gold et al., 1997; Pham et al., 2012). The virulence of each treatment group was scored by a disease index (DI) on a scale of 0 to 5, where 0= No Symptoms, 1= Chlorosis, 2= Small leaf tumors, 3= Large leaf tumors or small stem tumors, 4= Large stem tumors with bending, and 5= Death (Doyle et al., 2016; Gold et al., 1997). Thirty plants were used in each experiment and the trials were repeated three times, with plants scored for disease symptoms on 14- and 21-days post infection (dpi). A haploid *alb1* background mutant strain crossed with a haploid *a2b2* mutant strain was compared in each case to the corresponding wild type cross. Additional measures of virulence included estimations of biomass, numbers of leaves, plant length, and chlorophyll content of infected plants. The dry biomass index of the infected plants was measured as previously described (Akhtar et al., 2017). The above ground parts of the infected plants where both partners were wild type, or both were mutant (*i.e.*,  $\Delta ptn1 \times \Delta ptn1$  or  $ptn1^{otef} \times ptn1^{otef}$ ) were collected 8 days post infection (dpi) and washed once with tap water and twice with distilled water. Plants were blotted dry and the samples were stored in labeled paper bags and dried at  $65 \pm 5$  °C in an incubator until a constant weight and dry biomass was recorded. Chlorophyll extraction was performed by the DMSO method and content was determined spectrophotometrically as described previously (Hiscox & Israelstam, 1979; Manolopoulou, Varzakas, & Petsalaki, 2016). Plant infections were also performed on a dwarf variety of maize (Tom Thumb popcorn, High Mowing Organic Seeds, Walcott, VT) mainly to facilitate maize cob infections. For

maize cob infection, maize plants were de-tasseled to increase the prospect of cob infection by preventing the pollination of ovules. Cobs were injected, as described previously (Doyle et al., 2016; Morrison, Emery, & Saville, 2015). In separate experiments, dwarf maize plants were infected with wild type (WT) and mutant strains on the leaf following the protocol described (Gold et al., 1997).

**Statistical analysis.** Statistical analysis of the disease index data from plant infection was conducted using Kruskal-Wallis Test with a Multiple Comparison Test using R software (Conover, 1999; Redkar et al., 2015). The data of plant morphological characteristics such plant length, leaf number, dry biomass, chlorophyll content, spore germination rate and spore count were analyzed using ANOVA followed by Tukey's test (Torró, Bretó, & García-Yzaguirre, 2016) using GraphPad Prism software and the probability values of  $P < 0.05$  were considered as significant.

## RESULTS

**In silico analysis of *ptn1*.** Initial analysis of the *U. maydis* genome sequence revealed the presence of a hypothetical *PTEN*-like gene (UMAG\_03760), hereafter known as *ptn1*, predicted to encode a protein of 848 amino acids. The nucleotide sequence analysis (blastn) of the *ptn1* gene found greatest similarity to the *PTENB* gene (XM\_012330711.1) of *Pseudozyma hubeiensis*, a fungus also belonging to the order Ustilaginales. The *U. maydis* Ptn1 protein is characterized by the conserved Protein tyrosine phosphatase catalytic (PTPc) domain motif (more specifically CDC14 subgroup of PTP proteins) present in other *PTEN* orthologues, as well as a phosphatase tensin-type domain, which is characteristic of all *PTEN* proteins (Figure 2.1 and 2.12). In silico prediction tools such as SignalP

(<http://www.cbs.dtu.dk/services/SignalP>) and TargetP (<http://www.cbs.dtu.dk/services/TargetP>) suggested that Ptn1 is a cytoplasmic protein (Figure 2.13 and 2.14).

Predicted PTEN protein <i>Ustilago maydis</i>	1	<b>MTSIARRIVSGQKARFKDPLLDLDDLTYYVDHLIIMGFPASGVASL-YRNKRSVRRFLDKRH-DDLYRVYNFCP</b>	74
PTENB  <i>Pseudozyma hubeiensis</i>	1	<b>MTSIARRIVSGQKARFKDPTLDLDDLTYYVDHLIIMGFPASGVASL-YRNKRSVRRFLDKRH-DDLYRVYNFCP</b>	74
PTEN  <i>Sporisorium scitamineum</i>	1	<b>MASIARRIVSGQKTRFQDPLLDLDDLTYYVDHLIIMGFPASGVASL-YRNKRSVRRFLDKRH-DDLYRVYNFCP</b>	74
TEP1  <i>Sacharomycetes cerevisiae</i>	1	[18] <b>FVNLMKKILSLPMKKTND-IGLRLDISYILVNLIVCSYPVNTYPKLLYRNSLDDLILFLTVYHGKGNFRIFNFRG</b>	93
PTEN  <i>Mus musculus</i>	1	<b>MTAIIKEIVSENKRRYQED--GFDDLTYYIYPNILAMGFFAERLEGV-YRNKIDVVRFLDKKH-KNHYYKIYNLC-</b>	71
TPTE2  <i>Homo sapiens</i>	1	[85] <b>LEKLMRRLVSENKRRYTRD--GFDDLTYYVTERIAMSFPSSGRQSF-YRNPIEEVVRFLDKKH-RNHRYVYNLC-</b>	156
Predicted PTEN protein <i>Ustilago maydis</i>	75	<b>VTENA YDADEFYGR VSRFPFDHVPPLSLIPLFVADVTEYLESDFDATAVIHCKAGKGRSGMTCCYLVS</b>	146
PTENB  <i>Pseudozyma hubeiensis</i>	75	<b>VIENS YDADEFYGR VSRFPFDHVPPLSLIPLFVADITEYLESDFDATAVIHCKAGKGRSGMTCCYLVS</b>	146
PTEN  <i>Sporisorium scitamineum</i>	75	<b>VTENS YDADEFYAR VSRFPFDHVPPLSLIPLFVADITEYLESDFDATAVIHCKAGKGRSGMTCCYLVS</b>	146
TEP1  <i>Sacharomycetes cerevisiae</i>	94	<b>EKEDS [13] FESKDFEIQ [33] CERIGWLDHFPFPELLLEIIVDGIENYLSVSKNRVAVLHCRMGKGRSGMITVAYLMKY</b>	211
PTEN  <i>Mus musculus</i>	72	<b>-AERH YDTAKFNCR VAQYFPEDHNPQLELIKPFCELDQWLEDDNHVAIHCAGKGRSGTGMICAYLLHR</b>	142
TPTE2  <i>Homo sapiens</i>	157	<b>-SERA YDPKHFHNR VSRIMIDHNVPTLHEMVVFTKEVNEWMAQDLENIVAHCAGKGRSGTGMICAYLLAS</b>	227
Predicted PTEN protein <i>Ustilago maydis</i>	147	<b>PYLPTAPTSMFNYSKMQRPpKQSIAPSPFATI [10] HEQNATQapTVMQLQPP [7] PPRSSMTLQIPRSAANGVSS [5]</b>	239
PTENB  <i>Pseudozyma hubeiensis</i>	147	<b>PYLPTAPTSIKNYSKMQRPpQQTVSPPELPTI [10] DGQNAQ-pQAATLMPP PQARSSMTLQIPRSAAWADPCS [5]</b>	231
PTEN  <i>Sporisorium scitamineum</i>	147	<b>PYLPTAPTSIKNYSKMQRP-SNAVTPPELATN DGQNPQ--TSMQMP [8] PPRSSMTLQIPRSAANTQPST</b>	222
TEP1  <i>Sacharomycetes cerevisiae</i>	212	-----LQCPGLEA-----	219
PTEN  <i>Mus musculus</i>	143	<b>GKFLKAQEALDFYGEVTR-----</b>	161
TPTE2  <i>Homo sapiens</i>	228	<b>EIFLTAESLYYFGERRTN-----</b>	246

**Figure 2.1.** Sequence alignment of *U. maydis* Ptn1 and other PTEN proteins. Ptn1 protein was compared to selected proteins from Basidiomycete fungi, *Pseudozyma hubeiensis* and *Sporisorium scitamineum*; Ascomycete fungi, *Sacharomycetes cerevisiae*; and Mammals, *Mus musculus* and *Homo sapiens*. The red color shows a high degree of sequence similarity in amino acids at the N-terminal regions between Ptn1 and the other identified proteins.

**Deletion of *ptn1* led to reduced production of aerial hyphae characteristic of the mating reaction on charcoal media.** Wild type,  $\Delta$ *ptn1* and overexpression strains (*ptn1*<sup>otef</sup>) were spotted onto PDA charcoal plates to assess any defects in mating or post-mating filamentation (Figure 2.2). Compatible wild type haploids (1/2 *a1b1* x 2/9 *a2b2*) produced dikaryotic hyphae that appeared as white ‘fuzz’ growth when co-spotted. However, compatible *ptn1* deletion strains when co-spotted, showed a reduction in ‘fuzz’, especially when examined after the first 24 hrs. However, overexpression strains did not show a major change in ability to produce aerial hyphae. The complemented mutants,

$\Delta ptn1c$ , were able to partially recover the wild type phenotype, indicative of successful mating.

To determine whether  $\Delta ptn1$  cells produce pheromone, mating was performed using *U. maydis* tester strains, FBD11-7 and FBD12-17 (Figure 2.2). Such diploid strains are homozygous at the *a* mating locus and do not produce aerial hyphae when spotted alone on charcoal, but will become filamentous when they are plated together with cells that produce a different pheromone. The ‘fuzz’ appearance appeared in the case of both the wild type *a1b1* and *a2b2* partners with their respective tester strains; on the other hand, there was a slight reduction in the production of aerial hyphae for the *ptn1* deletion strain in the *a2b2* background when paired with tester strain FBD11-7, suggesting reduced production of the *a2* pheromone by this mutant.

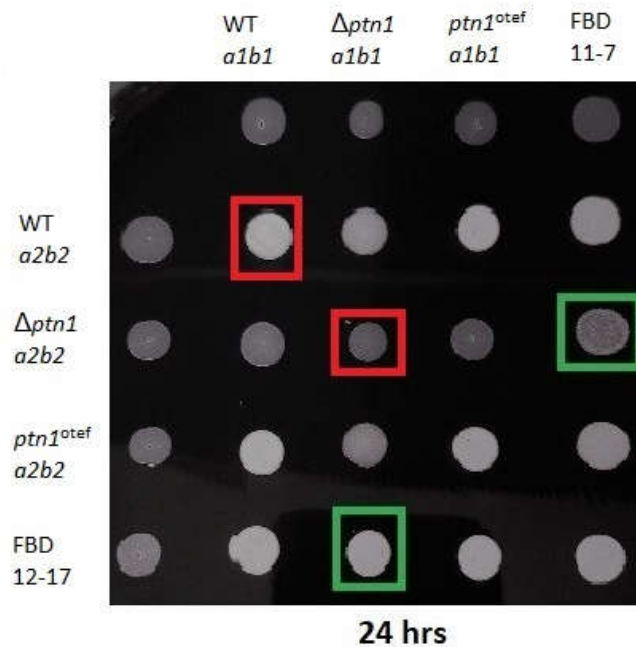
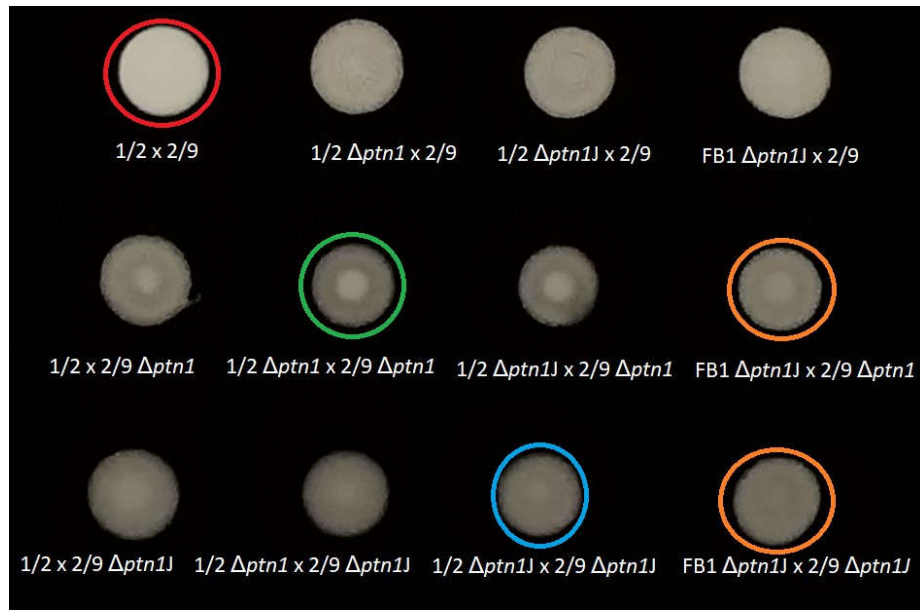


**Figure 2.2.** Mating assay and testing for pheromone production. Charcoal plate mating assay with wild type,  $\Delta ptn1$ ,  $\Delta ptn1c$ , and FBD - tester strains. A positive mating reaction is indicated by a white “fuzz” phenotype of aerial hyphae production. The reduction in filamentation was noticeable at 24 h, while such differences disappeared by 48 h (not shown). Red boxes compare the ‘fuzz’ produced between wild type mating and  $\Delta ptn1$

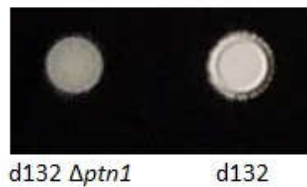


mating. Green boxes indicate the ‘fuzz’ produced when  $\Delta ptn1$  strains were mixed with tester strains.

As an additional level of confirmation for the observed defects in ‘fuzz’ phenotype, the mating assay was performed using deletion strains in an additional genetic background (FB1). When mating of the wild type ( $1/2 \times 2/9$ ) was compared with that of  $ptn1$  deletion strains ( $1/2 \Delta ptn1 \times 2/9 \Delta ptn1$ ,  $1/2 \Delta ptn1J \times 2/9 \Delta ptn1J$ , FB1  $\Delta ptn1J \times 2/9 \Delta ptn1J$ ), similar results were obtained as in Figure 2.2, *i.e.*, there was reduction in mating at 24 h for deletion strains, irrespective of the construct or background (Figure 2.3 A).



A



B

**Figure 2.3.** (A) Mating compared between deletion strains using two different constructs and different genetic backgrounds. Compared to wild type mating ( $1/2 \times 2/9$ ) denoted by the red circles, mating of deletion strains ( $1/2 \Delta ptn1 \times 2/9 \Delta ptn1$ , green circle, as well as  $1/2 \Delta ptn1J \times 2/9 \Delta ptn1J$ , blue circle) showed reduction in mating at 24 hrs. This result

matched the observation made when a haploid deletion strain  $\Delta ptn1J$  in the FB1 background was mated with a haploid  $\Delta ptn1$  or  $\Delta ptn1J$  strain in the 2/9 background (indicated by orange circles). (B) Formation of aerial hyphae for wild type  $ptn1ptn1$  or mutant  $ptn1\Delta ptn1$  diploid d132 background at 24 h.

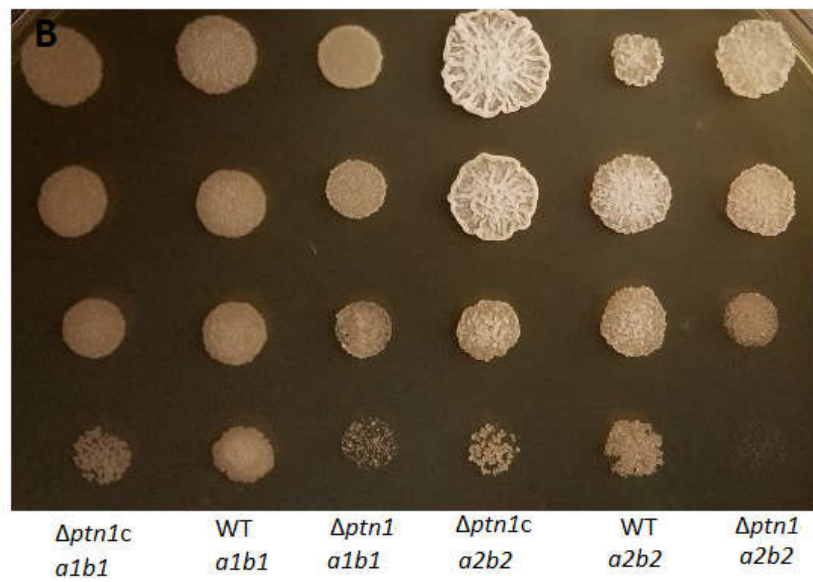
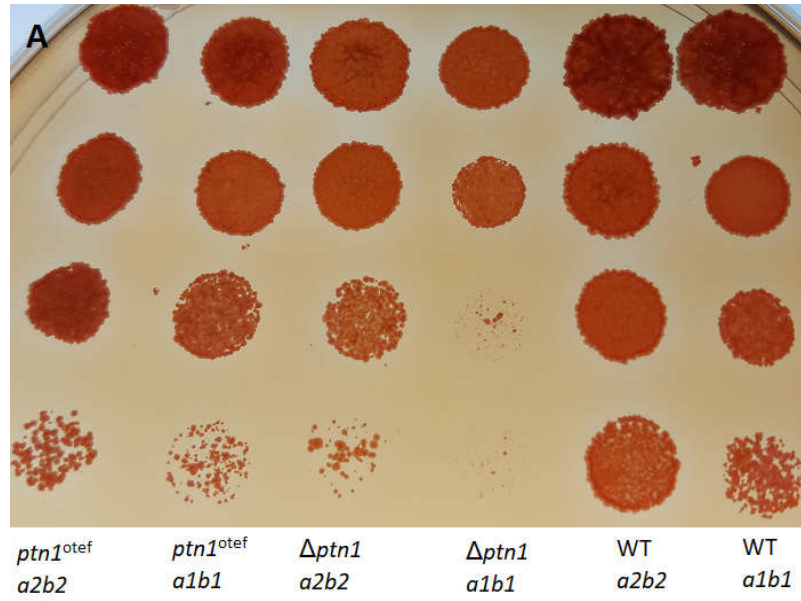
Formation of aerial hyphae on charcoal was also examined for  $ptn1$  deletion mutants in the diploid background (d132  $\Delta ptn1$ ) and in the solopathogenic SG200 background (SG200  $\Delta ptn1$ ). The deletion strain in the SG200 background did not show any change in the ‘fuzz’ intensity (Figure 2.15). However, the d132 $\Delta ptn1$  strain showed reduced formation of aerial hyphae (Figure 2.3 B), compared to wild type. This result indicates that  $ptn1$  gene does show some level of haplo-insufficiency in the d132 diploid background, as has been observed for other genes in this species (Pham et al., 2012). In contrast, the loss of  $ptn1$  appears to be at least partially compensated by the presence of the wild type allele in dikaryons as demonstrated by 2/9 x 1/2  $\Delta ptn1$ .

***prf1* is upregulated in  $\Delta ptn1$  under low ammonium conditions.** The lower than expected formation of aerial hyphae during the mating of the 2/9  $\Delta ptn1 a2b2$  with the tester strain, FBD 11-7 strain led us to speculate whether there was an alteration in the expression of mating genes affecting pheromone production. The fusion of haploid cells during mating leads to the differentiation of *U. maydis* into the subsequent filamentous dikaryon (Muller et al., 1999). Also, environmental conditions such as acidic pH, lipids and low ammonium conditions can trigger the filamentous response in *U. maydis* (Klose, de Sa, & Kronstad, 2004; Ruiz-Herrera, Leon, Guevara-Olvera, & Carabez-Trejo, 1995; Smith et al., 2003), while acetate inhibits filamentation due to mating or to exposure to oleic acid (Kretschmer, Lambie, Croll, & Kronstad, 2018). Hence, a qRT-PCR analysis was conducted of several genes involved in the mating pathway, e.g., *mfa2*, encoding a2 pheromone precursor, *pra2*,

encoding pheromone receptor, and *prf1*, encoding a transcription factor (Kaffarnik et al., 2003). The analysis involved comparing the expression levels between wild type 2/9 and 2/9  $\Delta$ *ptn1* under high and low ammonium conditions. The expression of all the strains were compared to the wild type 2/9 strain in high ammonium (Figure 2.16). The data indicated that the *prf1* levels decreased between high and low ammonium conditions in wild type, whereas it significantly increased in the  $\Delta$ *ptn1* mutant from high to low ammonium. There was a significant difference between the relative expression of *prf1* between wild type under low ammonium and  $\Delta$ *ptn1* mutants under low ammonium. Even though there was no significant difference in the expression of *mfa2* and *pra2* under similar conditions, the trend showed that while the *mfa2* and *pra2* genes tended to be less expressed under low ammonium conditions in wild type, for the  $\Delta$ *ptn1* mutant their expression appeared to be in the opposite direction.

**Cell growth of *ptn1* mutants is largely unaffected, while stress tolerance is reduced under certain conditions.** In standard growth media such as yeast extract-peptone-sucrose (YEPS) or potato dextrose broth (PDB), *ptn1* mutants were able to grow and showed no significant differences from wild type cells in terms of growth rate (Figure 2.17). The effects of stressors, including high osmotic medium, *i.e.*, YEPS supplemented with 1 M sorbitol or 1M NaCl was tested but not found to affect growth (data not shown). However, *ptn1* mutants showed a difference from wild type strains on YEPS media supplemented with Congo red (CR) or calcofluor white (CFW). Both *ptn1* deletion and overexpression strains showed a reduced tolerance when compared to the respective wild type strains (Figure 2.4 A) while the complemented strains were able to partially recover the wild type

growth (Figure 2.4 B) in CR media as well as on CFW media (Figure 2.4 C). Overall, these experiments suggested that the mutation of *ptn1* has an impact on the integrity of cell wall.



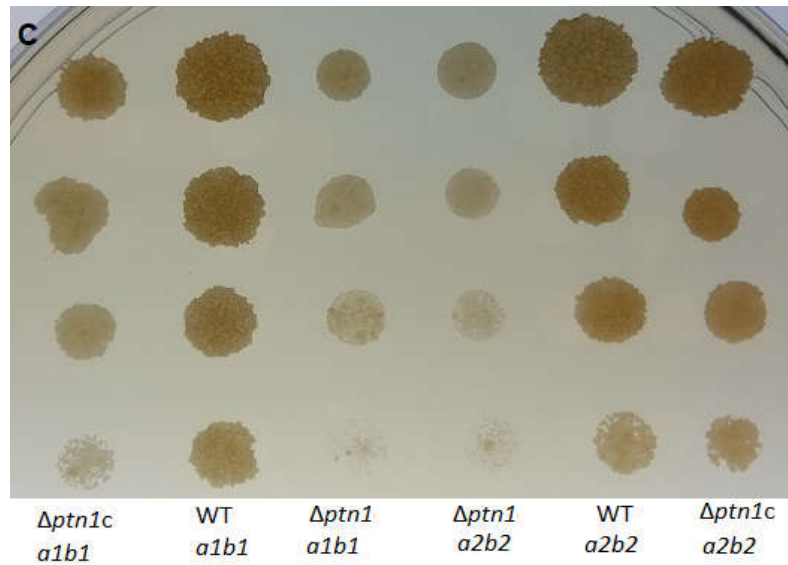


**Figure 2.4.** Response of mutants to cell wall stress. (A) 10-fold serial dilutions of the 1/2 *a1b1*, 2/9 *a2b2*,  $\Delta ptn1$  *a1b1*,  $\Delta ptn1$  *a2b2*, *ptn1*<sup>otef</sup> *a1b1*, and *ptn1*<sup>otef</sup> *a2b2* strains were spotted onto media containing 1 mM Congo red and observations were made at 48 hours. Congo red is a cell wall stressor which prevents glycan microfibril assembly by binding to  $\beta$ -glucans. The 1/2 *a1b1* strains were compared with *a1b1* mutant strains while *a2b2* background strains were compared amongst themselves. Growth defects were observed in  $\Delta ptn1$  strains as well as *ptn1*<sup>otef</sup> as reduction in colony numbers at higher dilutions compared to comparable wild type, for both *a1b1* and *a2b2* backgrounds. The overexpression of *ptn1* ectopically in deletion mutants was able to partially rescue the growth defect in (B) Congo red media and (C) calcofluor white media.

**Pathogenicity is reduced by *ptn1* deletion.** Compatible opposite mating type strains were mixed and injected into maize seedlings to assess the effect of deletion of *ptn1* on *U. maydis* virulence. The results at 14 dpi are presented in the graph as a percentage of symptom formation in infected plants. Statistical analysis was performed on the disease index score (mean +/- standard deviation) with a Kruskal-Wallis test and a multiple-comparison test. The results (Figure 2.5) indicate that deletion of *ptn1* results in reduced virulence compared to the wild type, and this reduction was statistically significant compared to the other infections. There were significantly more healthy plants surviving at the end of the study among the plants infected with *ptn1* deletion mutants. On the other hand, overexpression of *ptn1* did not yield significant change in the virulence. For

infections where both partners carried the *ptn1* deletion, the ability of the fungus to form tumors was severely reduced. While in infections with both wild type partners approximately 82% of infected plants had tumors, only roughly 30% of infections had tumors where both mating partners carried the  $\Delta ptn1$  lesion. The complemented  $\Delta ptn1c$  mating partners were partially able to rescue this defect. More plants (~90%) showed signs of infection in  $\Delta ptn1c$  infected group when compared to  $\Delta ptn1$  infected plants (~68%).

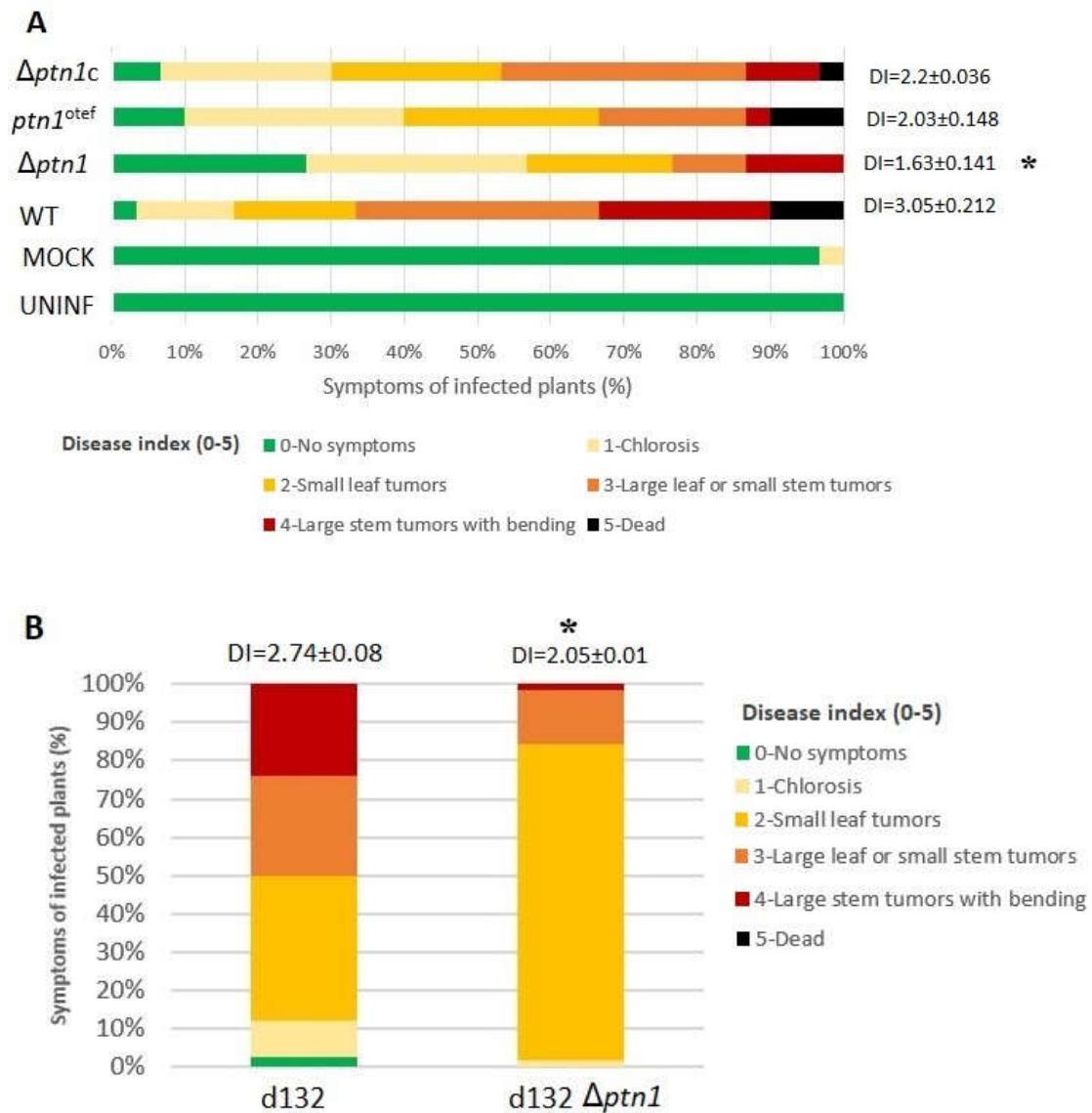


**Figure 2.5.** Plant infection. (A) One-week old maize seedlings were infected with indicated strains of *U. maydis*. Disease symptoms were scored 14 days post infection (dpi) and

compared to those where both partners were wild type (WT) strains (1/2 *a1b1* x 2/9 *a2b2*). Plants were inoculated with one paired background, indicated on the Y-axis. Disease symptom categories are depicted at the bottom. Numbers to the right of each bar represent mean (+/- standard deviation) for disease indices (DI). The graphs display the percentage of plants with specific symptoms of infection. The  $\Delta ptn1$  (*a1b1* x *a2b2*) and *ptn1*<sup>otef</sup> (*a1b1* x *a2b2*) infections, here both partners contained the indicated mutations/modifications, displayed reduced pathogenicity. The reduction in  $\Delta ptn1$  strains was statistically significant ( $P < 0.05$ ) compared to the wild type used in this study. B) Experiment conducted using diploid strains d132 WT and d132  $\Delta ptn1$  showed that deletion of one copy of *ptn1* reduces pathogenicity. Numbers above each bar represent mean (+/- standard deviation) for disease indices (DI). The data were analyzed using Kruskal-Wallis test followed by post-hoc comparison and an asterisk (\*) indicates significant difference ( $P < 0.05$ ).

In a separate experiment, deletion strain d132  $\Delta ptn1$  also showed reduced severity of infection compared to its wild type progenitor, indicating that one functional copy of *ptn1* was insufficient for full pathogenicity (Figure 2.5 B). The phenotypic trend of reduced pathogenicity was confirmed using deletion mutant in SG200 background though the difference ( $P=0.05048$ ) was only marginally significant (Figure 2.18). In addition to the above-mentioned infections using d132 background strains, *ptn1* deletion strain in the *a1b1* background mixed with WT strain in *a2b2* background was examined for the effect of virulence when one wild type copy of the gene was present, *i.e.*, 1/2 *a1b1*  $\Delta ptn1$  strain was crossed with 2/9 *a2b2* strain and vice versa. This was compared with wild type (1/2 x 2/9) infection and deletion mutant infection (1/2  $\Delta ptn1$  x 2/9  $\Delta ptn1$ ). The results are shown in Figure 2.6 and they indicate that presence of one wild type copy can rescue the phenotype to some extent.

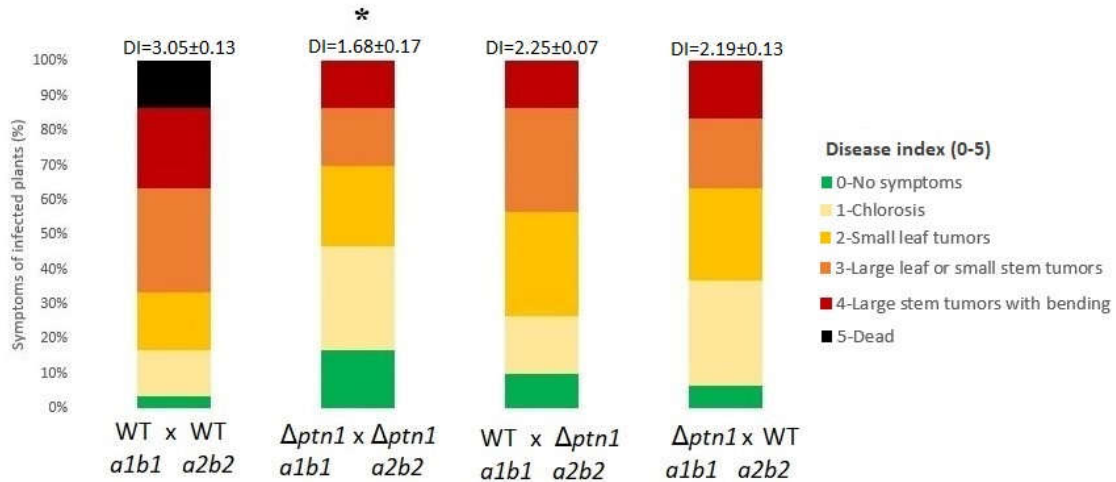
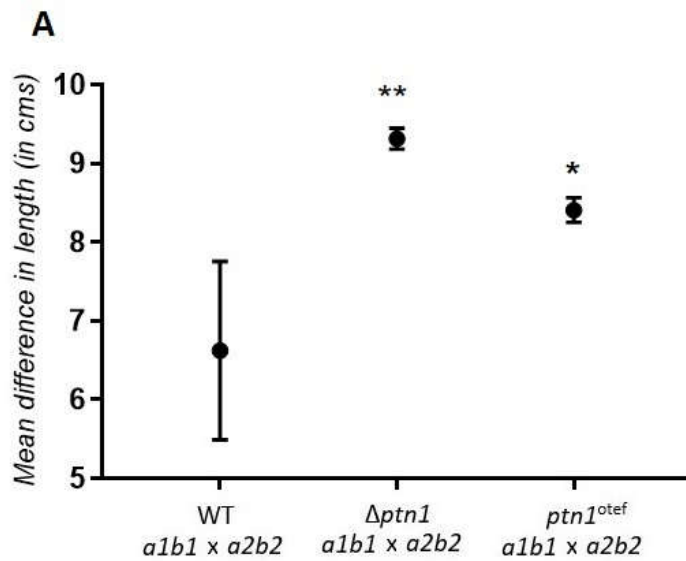


**Figure 2.6.** Are functional copies of the *ptn1* gene in both partners required for pathogenicity? The  $\Delta ptn1$  strains were mated with the wild type strain of opposite mating-type and compared with infections due to either both wild type or both mutant pairings. The graphs display the percentage of plants with specific symptoms of infection. The combinations  $1/2 \Delta ptn1 a1b1 \times 2/9 a2b2$  and  $1/2 a1b1 \times 2/9 \Delta ptn1 a2b2$  were more virulent when compared to  $\Delta ptn1 (a1b1 \times a2b2)$  but less when compared to the  $1/2 \times 2/9$ . Numbers above each bar represent mean ( $\pm$  standard deviation) for disease indices (DI). The data were analyzed using Kruskal-Wallis test followed by post-hoc comparison and an asterisk (\*) indicates significant difference ( $P < 0.05$ ).

**Pathogenicity calculated by additional plant growth indicators.** The effect of deletion of *ptn1* on the virulence of the fungus was measured by a range of plant growth indicators. This provided a more comprehensive view of the extent of the effect on pathogenicity. In this experiment plants infected with wild type cross ( $1/2 \times 2/9$ ) strains were compared with those infected with deletion cross and overexpression cross strains. A total of 28 plants were used per treatment group and the experiment was repeated a total of three times. The total number of leaves and the length of the plants were measured on the day of infection, as well as on 4 dpi (days post infection) and 8 dpi. Measurements were not taken after 8 dpi as many plants were drooping and unable to stand erect due to infection, thereby posing difficulty in making accurate length measurements. Both the  $\Delta ptn1$  and *ptn1* overexpression infections yielded significantly taller plants (*i.e.*, reduced infection)



compared to wild type (Figure 2.7 A). The average number of leaves produced was significantly lower in plants infected with wild type partners compared to plants infected with overexpression strains or deletion strains, with the latter showing the highest average number of leaves (Figure 2.7 B). The dry biomass index of the plants infected with wild type strains was significantly lower when compared to  $\Delta ptn1$  infections. The  $ptn1^{otef}$  infected plants had a lower biomass index than  $\Delta ptn1$  infected plants but higher than for wild type infections. However, the differences in biomass, plant length or leaf number of the plants infected with overexpression strain were closer to wild type infection which indirectly indicates that only the deletion of  $ptn1$  results in significant alteration in virulence of the fungus.



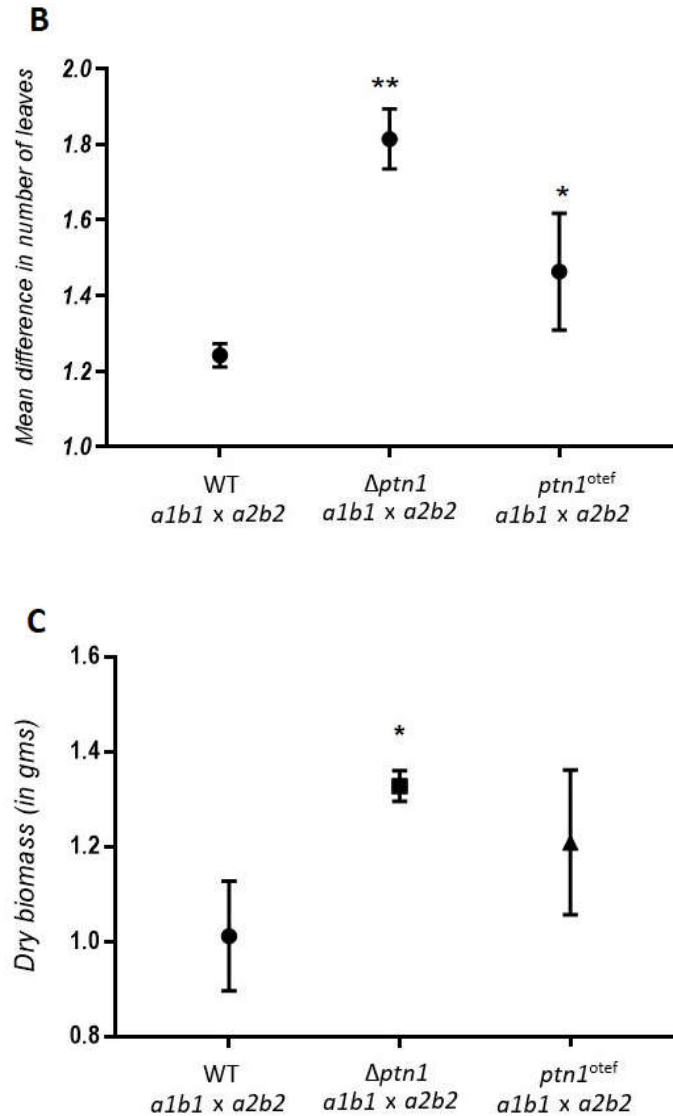


**Figure 2.7.** Plant growth parameters. Effect on (A) plant length, (B) leaf count and (C) plant dry weight. The plants were infected with 1/2 *a1b1* x 2/9 *a2b2*,  $\Delta$ *ptn1* (*a1b1* x *a2b2*) and *ptn1*<sup>otef</sup> (*a1b1* x *a2b2*) and the length and the number of leaves produced were measured on dpi-0 (0 days post infection), dpi-4 and dpi-8. The  $\Delta$ *ptn1* strains showed a significant reduction in their effect on plant length and leaf production when compared to WT. Means (+/- standard deviation) of plant lengths and number of leaves of  $\Delta$ *ptn1* marked by an asterisk (\*\*) were significantly different ( $P \leq 0.01$ ) from those of WT; the mean length and number of leaves of *ptn1*<sup>otef</sup> was significantly different ( $P \leq 0.05$ ) from WT and  $\Delta$ *ptn1*, respectively. The dry biomass of the plants infected with WT (*a1b1* x *a2b2*),  $\Delta$ *ptn1* (*a1b1* x *a2b2*) and *ptn1*<sup>otef</sup> (*a1b1* x *a2b2*) were measured. The  $\Delta$ *ptn1* strains showed an increase in plant biomass (+/- standard deviation) when compared to WT, indicating a reduction in virulence. Mean of dry mass of plants infected by  $\Delta$ *ptn1* was significantly different ( $P \leq 0.05$ ) from those of wild type infections. Statistical analysis was done by ANOVA followed by Tukey's test.

During infection there was normally a color change in the leaves of infected plants due to chlorosis. The wild type infected plant leaves had more yellow coloration/chlorosis compared to  $\Delta ptn1$  infected plants. Several papers have shown in wild type *U. maydis* infections an increase in chlorosis and decrease in chlorophyll content of infected leaves (Doehlemann et al., 2008; Horst, Engelsdorf, Sonnewald, & Voll, 2008). Thus, chlorophyll estimation was performed to examine whether there was a corresponding change in the level of photosynthetic pigments such as chlorophyll a and chlorophyll b between the different treatment groups. The concentrations of both chlorophyll a and chlorophyll b pigments were significantly reduced in wild type infected plants when compared to comparable infections using the deletion strain partners (Figure 2.8). The chlorophyll a and chlorophyll b data were used to calculate chlorophyll a/b ratio which is indicative of the level of stress in plants (Funayama-Noguchi & Terashima, 2006; Pavlovic et al., 2014). The chlorophyll a/b ratio for plants from the  $\Delta ptn1$  infection was significantly higher compared to that for wild type.

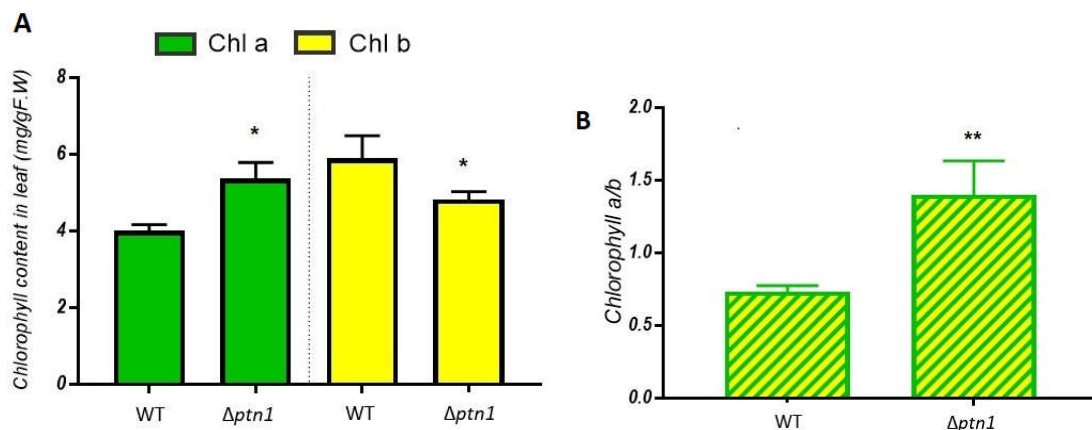


**Figure 2.8.** Chlorophyll estimation. (A) Chlorophyll count of leaves of plants infected with WT (1/2 *a1b1* x 2/9 *a2b2*) and  $\Delta ptn1$  (*a1b1* x *a2b2*) were measured using the DMSO method (Manolopoulou et al., 2016). (B) The plants infected with  $\Delta ptn1$  strains had higher a/b ratio and such plants had chlorophyll levels more comparable to “Mock” infections. Means of chlorophyll a, chlorophyll b, and chlorophyll a/b ratio marked with an asterisk

(\*) or two asterisks (\*\*) were significantly different ( $P \leq 0.05$ ) and ( $P \leq 0.01$ ), respectively, by Tukey's test.

**Impact of *ptn1* mutations on spore formation and germination.** The plants infected with *ptn1* deletion strains showed visibly reduced production in tumors in terms of size and number (Figure 2.20). Tumors were collected from all three treatment groups, 1/2 x 2/9,  $\Delta pt n1 \times \Delta pt n1$  and  $pt n1^{ote f} \times pt n1^{ote f}$  and weighed. The experiment was repeated three times. These data indicated that the WT (1/2 x 2/9) fungus produced far more tumors in plants when compared to the deletion strain or the overexpression strain. In the case of deletion strain, tumors produced were significantly fewer than for the WT or overexpression strain infections ( $P = 0.011$ , Tukey's test). Microscopic analyses of tumors from plants infected with compatible wild type strains or compatible  $\Delta pt n1$  strains, showed that the number of mature spores were relatively low in deletion strains (Figure 2.21). The teliospores from wild type infections overall were spherical and darkly pigmented, the number of mature teliospores increased in quantity with age/size of tumor, becoming clearly visible without magnification. However, while the  $\Delta pt n1 \times \Delta pt n1$  infected plants produced some tumors, the quantity of darkly pigmented teliospores was less (Figure 2.9) and in most cases were not obviously visible. It was difficult to quantify the presence of immature spores due to the inconsistency in the stages of infection between tumors and even within different parts of the same tumor. However, observations made from multiple independent infections indicated that the number of spores matched the intensity of infection. Crosses between  $\Delta pt n1$  derivatives constitutively expressing an ectopic copy of *ptn1* saw an improvement in tumor number and size, as well as spore number, but did not show a complete return to the wild type levels for these traits. Rather, the spore count from

$\Delta ptn1c$  was closer to that of  $ptn1^{otef}$  than  $\Delta ptn1$ , but it was still less compared to wild type (Figure 2.9).

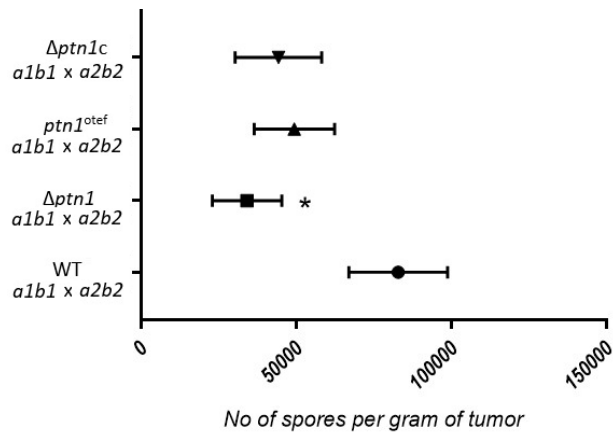


**Figure 2.9.** Spore count. Tumors were collected from plants infected with 1/2  $a1b1 \times 2/9 a2b2$ ,  $\Delta ptn1$  ( $a1b1 \times a2b2$ ),  $ptn1^{otef}$  ( $a1b1 \times a2b2$ ) and  $\Delta ptn1c$  ( $a1b1 \times a2b2$ ). From each type of infection (e.g., 1/2  $a1b1 \times 2/9 a2b2$ ) tumors were pooled and used to extract spores. The spore count was obtained using a hemocytometer for each pooled extraction. Presented here are the mean spore count (+/- standard deviation) for three biological replicates of each infection experiment. There was a significant reduction in spore production in infections by the  $\Delta ptn1$  strains ( $P < 0.05$ , by Tukey's Test).

The teliospores were extracted from tumors and allowed to germinate using previously published methods (Boyce, Chang, D'Souza, & Kronstad, 2005). Tumors from maize plants inoculated with wild type cross (1/2 x 2/9), deletion strain cross ( $\Delta ptn1 \times \Delta ptn1$ ), and the cross of overexpression strains ( $ptn1^{otef} \times ptn1^{otef}$ ) were used for germination studies. Since spore production was reduced in infections with the deletion strain cross, we examined whether there were also defects in spores from such infections. The  $\Delta ptn1$  strains showed a significantly lower rate of germination when compared to that for wild type infections ( $P < 0.05$ , Tukey's test); the complemented  $\Delta ptn1$  derivatives could only partially overcome the defect in spore germination rates (Figure 2.10). The formation of germination tubes from the spores (Figure 2.11) was examined to see if such defects could explain the reduced germination rates observed. Spores collected from tumors of plants

infected with 1/2 *a1b1* x 2/9 *a2b2* and  $\Delta$ *ptn1 a1b1* x  $\Delta$ *ptn1 a2b2* strains were plated onto 2% water agar plates. The formation of germination tubes was observed microscopically after 24 to 48 hrs.

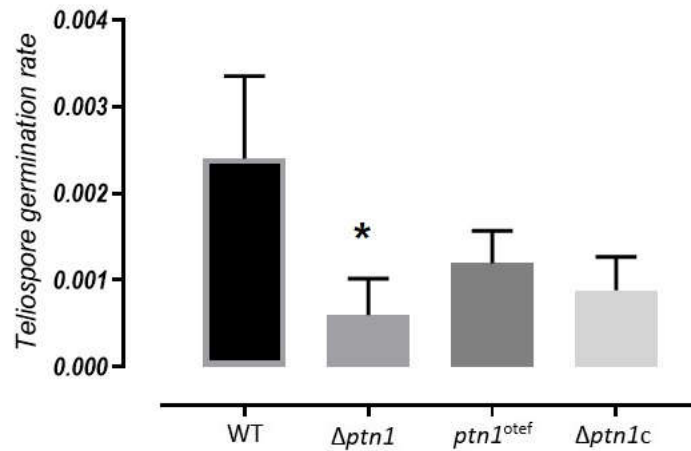


**Figure 2.10.** Spore germination assay. Spores were extracted from the plant tumors produced from the infection of 1/2 *a1b1* x 2/9 *a2b2*,  $\Delta$ *ptn1 a1b1* x  $\Delta$ *ptn1 a2b2*, *ptn1*<sup>otef</sup> *a1b1* x *ptn1*<sup>otef</sup> *a2b2* and  $\Delta$ *ptn1c a1b1* x  $\Delta$ *ptn1c a2b2* and plated onto water agar plates. The plates were incubated at 30 °C for 72 hours and observed for the presence of colonies formed from the germination of spores. The spore germination was reduced in  $\Delta$ *ptn1 a1b1* x  $\Delta$ *ptn1 a2b2* and *ptn1*<sup>otef</sup> *a1b1* x *ptn1*<sup>otef</sup> *a2b2* combinations, with few colonies being observed after germination. The difference in germination rate (percent germination per spores plated +/- standard deviation) for  $\Delta$ *ptn1* was statistically significant ( $P < 0.05$ ) by Tukey's Test; the differences for the overexpression strain were not statistically significant.

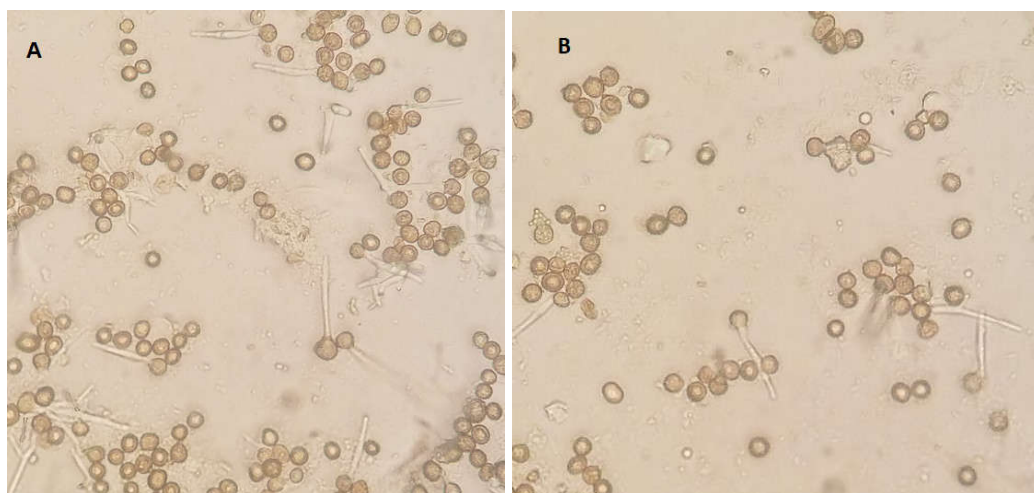


**Figure 2.11.** Spore germination tube formation. Microscopic analysis of spores collected from tumors of plants infected with (A) 1/2 *a1b1* x 2/9 *a2b2* and (B)  $\Delta$ *ptn1 a1b1* x  $\Delta$ *ptn1 a2b2* strains to examine possible defects in the formation of germination tube. Spore

germination on water agar plates incubated at 29 °C for 30 h was examined using differential interference contrast (DIC) microscopy.

In a pilot experiment to examine additional possible defects of the *ptn1* deletion crosses, plant infections were performed on maize ears of a dwarf variety of maize (n= 2) (Figure 2.22). In this way we investigated whether the deletion of *ptn1* affected teliospore production when inoculated into the developing embryos (ears) of plants with mixtures of compatible wild type or mutant strains. Only the wild type inoculation produced tumors, and these were filled with black teliospores (Figure 2.22 A); in contrast, the deletion strains did not show ear infection (Figure 2.22 B). As a control for differences in infection rates on different varieties of maize, the same dwarf variety was infected on the stems of plants; deletion strains failed to yield infection progression beyond chlorosis and over time infected plants appeared to be as healthy as uninfected plants. However, the wild type infection produced severe infections symptoms, with death of most infected plants (not shown).

## DISCUSSION

In this study the role of the *PTEN* orthologue of *U. maydis*, *ptn1*, in the pathogenic program of the fungus and in teliospore formation was examined. The predicted Ptn1 protein of *U. maydis* has a conserved protein tyrosine phosphatase catalytic motif (PTPc) in its N-terminal region, a motif present in PTEN proteins of most other organisms (Figure 2.12, Table 2.3). This is consistent with the finding that the PTEN orthologue of *Arabidopsis thaliana*, AtPTEN1, shares the similarity to higher eukaryotes only in the N-terminal region where the catalytic domain is present (Gupta et al., 2002). However, lack of conservation outside of the catalytic PTPc motif suggests that *ptn1* may respond mostly

to signals that are unique to *U. maydis*. In our study, a mutation in *ptn1* may led to a decrease in tolerance to stress conditions, especially in media supplemented with cell wall stress agents such as Congo red and calcofluor white. Dual specificity protein tyrosine phosphatases such as Ptp2 and Ptp3 in *S. cerevisiae* play a regulatory role in cell integrity pathways (Mattison, Spencer, Kresge, Lee, & Ota, 1999). It has also been reported in mouse model studies that *PTEN* is involved in stress response pathways connected to oxidative stress (Bankoglu et al., 2016).

In *U. maydis*, successful mating is indispensable for formation of the dikaryon, which is the infectious form of the fungus (Banuett & Herskowitz, 1996). Mating assays on charcoal plates and subsequent aerial hyphae indicative of infectious filament formation were used to measure this prerequisite for successful infection. The *ptn1* deletion strains had reduced fuzz formation during the initial 24 h. Since the difference was unnoticeable after 48 h, this indicates that the deletion caused delay in the onset of mating, and thus, only a minor defect in the mating capability. The RNA expression pattern of *mfa2* and *pra2* under low ammonium conditions also could not explain the reduced aerial hyphal production in matings involving 2/9  $\Delta$ *ptn1*. On the other hand, we did observe altered expression of *prf1* in the  $\Delta$ *ptn1 a2b2* mutant. Since Prf1 is a transcription factor, its dysregulation could alter expression of unidentified downstream targets, leading to translational or post-translation effects on mating specific targets. Overexpression of *ras1*(um02832) results in elevated levels of *mfa* (pheromone precursor) in *U. maydis* (Muller, Katzenberger, Loubradou, & Kahmann, 2003). A bioinformatic analysis looking for potential binding partners of Ptn1 indicated um02832 is a potential binding partner (Figure 2.23). Thus, it is plausible that um02832 is a potential downstream target for Ptn1.



In humans, the dosage of *PTEN* is important for tumor suppression as is evident from the data that monoallelic mutations (*i.e.*, heterozygous) at the *PTEN* locus have been found in various cancer types, including prostate cancer, breast cancer, colon cancer, and lung cancer (Salmena, Carracedo, & Pandolfi, 2008). Our data from the mating and plant infection experiments using *ptn1* deletion strains in the d132 diploid background are in accord with this observation, *i.e.*, loss of one copy of the *ptn1* gene is only partially compensated by the presence of the wild type allele in dikaryons and diploids. Deletion strains of *biz1* gene in SG200 background could filament normally while showing reduced virulence in plant infection (I. Flor-Parra, Vranes, Kamper, & Perez-Martin, 2006). We observed a similar phenotype with SG200  $\Delta$ *ptn1*.

Infection of maize plants with compatible wild type strains (1/2 *alb1* x 2/9 *a2b2*) and mutant strains ( $\Delta$ *ptn1 alb1* x  $\Delta$ *ptn1 a2b2* or *ptn1*<sup>otef</sup> x *ptn1*<sup>otef</sup>) showed that the *ptn1* deletion mutants were less virulent than wild type strains. Though the  $\Delta$ *ptn1* mutants were able to infect maize plants, they showed reduced symptoms, especially in tumor number and size (Figure 2.20); *ptn1* overexpression did not significantly alter virulence. We were able to rescue the virulence partially by complementing the deletion strains with a wild type copy of the *ptn1* gene. Although deletion strains constitutively expressing *ptn1* ectopically were only partially rescued, the fact that independently-isolated *ptn1* deletion mutants, produced by different means and in different genetic backgrounds, had similar levels of defects in measures of pathogenicity (Figure 2.19), strongly supports the role of the *ptn1* gene in virulence for *U. maydis*. A study of the pathogenic fungus, *Thielaviopsis basicola*, causing black root rot disease of cotton plants, shows plant growth factors such as plant height, dry biomass, etc., are valid indicators of pathogen infection

(Ma, Jaraba, Kirkpatrick, & Rothrock, 2013). Similarly, biochemical indicators like chlorophyll content or chlorophyll (a/b) ratio can be used as indicators of level of fungal infection in plants, as shown with *Crinipellis pernicioso*, causing witches broom disease in cocoa plants (Scarpari et al., 2005) and *Colletotrichum lindemuthianum* infecting *Phaseolus vulgaris* (common bean) plants (Lobato et al., 2010). In oxeye daisy (*Leucanthemum vulgare*) plants infected with the fungus *Rhizoctonia solani*, an 81% reduction in shoot and a 70% reduction in root biomass were observed (Lewandowski, Dunfield, & Antunes, 2013). In our study, the reduction in pathogenicity was confirmed in measures of plant height, numbers of leaves, and levels of chlorophyll content. The plants infected with deletion strains were significantly healthier compared to the wild type infected plants.

The dissection and microscopic analysis of the tumors from plants infected with  $\Delta ptn1$  mutants showed that while tumors were produced, a large proportion of those tumors lacked black teliospores. Moreover, tumors from infections with the deletion strains had significantly fewer spores than tumors from wild type infections. The spore germination assay found a significantly lower rate of germination of spores from infections by the  $\Delta ptn1$  mutants. However, there was no obvious difference between the wild type and mutant strains in germination tube formation.

Effects of the *ptn1* deletion in vitro, especially in haploid or diploid sporidia, were subtle (Figures 2.1, 2.3). Slight reduction in aerial hyphae production on charcoal and increased sensitivity to cell wall stressors were seen for such mutants. A similar cell wall defect was reported for *ptn1* (*PTEN* orthologue) mutants in fission yeast, *Schizosaccharomyces pombe*. (Mitra et al., 2004). Our study indicates that while

appressoria formation and penetration (not shown) were not impaired for the *ptn1* mutants, pathogenic development was obstructed at stages after penetration.

It has been noted in the case of some signaling proteins that aberrant expression in either direction can end up in same phenotypes. For example, when tumor suppressor SRPK1 (serine/Arginine-Rich Splicing Factor Kinase) which mediates the recruitment of the phosphatase PHLPP1 to Akt was deleted or overexpressed, it resulted in the promotion of cancer (Wang et al., 2014). This is especially relevant when the same protein has multiple roles in interconnected signal transduction pathways. This may be a reasonable explanation for our observation that overexpression strains (*ptn1<sup>otef</sup>* x *ptn1<sup>otef</sup>*) also displayed a reduction in virulence and the haploid mutant cells were also more susceptible to cell wall stressors than wild type.

*U. maydis* infection of maize leads to the formation of galls or tumors that are filled with fungal hyphae that ultimately develop into teliospores (Banuett & Herskowitz, 1996). Several individual processes inside the tumor lead to the formation of teliospores. These include rounding and swelling of hyphal tips of fungal mycelia for which functional *rum1* and *hda1* are necessary (Quadbeck-Seeger et al., 2000; Reichmann et al., 2002). The subsequent hyphal fragmentation needs *fuz1* (Banuett & Herskowitz, 1996). Other studies have shown that several genes, including *cru1*, *hgl1*, *unh1*, *ust1*, and *ros1* influence the formation and maturation of teliospores and some of the phenotypes of mutants in these genes resemble those shown by *ptn1* mutants. For instance, *cru1* mutants produced tumors that were considerably smaller and contained very few teliospores (Ignacio Flor-Parra, Castillo-Lluva, & Pérez-Martín, 2007). On a similar note, *hgl1* mutants produced tumors but failed to produce teliospores (Durrenberger et al., 2001). The deletion of *unh1* showed

a defect in the formation, maturation and pigmentation of teliospores (Doyle et al., 2016). A recent study indicated that the transcription factor Ros1 is a master regulator of sporogenesis in *U. maydis*. Although *ros1* is not required for tumor formation, it is essential during late stages of infection for fungal karyogamy, proliferation of fungal hyphae and spore formation (Tollot et al., 2016). Data from most of these studies indicate that the process of tumor formation is separate from teliospore development, as is also evident in the case of *ptn1* mutants. This makes *ptn1* part of the growing number of genes that are vital to the complex process of teliospore formation and germination.

In *Arabidopsis thaliana*, *AtPTEN1* (*PTEN* orthologue) is expressed exclusively in pollen grains during the late stage of development; when expression of *AtPTEN1* was suppressed by RNA interference, it resulted in pollen cell death after mitosis (Gupta et al., 2002). This is interesting considering the observation that the *ptn1* gene in *U. maydis* is involved in sexual development of the fungus. Similarly, in *S. cerevisiae*, *TEP1* (*PTEN* orthologue) mutants showed a defect in the developmental process of sporulation. Moreover, *FgTep1p* (*PTEN* orthologue) deletion mutants in the wheat pathogen, *Fusarium graminearum*, produced fewer conidia and showed an attenuation in virulence on host plants (D. Zhang et al., 2010).

In conclusion, the results reported in this study illustrate that *ptn1* has a role in virulence, especially in tumor production and in the development of teliospores in *U. maydis*. A growing number of studies show that the process of teliospore formation and germination is intricate, requiring exquisite control of hyphal proliferation inside the plant, formation of teliospores, formation of a thick cell wall, and germination involving completion of meiosis to produce haploid cells. The cells must make appropriate

developmental decisions at each of these steps in response to the prevailing conditions. A defect in genes responsible for any of these steps can result in failure to produce mature and functional teliospores. Hence, further investigation into the proteins that interact with Ptn1 during spore formation will likely contribute to a deeper understanding of how the complex signaling networks regulate pathogenic development and teliospore development in *U. maydis*.

### Supplementary materials

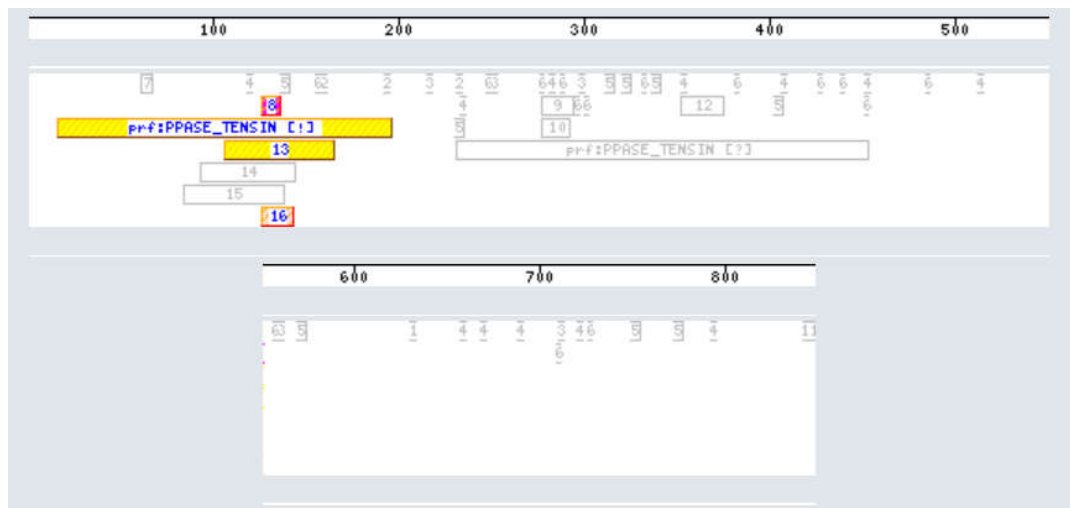


**Figure 2.12.** Motif scan analysis of Ptn1 using Hits (<https://myhits.isb-sib.ch/>) indicated the presence of Phosphatase tensin-type domain profile.

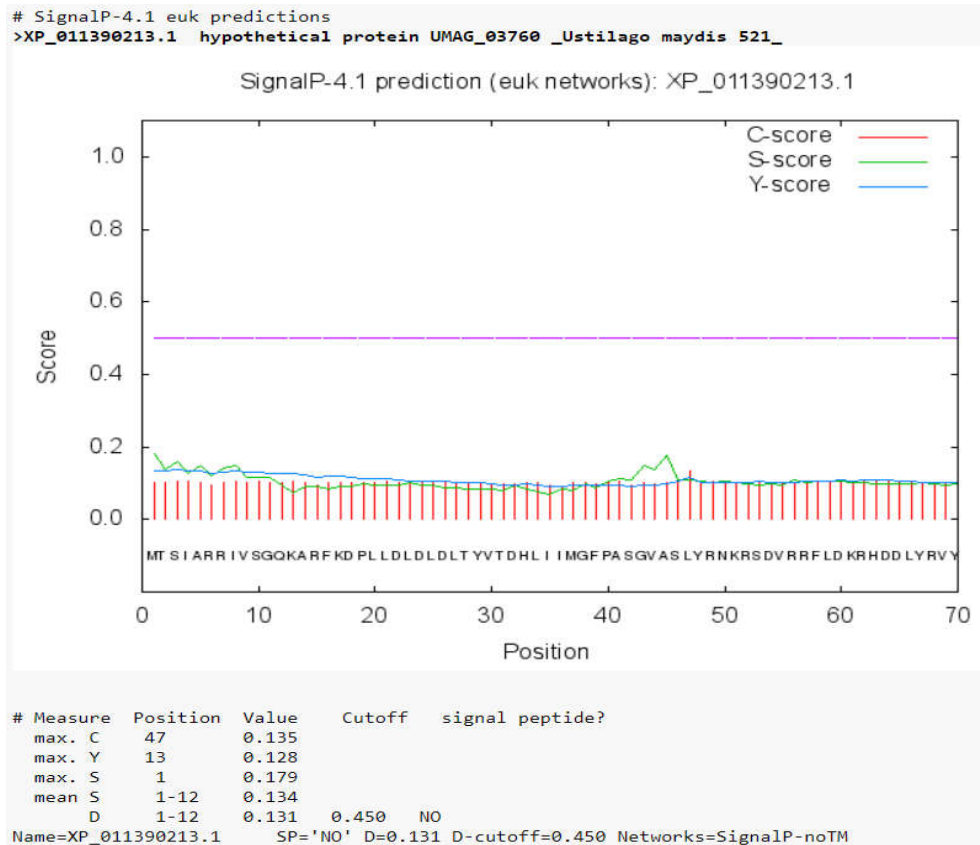


**Figure 2.13.** SignalP 4.1 prediction of the presence signal peptide. SignalP could not find a signal peptide in Ptn1.

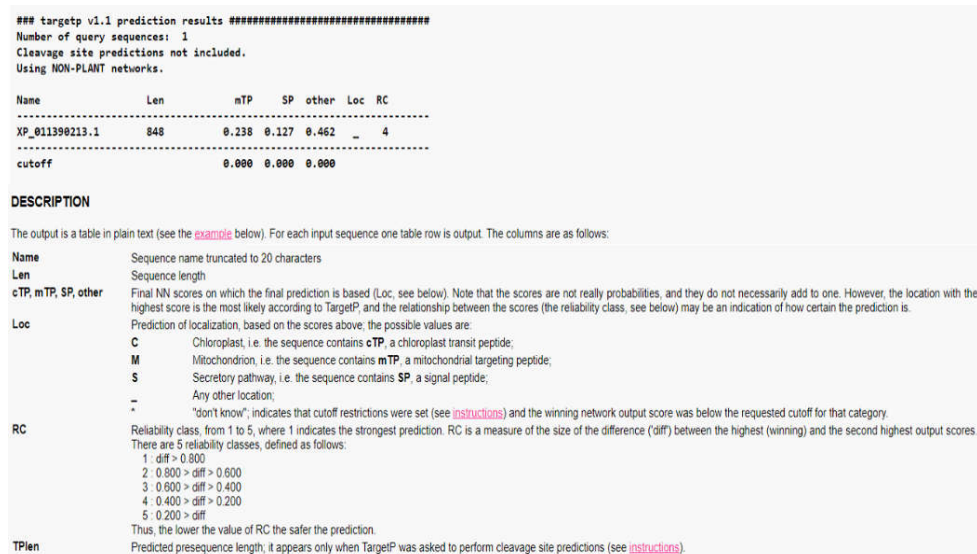


**Figure 2.14.** TargetP prediction of sub-cellular localization of Ptn1. TargetP analysis indicated that Ptn1 is not a secreted protein and may have a sub-cellular location other than mitochondria.



**Figure 2.15.** The charcoal assay for fuff production performed with SG200 and SG200  $\Delta ptn1$  strains. No differences were observed in the ability to produce aerial hyphae.

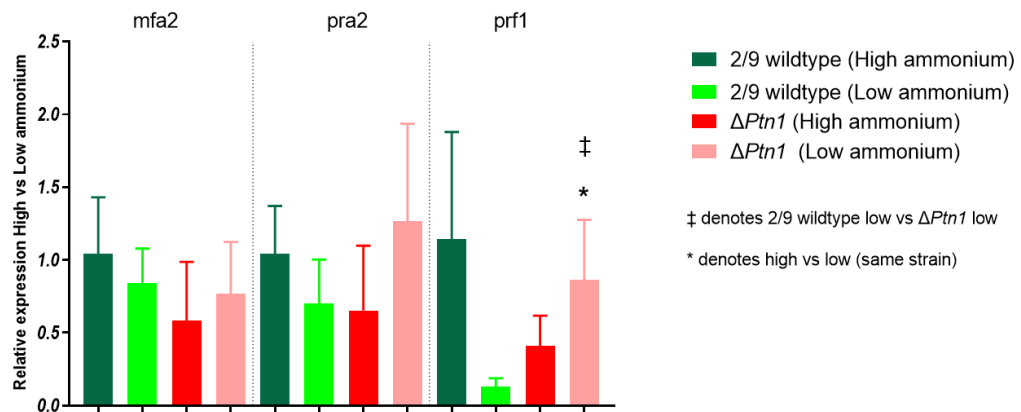


**Figure 2.16.** The relative expression analysis of *mfa2*, *pra2*, and *prf1* (*U. maydis* mating pathway genes) in wildtype and  $\Delta ptn1$  under high and low ammonium conditions. The expression of all the strains are compared to wildtype strain in high ammonium.

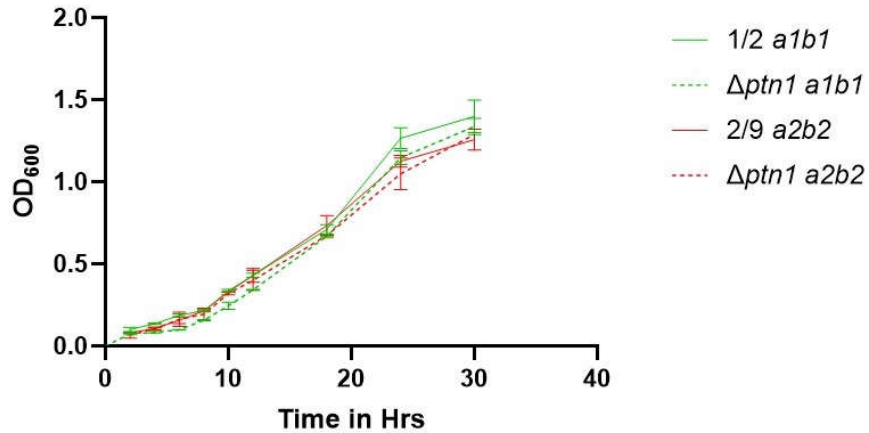


**Figure 2.17:** Growth assay of *ptn1*. Growth rates of 1/2, 2/9, 1/2  $\Delta ptn1$  and 2/9  $\Delta ptn1$  strains grown in YPS media were measured by OD<sub>600</sub> at an initial interval of 2 h until 12 hours and then every 6 hours until 30 hours. The data did not show any significant differences in growth rates.

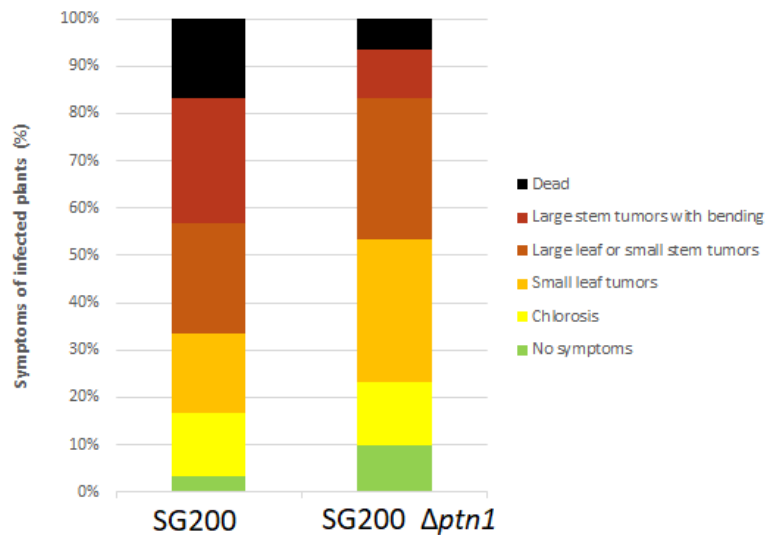


**Figure 2.18:** Infection of plants with  $\Delta ptn1$  deletion strains in SG200 background. The deletion strain SG200  $\Delta ptn1$  showed a reduction in pathogenicity compared to wildtype SG200 (nearly significant,  $P=0.05048$ , Kruskal-Wallis multiple comparison test)



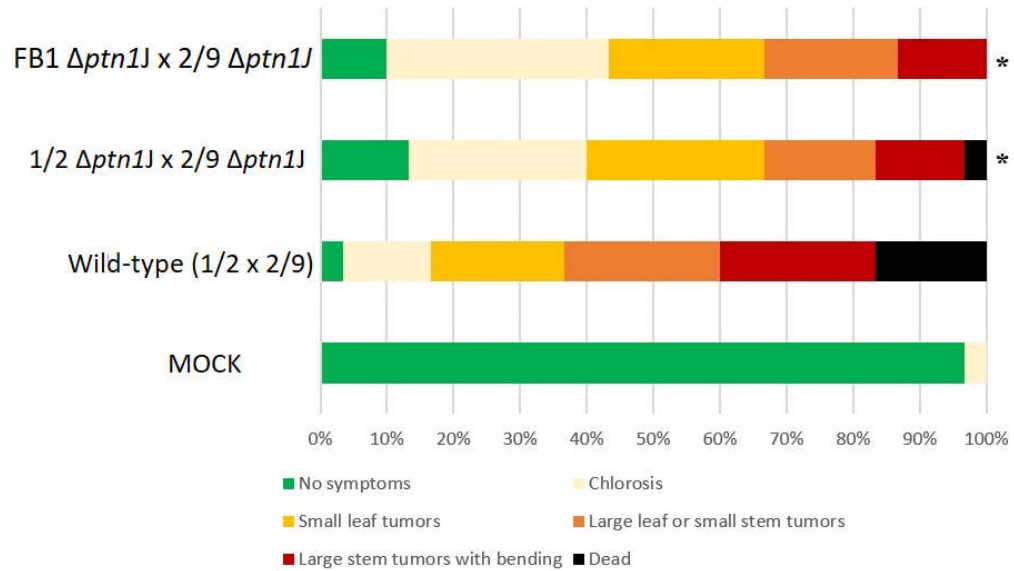


**Figure 2.19.** Infection of plants with  $\Delta pt n 1$  deletion strains in different backgrounds and created through two different methods. Similar reductions in pathogenicity were seen, regardless of the method used to generate the deletions or the genetic backgrounds of the compatible mating partners. 1/2  $\Delta pt n 1 J$  and 2/9  $\Delta pt n 1 J$  strains generated using the overlap- PCR method (Harrison et al., 2013; Kamper, 2004) were found to be less infectious compared to WT (1/2 and 2/9). Pathogenicity was similarly impaired for infections with strains FB1  $\Delta pt n 1 J$  x 2/9  $\Delta pt n 1 J$ ; FB1  $\Delta pt n 1$  was generated via the overlap method, while 2/9  $\Delta pt n 1$  as produced with the DelsGate method.

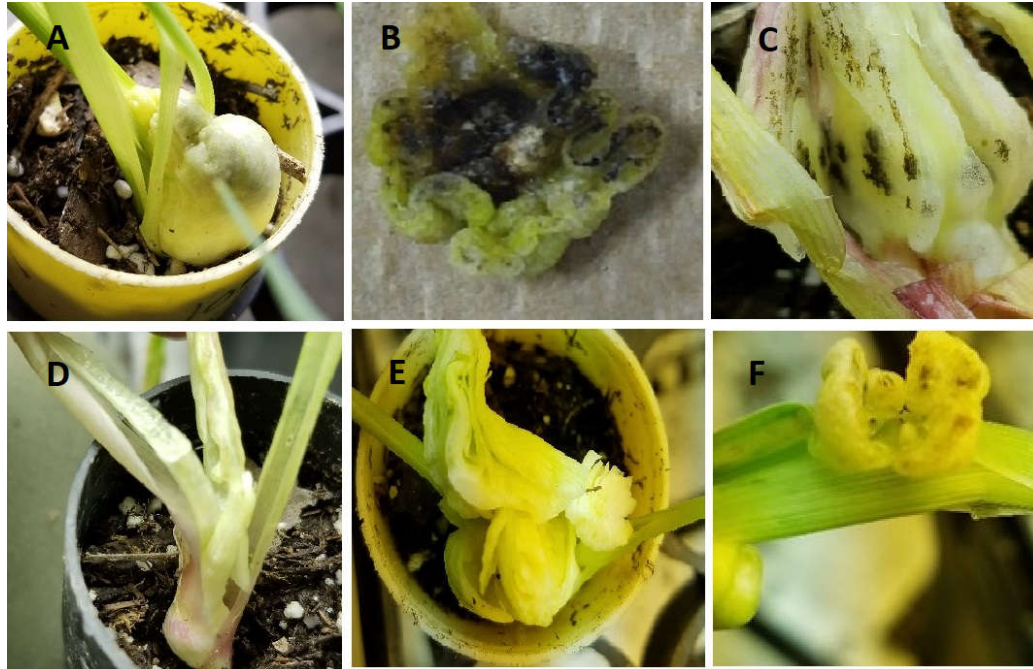


**Figure 2.20.** Teliospores from infected maize plants (Clockwise): A, B and C represent tumors from plants infected with both wild type partners 1/2 x 2/9 (*alb1* x *a2b2*). D, E, F represent tumors of plants from  $\Delta$ *ptn1* (*alb1* x *a2b2*) infection. WT (1/2 x 2/9) infected plants produced normal tumors which were filled with black teliospores, whereas mature black teliospores were not clearly visible in most of the tumors produced from  $\Delta$ *ptn1* infected plants.

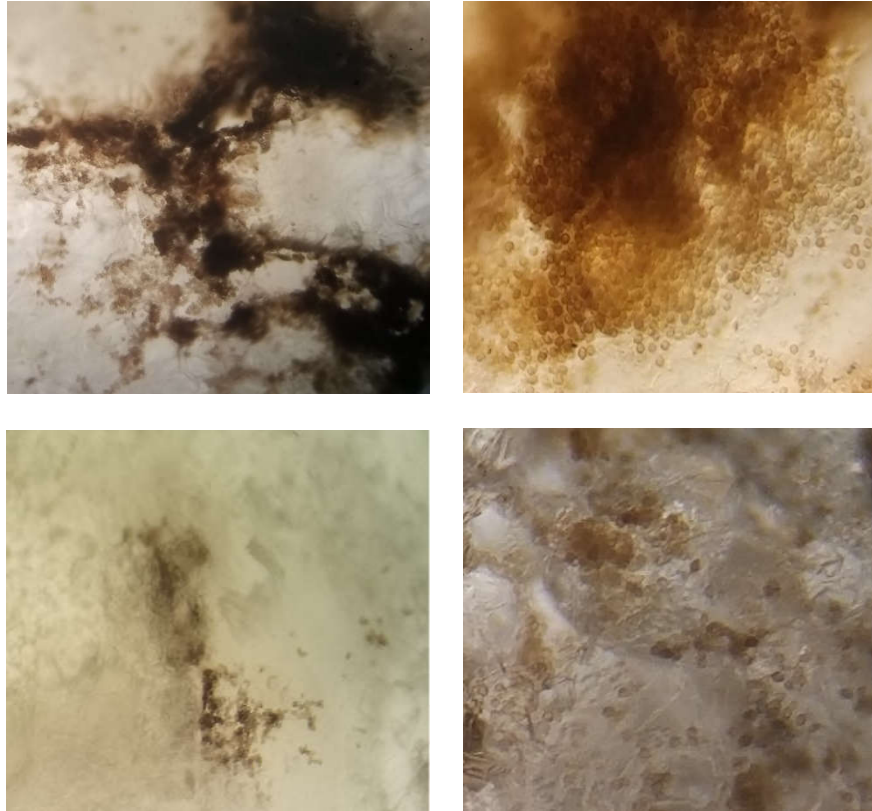


**Figure 2.21.** Dissection of tumors under microscope showing teliospores. Upper panels represent spores from WT 1/2 x WT 2/9 infected plants and lower panels show spores from  $\Delta pt n 1$  infected plants. WT tumors contained visibly more teliospores.

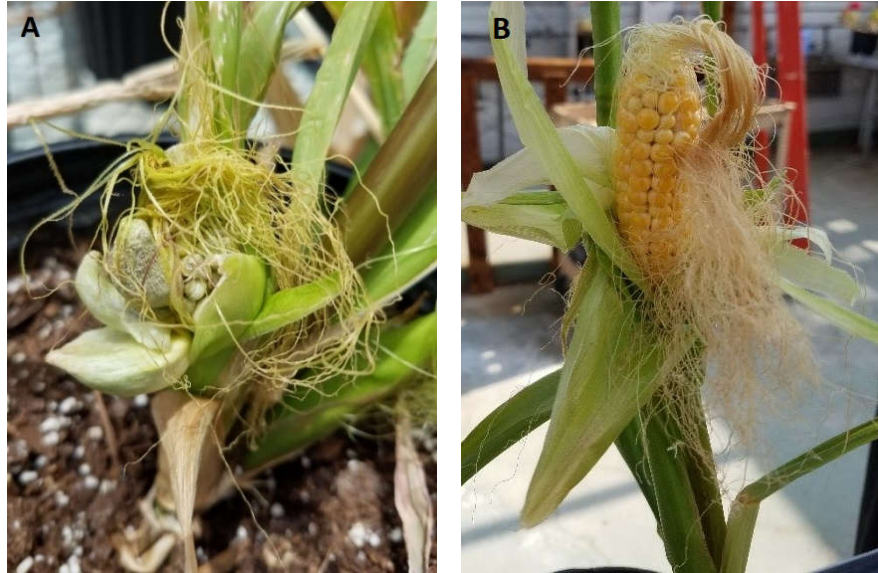


**Figure 2.22.** Deletion of *ptn1* alters ability to produce tumors in maize cobs. The deletion strains were not able to produce tumors with teliospores when infection was performed on maize ears (A) WT (1/2) × WT (2/9), (B)  $\Delta ptn1 \times \Delta ptn1$  in the same respective genetic backgrounds as in (A).

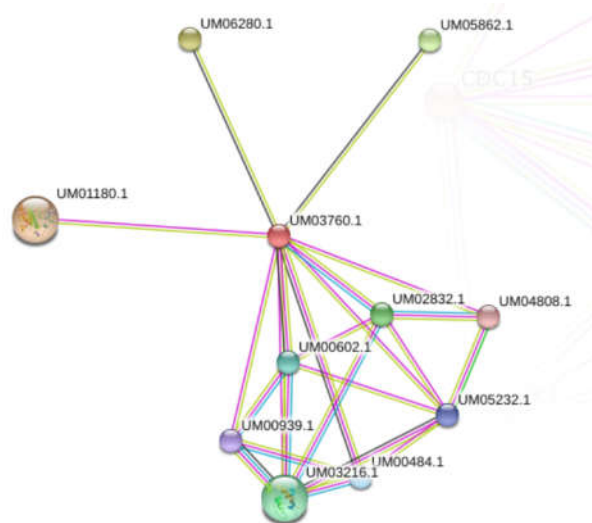


**Figure 2.23.** Interaction Network Analysis of Ptn1 protein sequence using STRING software (<https://string-db.org>) indicated one of the potential interactors as UM02832 (Ras1 protein) of *U. maydis*

Table 2.3 A. Aligned Proteins			
Protein Name	Identity	Expected Value	Matched Length
<a href="#">A0A0D1E0C2_USTMA</a>	1	0	848
<a href="#">R9NVM2_PSEHS</a>	0.76	e-163	850
<a href="#">I2FUC9_USTH4</a>	0.69	e-158	853
<a href="#">A0A1K0H8X3_9BASI</a>	0.69	e-156	853
<a href="#">E6ZMB4_SPORE</a>	0.68	e-144	852
<a href="#">W3VTN5_PSEA5</a>	0.67	e-162	860
<a href="#">M9LVY0_PSEA3</a>	0.67	e-162	860
<a href="#">A0A0F7S2A1_9BASI</a>	0.67	e-110	697
<a href="#">A0A081CHB7_PSEA2</a>	0.66	e-159	851
<a href="#">A0A127ZGP6_9BASI</a>	0.66	e-150	857
<a href="#">A0A077QWF3_9BASI</a>	0.65	e-159	859
<a href="#">V5EYU7_KALBG</a>	0.45	1.00E-96	844
<a href="#">TPTE2_MACFA</a>	0.38	1.00E-42	193
<a href="#">TPTE2_HUMAN</a>	0.38	7.00E-42	193
<a href="#">PTEN1_ARATH</a>	0.38	4.00E-36	189
<a href="#">A0A0D2PH34_9AGAR</a>	0.37	1.00E-31	311
<a href="#">TPTE_HUMAN</a>	0.37	2.00E-40	193
<a href="#">PTN2B_ARATH</a>	0.36	1.00E-38	204
<a href="#">A0A0C9WXR8_9AGAR</a>	0.35	1.00E-33	340
<a href="#">A0A066VX13_9BASI</a>	0.34	9.00E-90	877
<a href="#">CNRN_DICDI</a>	0.32	1.00E-37	237
<a href="#">PTEN_MOUSE</a>	0.31	2.00E-46	251
<a href="#">PTEN_HUMAN</a>	0.31	2.00E-46	251
<a href="#">PTEN_CANLF</a>	0.31	2.00E-46	251
<a href="#">PTEN_DICDI</a>	0.31	4.00E-44	237
<a href="#">PTEN_XENLA</a>	0.31	2.00E-42	239
<a href="#">5bzz_D Chain(D)</a>	0.3	6.00E-40	238
<a href="#">5bzz_C Chain(C)</a>	0.3	6.00E-40	238
<a href="#">5bzz_B Chain(B)</a>	0.3	6.00E-40	238
<a href="#">5bzz_A Chain(A)</a>	0.3	6.00E-40	238
<a href="#">5bzx_D Chain(D)</a>	0.3	6.00E-40	238
<a href="#">5bzx_C Chain(C)</a>	0.3	6.00E-40	238
<a href="#">5bzx_B Chain(B)</a>	0.3	6.00E-40	238
<a href="#">5bzx_A Chain(A)</a>	0.3	6.00E-40	238
<a href="#">1d5r_A Chain(A)</a>	0.3	6.00E-40	238
<a href="#">5bug_D Chain(D)</a>	0.3	6.00E-40	238
<a href="#">5bug_C Chain(C)</a>	0.3	6.00E-40	238
<a href="#">5bug_B Chain(B)</a>	0.3	6.00E-40	238

<a href="#">5bug_A Chain(A)</a>	0.3	6.00E-40	238
<a href="#">3v0h_B Chain(B)</a>	0.3	7.00E-36	240
<a href="#">3v0f_A Chain(A)</a>	0.3	1.00E-35	240
<a href="#">3v0g_C Chain(C)</a>	0.3	4.00E-35	239
<a href="#">3v0g_A Chain(A)</a>	0.3	4.00E-35	239
<a href="#">3v0h_A Chain(A)</a>	0.3	4.00E-35	239
<a href="#">3v0d_A Chain(A)</a>	0.3	1.00E-34	238
<a href="#">3v0f_B Chain(B)</a>	0.3	1.00E-34	238
<a href="#">K5WK49_AGABU</a>	0.29	8.00E-36	423
<a href="#">3v0g_B Chain(B)</a>	0.29	3.00E-36	249
<a href="#">3v0d_B Chain(B)</a>	0.29	3.00E-34	243
<a href="#">3v0g_D Chain(D)</a>	0.29	3.00E-34	243
<a href="#">A0A0C3CDL4_HEBCY</a>	0.28	4.00E-31	444
<a href="#">A0A177VUH2_9BASI</a>	0.26	4.00E-54	733
<a href="#">A0A177VHL6_9BASI</a>	0.26	4.00E-54	733
<a href="#">W4JQV9_9HOMO</a>	0.26	9.00E-51	616
<a href="#">A0A1J7GYH2_LUPAN</a>	0.24	7.00E-48	518
<a href="#">A0A166LBZ8_9HOMO</a>	0.23	8.00E-61	767
<a href="#">PTN2A_ARATH</a>	0.22	1.00E-38	463
<a href="#">A0A0C9WXR8_9AGAR</a>	0.18	8.00E-52	563
<a href="#">A0A0D2PH34_9AGAR</a>	0.18	3.00E-51	567
<a href="#">A0A0C3CDL4_HEBCY</a>	0.17	8.00E-49	572
<a href="#">A0A087UC66_9ARAC</a>	0.16	4.00E-49	775
<a href="#">TENS3_HUMAN</a>	0.16	6.00E-40	792
<a href="#">PTEN1_ARATH</a>	0.16	6.00E-04	219
<a href="#">TENS3_MOUSE</a>	0.16	6.00E-34	769
<a href="#">A0A177VUH2_9BASI</a>	0.15	1.00E-16	555
<a href="#">A0A177VHL6_9BASI</a>	0.15	1.00E-16	555
<a href="#">K5WK49_AGABU</a>	0.15	7.00E-48	607
<a href="#">K1RBC4_CRAGI</a>	0.14	4.00E-49	768

<b>Table 2.3 B. Matched Protein Structures</b>			
Protein Name	Identity	Expected Value	Matched Length
<a href="#">5bzz_D Chain(D)</a>	0.3	6.00E-40	238
<a href="#">5bzz_C Chain(C)</a>	0.3	6.00E-40	238
<a href="#">5bzz_B Chain(B)</a>	0.3	6.00E-40	238
<a href="#">5bzz_A Chain(A)</a>	0.3	6.00E-40	238
<a href="#">5bzx_D Chain(D)</a>	0.3	6.00E-40	238



<a href="#">5bzx_C Chain(C)</a>	0.3	6.00E-40	238
<a href="#">5bzx_B Chain(B)</a>	0.3	6.00E-40	238
<a href="#">5bzx_A Chain(A)</a>	0.3	6.00E-40	238
<a href="#">1d5r_A Chain(A)</a>	0.3	6.00E-40	238
<a href="#">5bug_D Chain(D)</a>	0.3	6.00E-40	238
<a href="#">5bug_C Chain(C)</a>	0.3	6.00E-40	238
<a href="#">5bug_B Chain(B)</a>	0.3	6.00E-40	238
<a href="#">5bug_A Chain(A)</a>	0.3	6.00E-40	238
<a href="#">3v0h_B Chain(B)</a>	0.3	7.00E-36	240
<a href="#">3v0f_A Chain(A)</a>	0.3	1.00E-35	240
<a href="#">3v0g_C Chain(C)</a>	0.3	4.00E-35	239
<a href="#">3v0g_A Chain(A)</a>	0.3	4.00E-35	239
<a href="#">3v0h_A Chain(A)</a>	0.3	4.00E-35	239
<a href="#">3v0d_A Chain(A)</a>	0.3	1.00E-34	238
<a href="#">3v0f_B Chain(B)</a>	0.3	1.00E-34	238
<a href="#">3v0g_B Chain(B)</a>	0.29	3.00E-36	249
<a href="#">3v0d_B Chain(B)</a>	0.29	3.00E-34	243
<a href="#">3v0g_D Chain(D)</a>	0.29	3.00E-34	243

**Table 2.3.** Protein prediction analysis of Ptn1 using PredictProtein (<https://www.predictprotein.org>). (A) Shows the list of aligned proteins. (B) Shows the list of matched protein structures.

## CHAPTER III

### INTERACTION OF PTN1 WITH RHO1 AND PDC1 IN *USTILAGO MAYDIS*

#### SUMMARY

The RhoA and 14-3-3 proteins play important roles in cell signaling in mammalian systems. Previous studies on the orthologues of these proteins in *Ustilago maydis*, such as Rho1 and Pdc1, respectively, showed that they play important roles in cell growth and filamentation. While the potential physical interaction of Rho1 and Pdc1 with Ptn1 was indicated in an earlier study, the current study aims to investigate the likely epistatic interactions between *rho1* and/or *pdcl* with *ptn1*. Our experiments demonstrate a functional connection between these genes, especially in processes that are related to stress tolerance, cellular morphology, and virulence of the fungus, indicating that they may be elements of the same regulatory pathway. Overexpressing *pdcl* in *ptn1* deleted strains resulted in reduced growth, mating efficiency, virulence, and stress tolerance relative to the  $\Delta$ *ptn1* strains while *rho1* overexpression in *ptn1* deleted strains did not have a significant effect on any of those parameters. In contrast, the overexpression of *rho1* alone in *U. maydis* negatively affected the infection rate, while *pdcl* overexpression did not result in any significant phenotype. Previous studies have demonstrated that Ptn1 physically interacts with Pdc1 and Rho1. When taken together these results indicate that the *pdcl* interaction with *ptn1* may be the reverse of that of *rho1* with *ptn1*. The current phenotypes



of the mutant strains when considered in the context of already available information about the role of these genes in other systems indicate that they may be part of a pathway that modulates cytoskeletal rearrangements.

## INTRODUCTION

GTPase proteins regulate several protein-protein interactions and cellular activities through conversion between the active GTP (guanosine-5-triphosphate)-bound state and inactive (guanosine 5-diphosphate (GDP)-bound) state (Bokoch, 2000). The GTPases can be multi-subunit G proteins or low molecular weight small GTPases belonging to the Ras/Rho superfamily (Hippenstiel et al., 2002; Wennerberg, Rossman, & Der, 2005). Rho GTPases act as molecular switches that modulate several fundamental cellular activities such as cellular defense, growth, differentiation, proliferation and cytoskeleton differentiation (Cherfils & Zeghouf, 2013; Wennerberg et al., 2005). In leukocytes, RhoA and Cdc42 proteins are activated by chemo-attractants and RhoA is localized to the posterior of the cell (Z. Li et al., 2003). A study in *Dictyostelium discoideum* showed the presence of another protein, PTEN, at the posterior of chemotaxing cells (Comer & Parent, 2002). Studies in mouse neutrophils undergoing chemotaxis showed that PTEN is colocalized with active RhoA at the posterior and provided evidence that RhoA/RhoA-associated kinase (Rock)-mediated phosphorylation of PTEN controls its localization and activation (Z. Li et al., 2005; Meili, Sasaki, & Firtel, 2005). In *Saccharomyces cerevisiae*, the mutation of *RHO1*, the ortholog of the mammalian *RHOA* gene, resulted in increased cell lysis and cell death. It also led to the accumulation of small budded cells in which cortical actin patches were clustered to buds, indicating its vital role in controlling cell growth (Yamochi et al., 1994).

14-3-3 proteins are a family of conserved regulatory proteins that interact with several different binding partners including kinases, phosphatases, and transmembrane receptors to regulate their cellular localization and function. These proteins modulate the function of substrate molecules through various ways, including protection from dephosphorylation, masking nuclear localization and export signals, blocking binding of other regulator proteins (*e.g.* phosphatases), or converting proteins into their active or inactive conformations (Pennington, Chan, Torres, & Andersen, 2018; Shimada, Fournier, & Yamagata, 2013). 14-3-3 proteins exist as homo- or hetero-dimers and bind to the target substrates mainly through phospho-serine/threonine motifs (Jones, Ley, & Aitken, 1995; Muslin, Tanner, Allen, & Shaw, 1996). Studies have repeatedly shown that they contribute to pathogenesis mainly by regulating the subcellular localization of target proteins (Shimada et al., 2013). Recently it has been found that 14-3-3 proteins control AKT (PKB/protein kinase B) activation by inhibiting its phosphorylation during inflammation and thereby playing a vital role in cell survival and apoptosis of intestinal epithelial cells (Gomez-Suarez et al., 2016). This is significant since an activated AKT is required for the phosphorylation of a series of substrates throughout the cell which are critical in mediating numerous aspects of cellular function, including nutrient uptake, anabolic reactions, cell growth, differentiation and survival (Yu & Cui, 2016). Disruption of 14-3-3 protein expression has been observed in the case of Parkinson's disease (Slone, Lavalley, McFerrin, Wang, & Yacoubian, 2015). *S. cerevisiae* has two isoforms of 14-3-3 proteins, Bmh1 and Bmh2, and these are essential since deleting them together led to non-viable cells (van Heusden et al., 1995). Studies in *S. cerevisiae*

indicated that these proteins play a role in actin cytoskeleton organization and cell wall integrity (Lottersberger, Panza, Lucchini, Piatti, & Longhese, 2006).

The dimorphic transition in *Ustilago maydis* requires the coordinated communication among different regulatory pathways of which the two important ones are the mitogen-activated protein (MAP) kinase pathway (Smith et al., 2004) and protein kinase A (PKA) pathway (Gold et al., 1997). Among the several proteins associated with this signaling cascade, the GTPase superfamily proteins such as Rho/Rac GTPases, as well as the 14-3-3 proteins, are of great significance. *U. maydis* contains six different Rho/Rac encoding genes; *rho1*, *rac1*, *cdc42* and three other *rho*-like genes (Kamper et al., 2006; Pham et al., 2009). Disruption of *rho1* in haploid cells is lethal, indicating that Rho1 is the only GTPase in *U. maydis* that is essential for cell viability (Pham et al., 2009). The deletion of *rac1* affected cellular morphology and interfered with hyphal growth, showing that it is necessary for the dimorphic switch from yeast to hyphal growth, while the cells deleted for *cdc42* failed to separate after cytokinesis in *U. maydis* (Mahlert, Leveleki, Hlubek, Sandroock, & Bolker, 2006). In *U. maydis*, there is only a single 14-3-3 orthologue, *pdcl*, and it is essential for cell viability; the depletion of *pdcl* resulted in severe growth impairment (Pham et al., 2009)

From the experiments described in chapter 2, it is evident that *ptn1* plays a role in pathogenicity and is required for the development and germination of teliospores in *U. maydis*. A previous study showed that Rho1 and Pdc1 proteins participate in the same regulatory pathway(s) that control morphogenesis in *U. maydis* and also that these proteins physically interact with Ptn1 (Pham et al., 2009). It would be interesting to explore this potential interaction in the context of plant pathogenicity and spore germination. The

current study indicates that *ptn1* interacts with *pdcl* since overexpression of *pdcl* in a *ptn1* deletion background further exacerbated the *ptn1* deletion phenotypes related to mating efficiency, virulence and stress tolerance. On the other hand, *rho1* overexpression in the *ptn1* deletion background did not result in any major phenotype, although overexpressing *rho1* alone resulted in a severe decline in virulence.

## MATERIALS AND METHODS

**Strains and growth conditions.** *U. maydis* strains used in this study are listed in Table 3.1. *Escherichia coli* strains DH5- $\alpha$  and TOP10 (Invitrogen/ Thermo Fisher) were used for all cloning and plasmid amplification reactions. *U. maydis* strains were grown in media and conditions as described in materials and methods (Chapter II).

**Table 3.1. Strains used in this study.**

<b>List of strains</b>		
<b><i>U. maydis</i> strain</b>	<b>Genotype</b>	<b>References</b>
1/2	<i>alb1</i>	(Gold et al., 1997)
2/9	<i>a2b2</i>	(Gold et al., 1997)
d132	<i>ala2b1b2</i>	(Kronstad & Leong, 1989a)
d132 $\Delta$ <i>ptn1</i>	<i>ala2b1b2 ptn1 ptn1::hyg<sup>R</sup></i>	Chapter 2
d132 $\Delta$ <i>pdcl</i>	<i>ala2b1b2 pdcl, pdcl::cbx<sup>R</sup></i>	(Pham et al., 2009)
d132 $\Delta$ <i>rho1</i>	<i>ala2b1b2 rho1, rho1::cbx<sup>R</sup></i>	(Pham et al., 2009)
d132 $\Delta$ <i>rho1</i> $\Delta$ <i>ptn1</i>	<i>ala2b1b2 <math>\Delta</math>rho1, ptn1::hyg<sup>R</sup></i>	This study
d132 $\Delta$ <i>pdcl</i> $\Delta$ <i>ptn1</i>	<i>ala2b1b2 <math>\Delta</math>pdcl, ptn1::hyg<sup>R</sup></i>	This study
1/2 <i>pdcl</i> <sup>Otef</sup>	<i>alb1 P<sub>otef</sub>-pdcl, hyg<sup>R</sup></i>	This study
2/9 <i>pdcl</i> <sup>Otef</sup>	<i>a2b2 P<sub>otef</sub>-pdcl, hyg<sup>R</sup></i>	This study
1/2 <i>rho1</i> <sup>Otef</sup>	<i>alb1 P<sub>otef</sub>-rho1, hyg<sup>R</sup></i>	This study
2/9 <i>rho1</i> <sup>Otef</sup>	<i>a2b2 P<sub>otef</sub>-rho1, hyg<sup>R</sup></i>	This study
1/2 $\Delta$ <i>ptn1 pdcl</i> <sup>Otef</sup>	<i>alb1 ptn1::cbx<sup>R</sup> P<sub>otef</sub>-pdcl, hyg<sup>R</sup></i>	This study
2/9 $\Delta$ <i>ptn1 pdcl</i> <sup>Otef</sup>	<i>a2b2 ptn1::cbx<sup>R</sup> P<sub>otef</sub>-pdcl, hyg<sup>R</sup></i>	This study
1/2 $\Delta$ <i>ptn1 rho1</i> <sup>Otef</sup>	<i>alb1 ptn1::cbx<sup>R</sup> P<sub>otef</sub>-rho1, hyg<sup>R</sup></i>	This study
2/9 $\Delta$ <i>ptn1 rho1</i> <sup>Otef</sup>	<i>a2b2 ptn1::cbx<sup>R</sup> P<sub>otef</sub>-rho1, hyg<sup>R</sup></i>	This study
<b>Plasmids</b>	<b>Genotype</b>	<b>References</b>
<i>Otef-rho1-hyg</i>	<i>P<sub>otef</sub>-rho1 hyg<sup>R</sup></i>	(Pham et al., 2009)
<i>Otef-pdcl-hyg</i>	<i>P<sub>otef</sub>-pdcl hyg<sup>R</sup></i>	(Pham et al., 2009)

**Genetic Manipulation and Vector construction.** Primer design, PCR reactions, vector construction, cloning reactions, deletion construction, and *U. maydis* transformations, were performed as described previously (Chapter II).

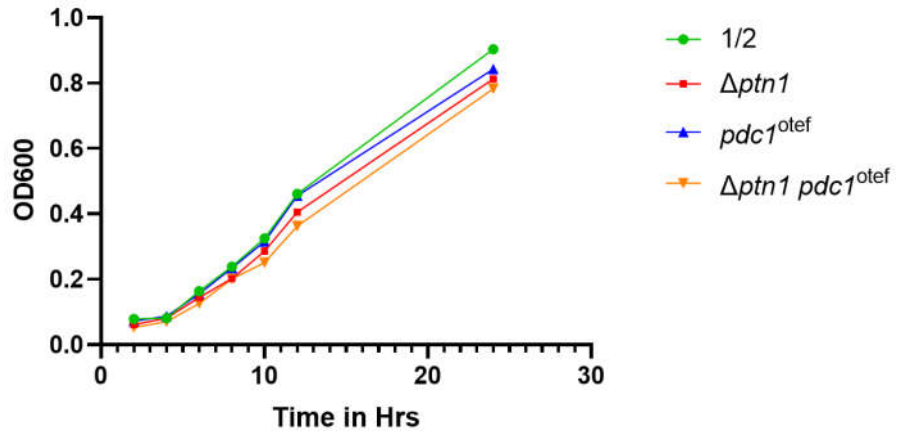
**Growth rate, cell wall stress tests, mating assays, plant infection, spore count and spore germination assays.** Cell wall stress tests, mating assays, plant infections, spore count and spore germination assays were performed as described (Chapter II).

**Staining and microscopy.** Staining of *U. maydis* strains and microscopic analyses were performed as described previously (Lovely, Aulakh, & Perlin, 2011; Pham et al., 2009).

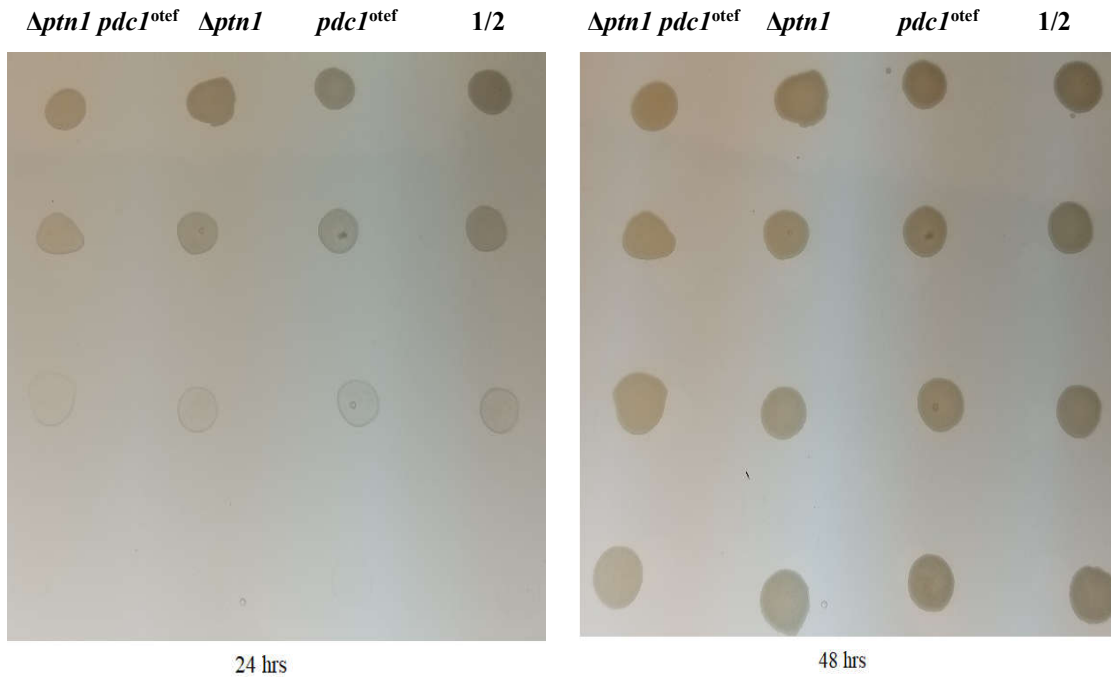
## RESULTS

**The overexpression of *pdcl* in *ptn1* deletion strains shows a background specific impairment in growth ability.** Previous studies of *pdcl* (Pham et al., 2009) demonstrated that lack of *pdcl* results in growth impairment in the haploid background. We were curious to determine the effect of overexpression of *pdcl* on the growth of the fungus, especially in a *ptn1* deletion background. Initially, the growth of  $\Delta ptn1 pdcl^{otef}$  strains were compared to that of the wild type,  $\Delta ptn1$ , and  $pdcl^{otef}$  strains on PDA agar plates by spotting serially diluted (undiluted,  $10^{-1}$ ,  $10^{-2}$ , and  $10^{-3}$ ) samples and observing the plates for growth of the strains after incubating for 24-48 hours at 27 ° C. The results indicated that the  $\Delta ptn1 pdcl^{otef}$  strains showed less growth compared to all the other strains and the effect was more dramatic in the 2/9 background. This led us to perform the growth assay experiment where the growth of these strains was compared to each other by plotting a growth curve (Figure 3.1).

A



B



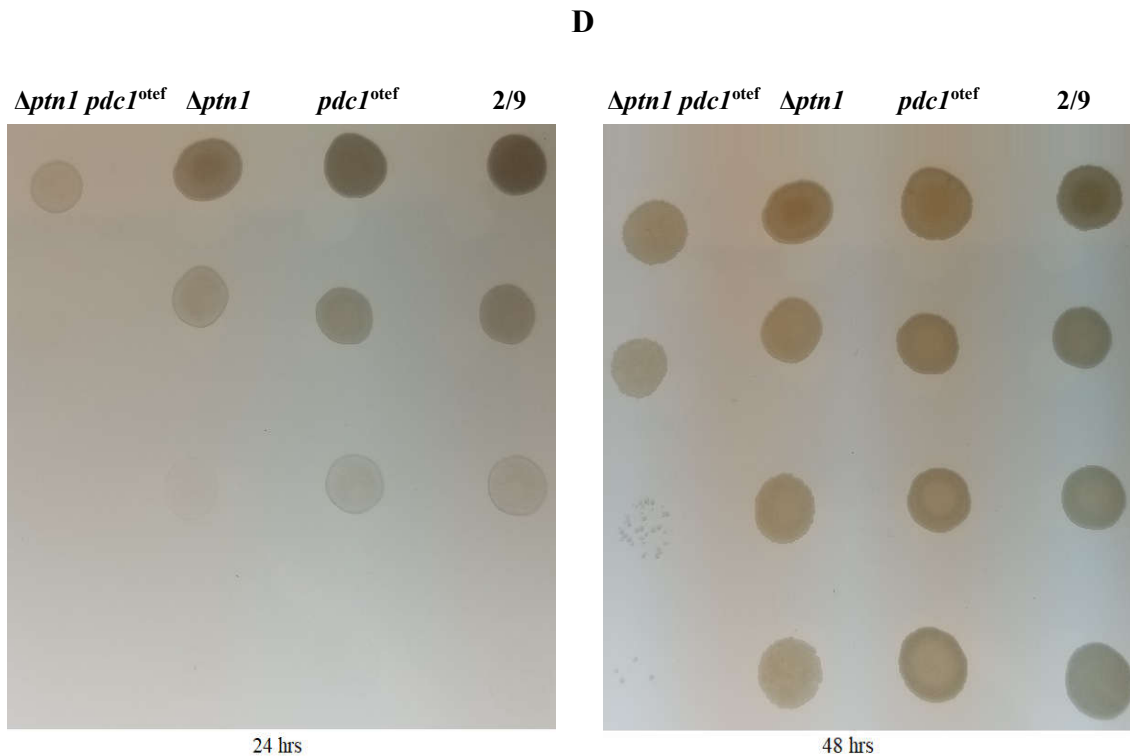
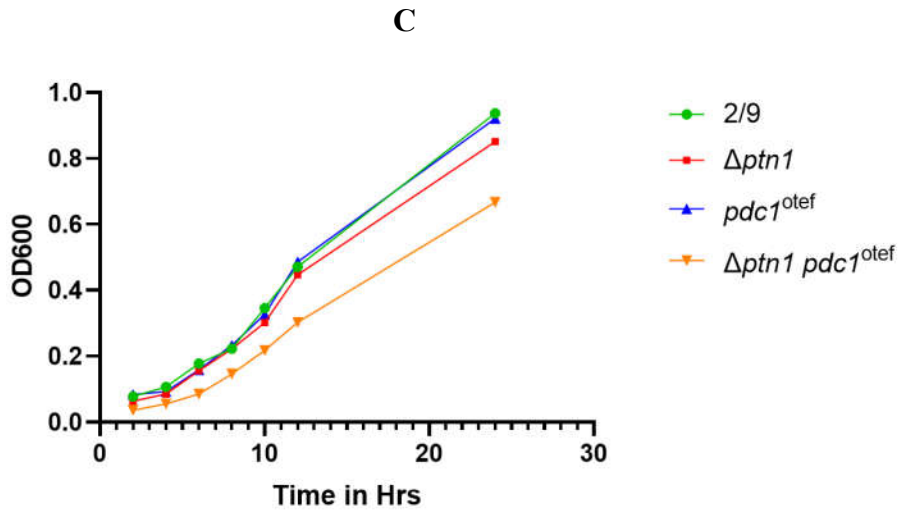


**Figure 3.1.** Overexpressing *pdc1* in *ptn1* deleted strains showed background specific growth effects with the 2/9  $\Delta ptn1 pdc1^{otef}$  more affected than the 1/2  $\Delta ptn1 pdc1^{otef}$  strain. Growth assays were performed following the protocol described in Chapter 2. *U. maydis* strains grown in YPS liquid media were used for the growth assay experiment to plot the growth curve. For the plate assay, serially diluted (undiluted,  $10^{-1}$ ,  $10^{-2}$ , and  $10^{-3}$ ) strains were spotted on PDA plates and growing them at 28 °C for 24-48 hours. **A.** The growth curve for the 1/2 background strains. **B.** PDA plate assay for the 1/2 background strains.

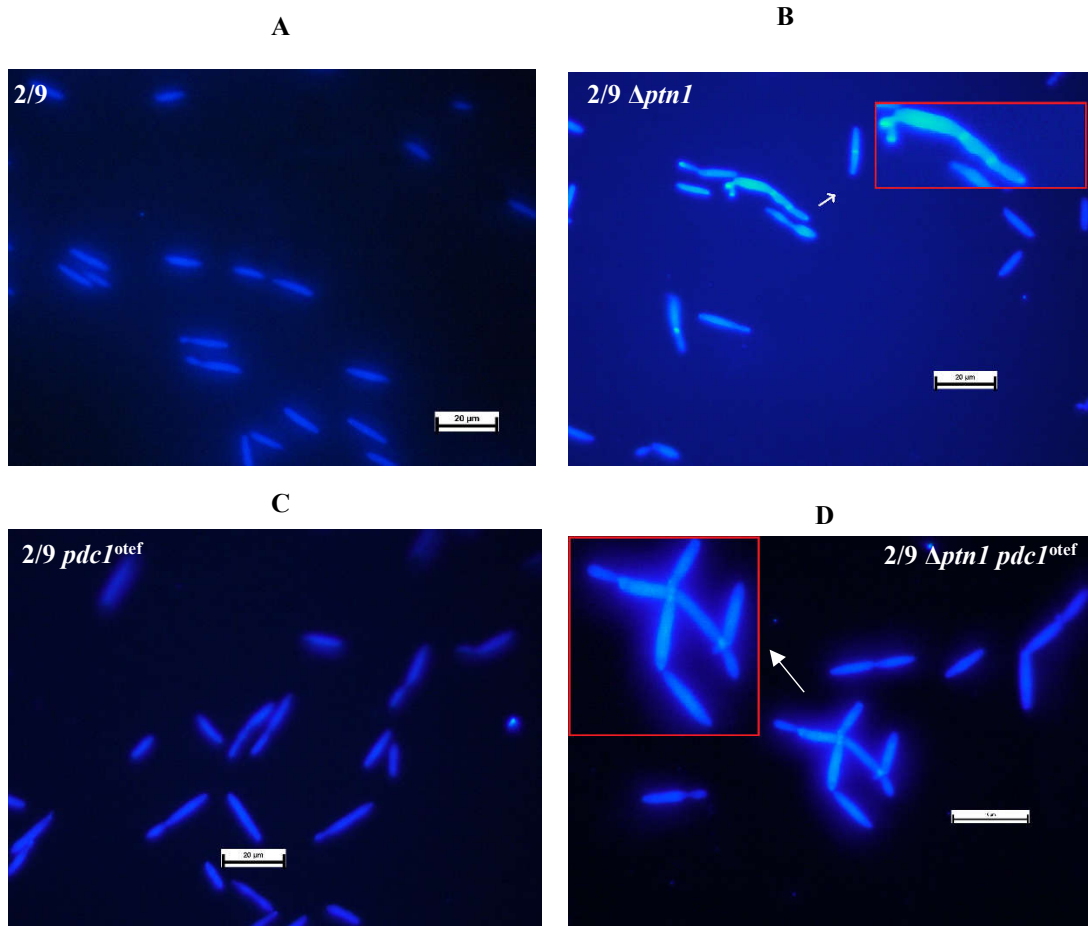
**C.** The growth curve for the 2/9 background strains. **D.** PDA plate assay for the 2/9 background strains.

The growth curve data were very similar to the growth profile on the PDA plates, *i.e.*, the deletion of *ptn1* coupled with *pdcl* overexpression led to reduced growth rates. This observation appeared to be background specific, as the 2/9  $\Delta ptn1$  *pdcl*<sup>otef</sup> strain was more affected than the 1/2  $\Delta ptn1$  *pdcl*<sup>otef</sup> strain.

**Overexpressing *pdcl* in *ptn1* backgrounds leads to an increase in aberrant cellular morphology.** To continue the examination of a possible genetic interaction between *ptn1* and *pdcl*, double deletion strain d132  $\Delta pdcl$   $\Delta ptn1$  and overexpression strains,  $\Delta ptn1$  *pdcl*<sup>otef</sup> (both 1/2 and 2/9 backgrounds) were used. Examination of cellular morphology indicated that d132  $\Delta pdcl$   $\Delta ptn1$  showed an increase in branching compared with d132  $\Delta pdcl$  cells, while the d132  $\Delta ptn1$  cells did not show any apparent difference in morphology from the wild type cells (Figure 3.2). A previous study (Pham et al., 2009) showed that depletion of *pdcl* in haploid cells results in aberrant morphology with an increase in branching of the cells. Our results showed that the overexpression of *pdcl* in the haploid background does not have an effect on cell morphology, however, that is not the case when it was overexpressed in a *ptn1* deletion background. The  $\Delta ptn1$  *pdcl*<sup>otef</sup> cells showed an increase in cells with aberrant morphology. These cells showed separation defects, with several cells attached to each other, resulting in a branched morphology (Figure 3.2 D). Also, the effect appeared to be background specific, *i.e.*, more of the 2/9 *ptn1* *pdcl*<sup>otef</sup> cells were defective than those made of the 1/2 background. The separation of the daughter cells from mother cells in *U. maydis* requires the formation of two distinct septa, a primary septum in the mother cell and subsequent formation of a secondary septum in the daughter cell, resulting in the formation of a fragmentation zone between the two



septa that eventually disintegrates, separating the daughter cell from the mother cell (Weinzierl et al., 2002). It is possible that the mutant strains may have some deficiencies in septum formation, however, the examination of cell wall localization with calcofluor white showed that the cell wall material was able to localize and deposit to the growing tip, while the cells remained connected. In the case of haploid *ptn1* deletion strains, a small number of cells produced cross wall septa, while not forming a branched phenotype. A similar type of morphology was described during the overexpression of *smu1* in *hsl1* deletion mutants (Lovely et al., 2011) and these genes are demonstrated to have a role in cell separation and cytokinesis in *S. cerevisiae* (Shulewitz, Inouye, & Thorner, 1999).



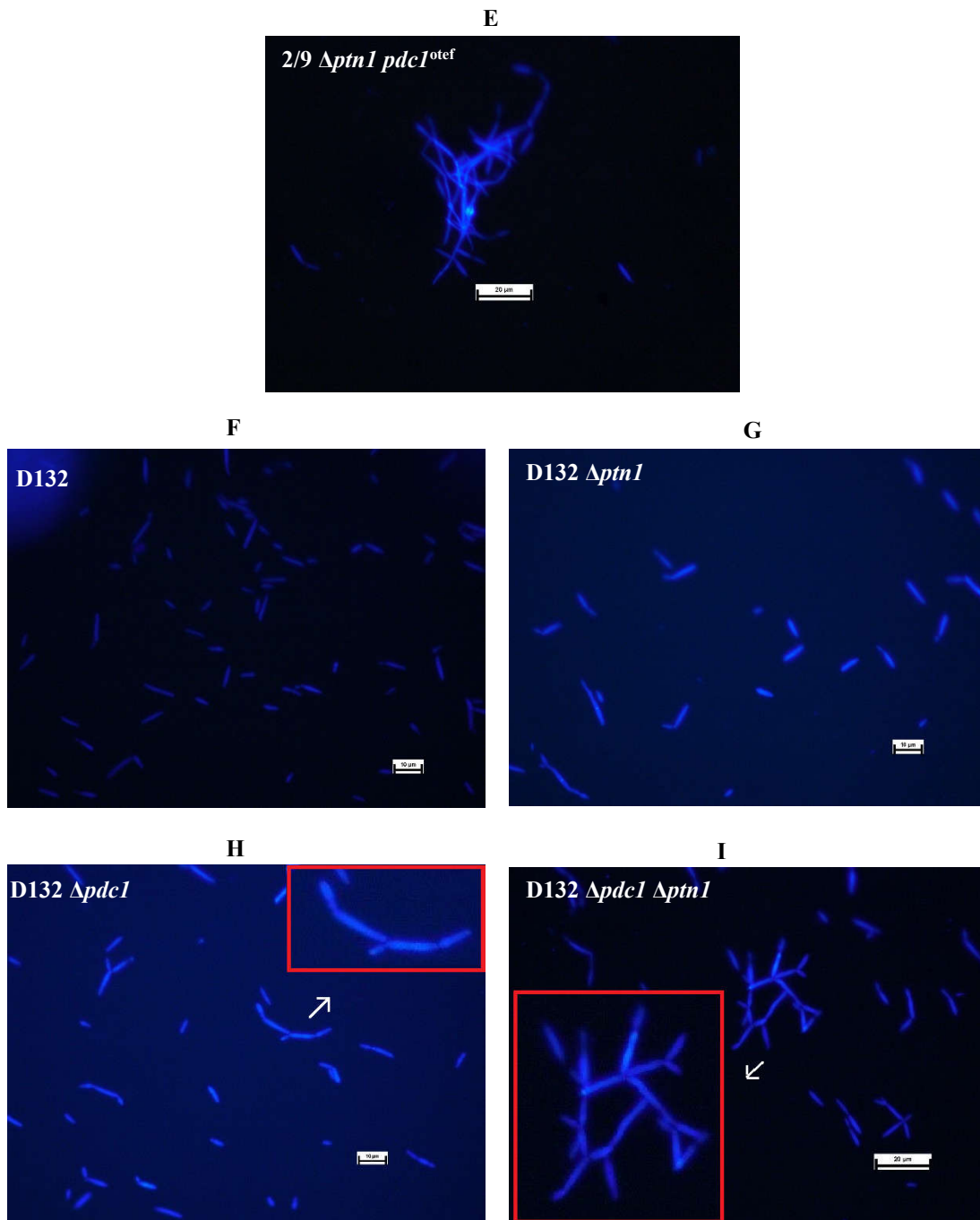


**Figure 3.2.** Calcofluor staining assay of *ptn1* and *pdc1* mutants. The staining shows that the deletion of both *pdc1* and *ptn1*, as well as the overexpression of *pdc1* in the *ptn1* deletion background leads to aberrant cell morphology showing a branched phenotype. The boxes represent magnified abnormal cell morphology. Size bar for A, B, C, E, and I is 20  $\mu m$ ; D, F, G, H is 10  $\mu m$ .

**Deletion of *ptn1* and *pdcl* reduces aerial hyphae while overexpressing *pdcl* in the *ptn1* deletion background has a severe effect on aerial hyphae formation.** In chapter 2, we demonstrated that the deletion of *ptn1* in haploid background influences the mating process, as evidenced by the reduction in the formation of filaments on charcoal plates during the initial 24 hours when two strains with compatible mating types were spotted together. Also, we have seen in chapter 2 that the deletion of a single copy of *ptn1* in diploid d132 background had a minor effect on filamentation especially during the initial 24 hours. It is known that when a single copy of *pdcl* is deleted as in d132  $\Delta pdcl$ , there were no effects on the aerial hyphal formation (Pham et al., 2012). However, the fact that Pdc1 physically interacts with Ptn1 led us to explore the effect of double deletion of *pdcl* and *ptn1*. Hence, we developed a strain, d132  $\Delta pdcl \Delta ptn1$ , where one copy each of *ptn1* and *pdcl* were deleted. The ability of this strain to form filaments was compared with that of wild type d132, d132  $\Delta pdcl$  and d132  $\Delta ptn1$  strains. The results indicated that simultaneous deletion of *pdcl* and *ptn1* affected the ability of the fungus to form filaments more than what was seen for the  $\Delta ptn1$  strains (Figure 3.3 A). A previous study conducted in our lab showed that *pdcl* is not essential for aerial hyphal formation in *U. maydis* (Pham et al., 2009). When mating assays were conducted using compatible mating type strains of *U. maydis* where *pdcl* gene was expressed under the control of nitrate reductase promoter,  $P_{nar1}$ , when *pdcl* was overexpressed, no significant difference in aerial hyphae formation was observed when compared to those between wild type strains (Pham et al., 2009). Similar results were obtained when *pdcl* was expressed under the control of *otef* (overexpressing) promoter (Figure 3.3 B). However, when mating was conducted using

strains where *pdcl* gene was overexpressed in the *ptn1* deletion background, as shown in Figure 3.3 B, there was a defect in mating hyphae formation.

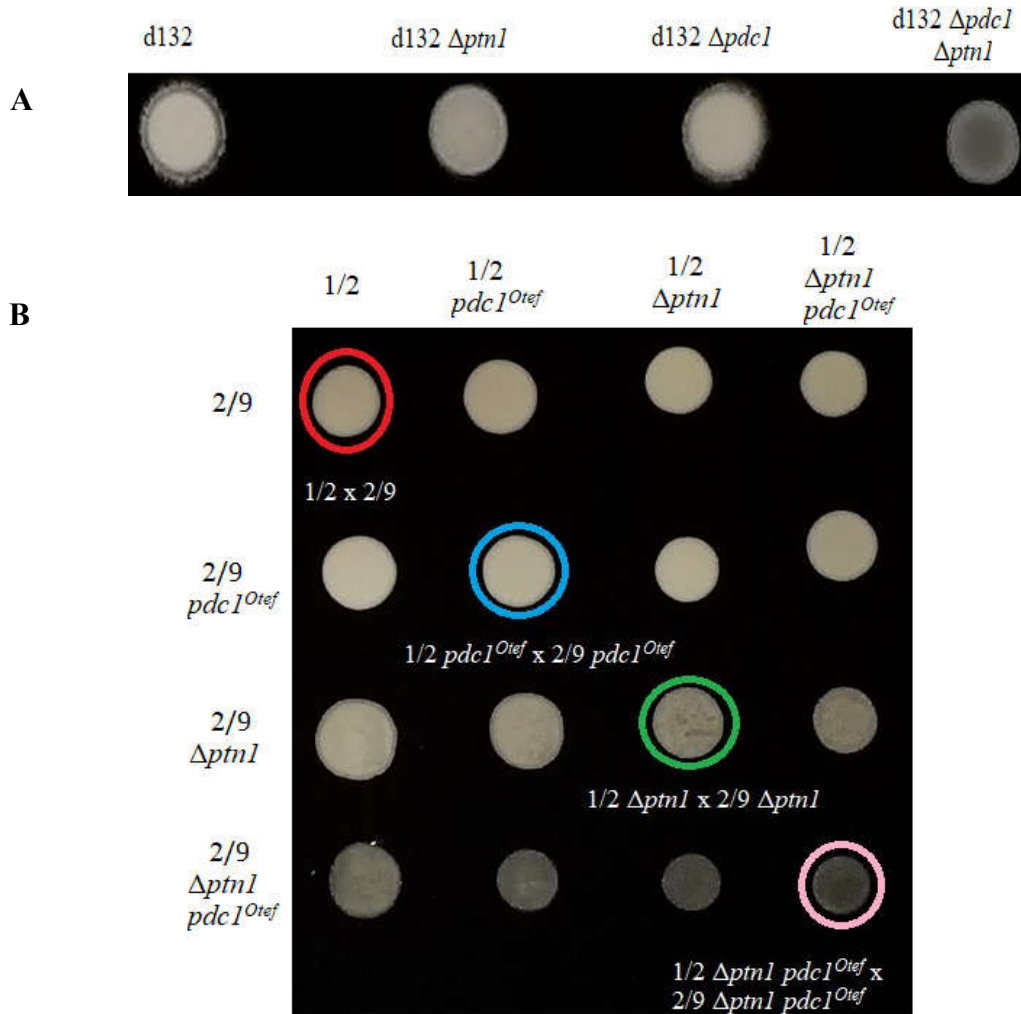
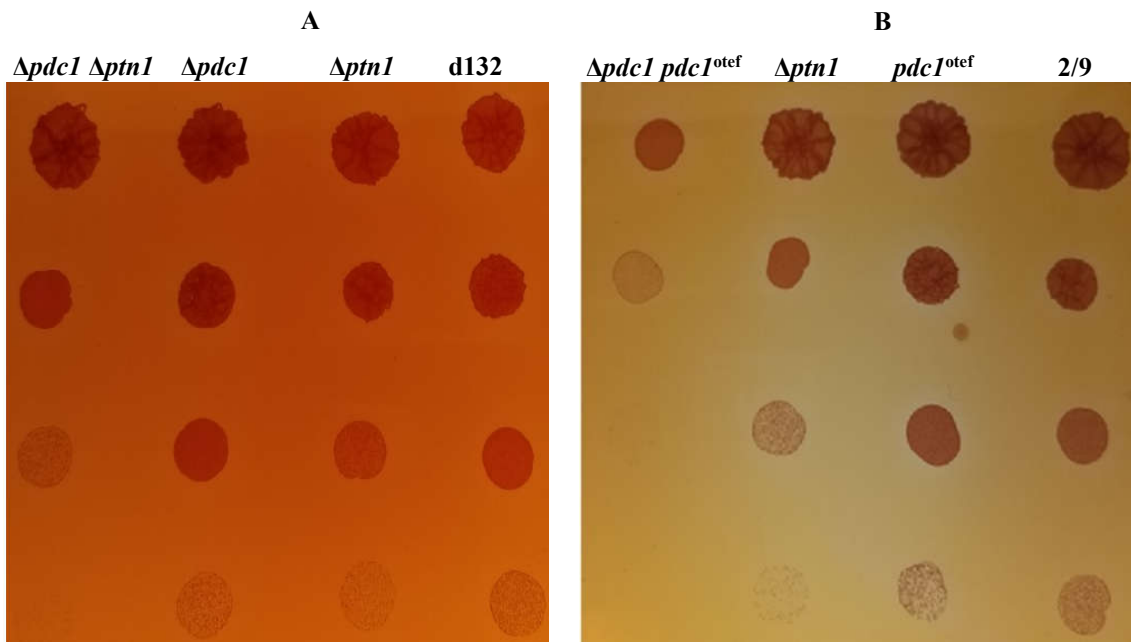


**Figure 3.3** Deletion or overexpression of *pdcl* reduces aerial hyphal formation in the *ptn1* deletion background. The strains were spotted on YPD charcoal plates and observed after 24 hours. **A.** Deletion of both *ptn1* and *pdcl* in d132 diploid background reduced the aerial hyphae formation while *pdcl* overexpression on its own did not show an effect. **B.** Compatible haploid mating type strains were mixed and spotted onto charcoal plates. The results indicated that overexpressing *pdcl* in conjunction with a *ptn1* deletion severely impaired the ability to form aerial hyphae.

#### Overexpression of *pdcl* in the *ptn1* deletion background reduces stress tolerance.

From chapter 2, we have seen that haploid *ptn1* deletion strains were slightly more sensitive to cell wall stress agents such as Congo red and calcofluor white. However, the diploid

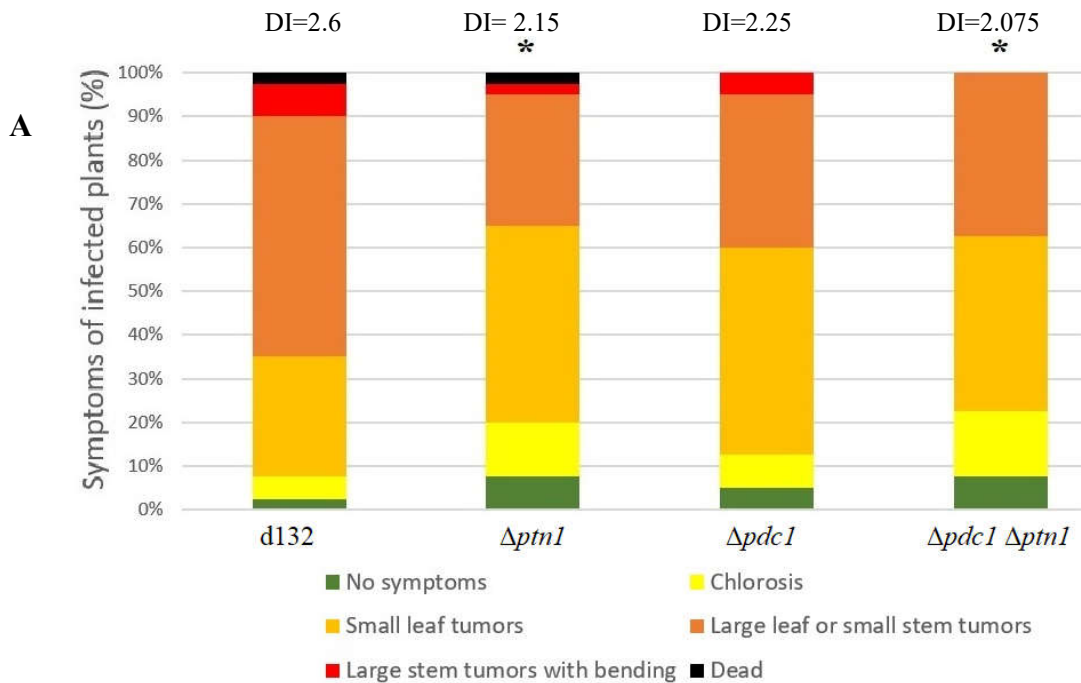
d132  $\Delta ptn1$  strain was not as sensitive as the haploid strains, but it appeared to be more sensitive than the wild type d132 strain (Figure 3.4 A). While the *pdcl* gene has a major role in pathways controlling cell separation and cell polarity (Pham et al., 2009), it appears that the deletion of *pdcl* does not significantly change the ability of the fungus to deal with cell wall stress in the d132 background. The effect of deletion of both *ptn1* and *pdcl* on the ability of the fungus to tolerate cell wall stress was examined. The results (Figure 3.4 A) indicated that the simultaneous deletion of the two genes made the strain more sensitive to cell wall stress than either of the mutant controls, d132  $\Delta ptn1$  or d132  $\Delta pdcl$ . When *pdcl* was overexpressed in the haploid background strains, it did not significantly alter the cell wall stress tolerance ability. However, when *pdcl* overexpression was coupled with *ptn1* deletion, the cells were more sensitive to cell wall stress associated with Congo red (Figure 3.4 B). This was especially true in the 2/9 (a2b2) background.



**Figure 3.4.** Stress sensitivity of *pdcl* and *ptn1* mutant strains. The strains were spotted onto YPS agar plates supplemented with cell wall stressor, Congo red, in decreasing order of cell concentration, undiluted,  $10^{-1}$ ,  $10^{-2}$ , and  $10^{-3}$ . **A.** In the diploid background, deletion of *pdcl* and *ptn1* appears to reduce the ability to tolerate cell wall stress more than for the

individual *pdcl* or *ptn1* deletion strains. **B.** The overexpression of *pdcl* in *ptn1* deletion background severely affects cell wall stress tolerance ability.

**Double deletion of *pdcl* and *ptn1* reduces virulence while overexpression of *pdcl* in a *ptn1* deletion background does not rescue the virulence phenotype.** The previous plant infection study (Chapter 2) showed that *ptn1* deletion results in reduction in virulence in plants. Hence, the effect of deletion of both *ptn1* and *pdcl* on virulence was examined. In the initial experiment, maize plants were infected with the d132 wild type, d132  $\Delta pdcl$ , d132  $\Delta ptn1$  and d132  $\Delta pdcl \Delta ptn1$  strains. The disease symptoms were scored according to severity (Figure 3.5). The double deletion strain, d132  $\Delta pdcl \Delta ptn1$ , was less virulent than either d132  $\Delta pdcl$  or d132  $\Delta ptn1$  in these plant infections. While the d132  $\Delta pdcl$  strains were less virulent than the wild type, they were found to be statistically more virulent than d132  $\Delta ptn1$  strains. Plants infected with d132  $\Delta pdcl$  strains showed more tumors overall, especially leaf and stem tumors, compared to d132  $\Delta ptn1$  strains.



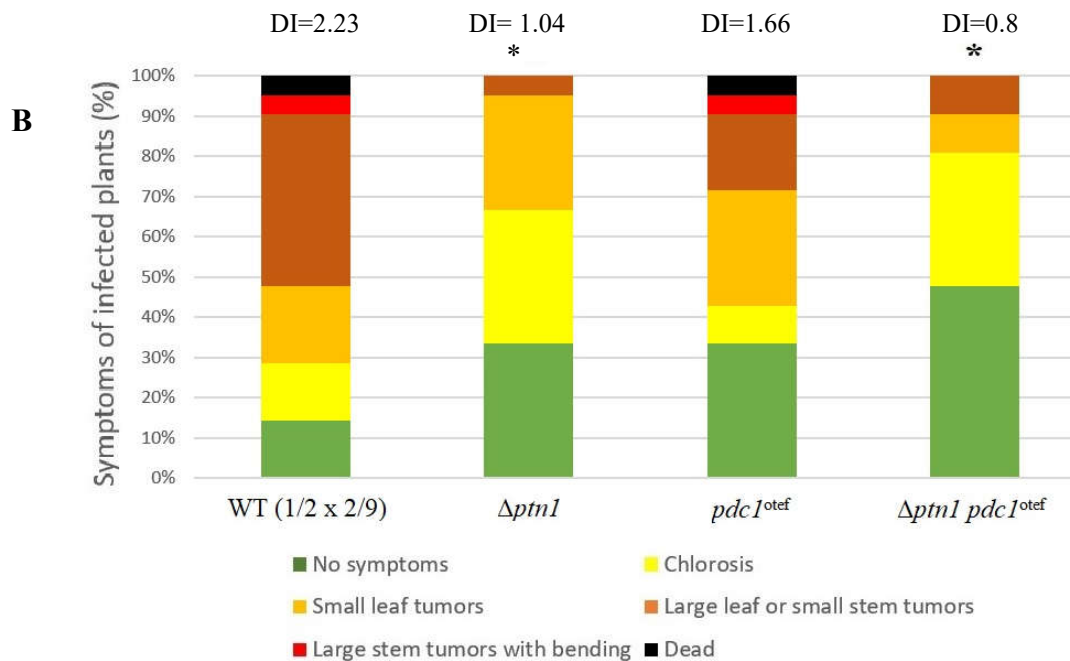


**Figure 3.5.** Plant infection profile of *ptn1* and *pdcl* mutants. For disease index (DI), the plants were scored based on symptoms of infection on a scale of 0-5. 0-no symptoms, 1-chlorosis, 2-small leaf tumors, 3 – several small leaf tumors/large leaf tumors/small stem tumors, 4- large stem tumors with bending, 5- plant death. Data analyzed using Kruskal Wallis, Multiple comparison test and a  $p < 0.05$  indicates significant difference (\*). **A.** The double deletion strains produced less symptoms than  $\Delta ptn1$ ;  $\Delta ptn1$  was less virulent compared to the wild type d132 progenitor;  $\Delta pdcl$  while less virulent, was not significantly different from wild type. **B.** Shown are crosses between compatible 1/2 and 2/9 wild type progenitors and also, as indicated the mutants of the respective progenitor strains. Overexpressing *pdcl* in *ptn1* knockout strains ( $\Delta ptn1 pdcl^{otef}$ ) led to decreased infection rates, while overexpressing *pdcl* by itself did not show any obvious difference from wild type.

**Aerial hyphae formation in  $\Delta rho1 \Delta ptn1$  strain appears to be the same as that of  $\Delta rho1$  phenotype, while *rho1* overexpression in  $\Delta ptn1$  did not have any effect.** The *U. maydis rho1* is the ortholog of the mammalian *RHOA* gene which codes for small GTPase protein. Disruption of *rho1* in the haploid background is lethal for *U. maydis* (Pham et al., 2009). On the other hand, the deletion of one copy of *rho1* in a diploid strain results in the loss of ability of the fungus to form aerial filaments on charcoal plates (Pham et al., 2012). To

explore the possible connection between *ptn1* and *rho1*, we attempted to delete *ptn1* in diploid d132 strains where one copy of *rho1* was deleted. The mating experiments from chapter 2 that a successful mating reaction in *U. maydis* can be measured in terms of the white ‘fuzz’ produced on a charcoal plate from the mating of strains of opposite mating types. Also, the diploid d132 strain by itself displays ‘fuzz’ reaction on a charcoal plate due to the presence of genetic elements of both mating types in the same strain. We observed that the double deletion strains have completely lost the ability to form aerial filaments (Figure 3.6 A). This phenotype was similar to that seen for d132  $\Delta\rho1$ .

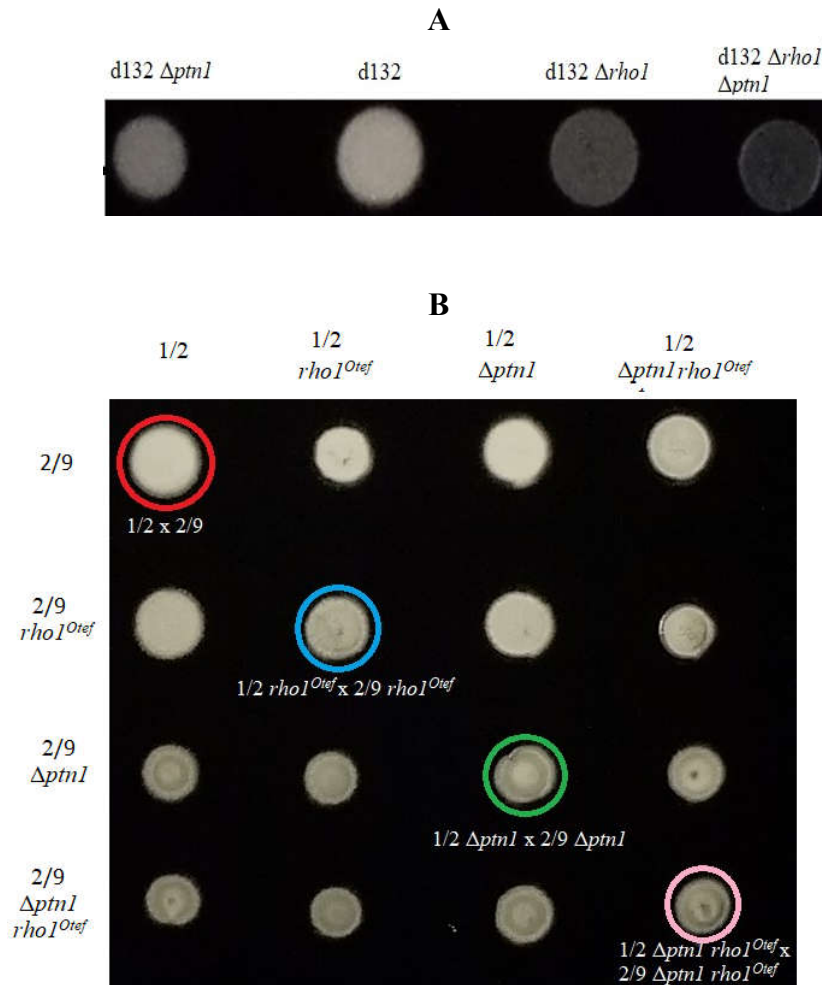


**Figure 3.6.** Deletion of both *ptn1* and *rho1* results in decreased mating deficiency. **A.** Charcoal plate assay of double deletion strain, d132  $\Delta\rho1$   $\Delta ptn1$ , was compared with that of wild type d132, d132  $\Delta\rho1$  and d132  $\Delta ptn1$ ; d132  $\Delta\rho1\Delta ptn1$  produced no aerial



filaments. **B.** The mating of haploid strains performed on activated charcoal plates. Overexpression of *rho1* in strains deleted for *ptn1* resulted in a slight reduction in white ‘fuzz’ mating filaments in the initial 24 hours.

We next examined the effect of overexpression of *rho1* in *ptn1* deletion strains. When haploid mutant strains 1/2  $\Delta pt n 1$  *rho1*<sup>otef</sup> and 2/9  $\Delta pt n 1$  *rho1*<sup>otef</sup> were mated, the phenotype was not as dramatic as in the case of corresponding double deletion strains. In this case, the strains showed defects in aerial hyphae formation, *i.e.*, relatively less amount of white ‘fuzz’ compared to the *ptn1* deletion strains (Figure 3.6 B). However, the  $\Delta pt n 1$  *rho1*<sup>otef</sup> strains were able to catch up to similar levels of aerial hyphal formation found in wild type by 48 hours, like the phenotype observed in the case of *ptn1* deletion strains, described in detail (Chapter 2). Additional controls for comparison included wild type strains and *rho1*<sup>otef</sup> strains, where the mating of *rho1*<sup>otef</sup> strains did not differ from that of wild type strains.

**Overexpression or deletion of *rho1* in *ptn1* deletion background does not have a major effect on cell wall stress tolerance.** We have seen that *ptn1* deletion in a haploid background makes the fungal cells more sensitive to cell wall stress and the deletion in a diploid background slightly increases the sensitivity of the strains to cell wall stress agents such as Congo red, an inhibitor of chitin microfibril assembly (Roncero & Durán, 1985). Here we tested the effect of *rho1* deletion or overexpression on this specific phenotype in *ptn1* deletion background strains. When *ptn1* was deleted in d132 strains where one copy of *rho1* was also deleted, it did not result in any significant change. The d132 *rho1* deletion strains were more sensitive to cell wall stress when compared to d132  $\Delta pt n 1$  strain, with the latter being slightly sensitive compared to the wild type strains. This indicates that *rho1* phenotype is dominant to the *ptn1* phenotype, and potentially may be downstream of *ptn1*.

We further examined if overexpressing *rho1* can rescue the *ptn1* deletion phenotype. Overexpression of *rho1* was examined in haploid strains deleted for *ptn1*. These mutants were compared with corresponding wild type, *ptn1* deletion, and *rho1* overexpression strains. However, these data (Figure 3.7) demonstrate that *rho1* overexpression does not rescue the defect seen in *ptn1* deletion strains. In addition, overexpressing *rho1* alone does not significantly alter the ability of the fungus to cope with stress. The results indicate that while a single copy of *rho1* is not enough to function normally in stress conditions, overexpressing *rho1* does not necessarily alter the stress sensitivity of the fungus.

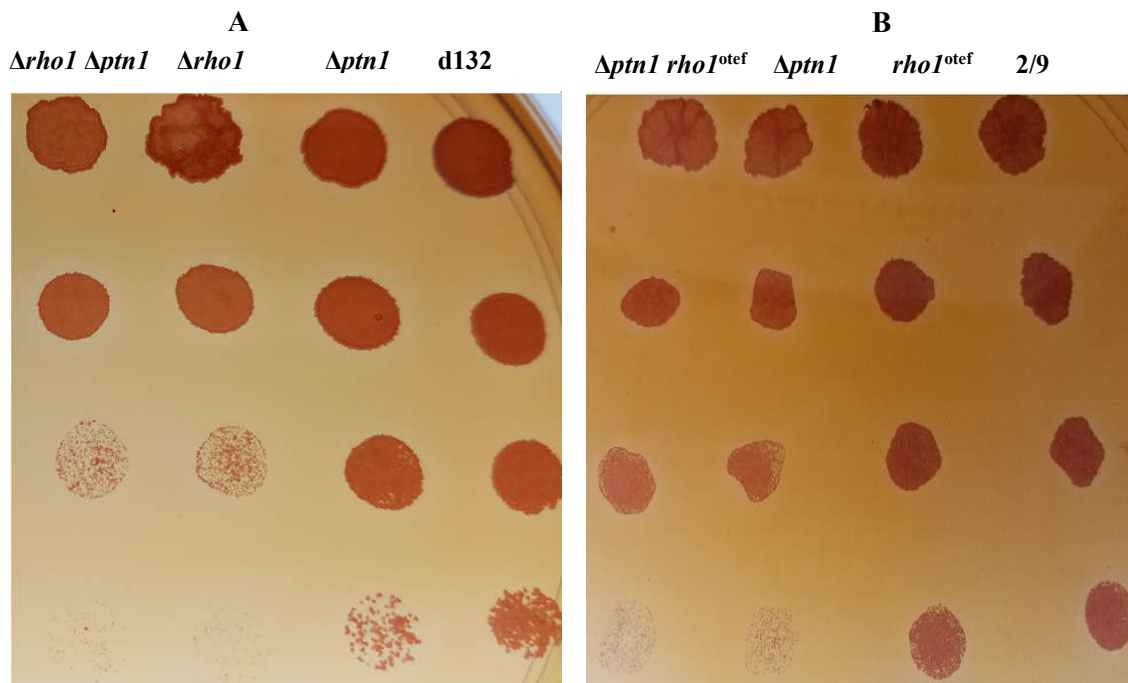


**Figure 3.7.** Cell wall sensitivity assay of *rho1* and *ptn1* mutants. *U. maydis* strains, mutant and wild type, were spotted on to Congo red media plates after serial dilution in the order of undiluted,  $10^{-1}$ ,  $10^{-2}$ , and  $10^{-3}$  (top to bottom). **A.** The deletion of *rho1* increases sensitivity to this cell wall inhibitor, while the deletion of both *rho1* and *ptn1* did not significantly alter the  $\Delta\rho1$  phenotype. **B.** The overexpression of *rho1* in haploid strains does not show any effect on cell wall stress tolerance.

**The deletion or overexpression of *rho1* leads to adverse effects on the virulence of *U. maydis*; overexpression of *rho1* in the *ptn1* deletion background does not significantly alter the virulence of  $\Delta$ *ptn1* strains.** Previous studies conducted in our lab showed that deleting *rho1* in d132 drastically reduces the pathogenicity of the fungus. Here we tested the effects of deletion of *ptn1* in the *rho1* deletion strain. When *ptn1* was deleted in the diploid d132 strain that contains only a single copy of *rho1*, the double deletion did not reverse the phenotype of *rho1* deletion. Both copies of *rho1* are essential for the fungus to infect maize as evidenced by the fact that the d132  $\Delta$ *rho1* deletion strain was unable to cause symptoms. While the deletion of *ptn1* decreased the pathogenicity of the fungus, the effect was not as dramatic as that of *rho1*. In addition, deleting *ptn1* in d132  $\Delta$ *rho1* strains did not rescue the phenotype, indicating that *rho1* may be downstream of *ptn1* if they are in the same pathway. In haploid strains, with and without a concomitant *ptn1* deletion, *rho1* was overexpressed (*i.e.*, 1/2 *rho1*<sup>otef</sup>, 2/9 *rho1*<sup>otef</sup>, 1/2  $\Delta$ *ptn1 rho1*<sup>otef</sup> and 1/2  $\Delta$ *ptn1 rho1*<sup>otef</sup> strains). When the plants were infected using these strains, the disease symptoms were substantially reduced in *rho1*<sup>otef</sup> infected plants compared to those of wild type,  $\Delta$ *ptn1*, and  $\Delta$ *ptn1 rho1*<sup>otef</sup> infected plants (Figure 3.8). The results indicated that normal levels of *rho1* are required for the normal pathological development of the fungus. However, deleting *ptn1* could partially ameliorate the negative effects of *rho1* overexpression. This is evident from the observation that  $\Delta$ *ptn1 rho1*<sup>otef</sup> strains showed significantly higher virulence measures than *rho1*<sup>otef</sup> strains (Kruskal Wallis test, Multiple comparison test, p-value < 0.05), even though  $\Delta$ *ptn1 rho1*<sup>otef</sup> had lower virulence than that of wild type strains.

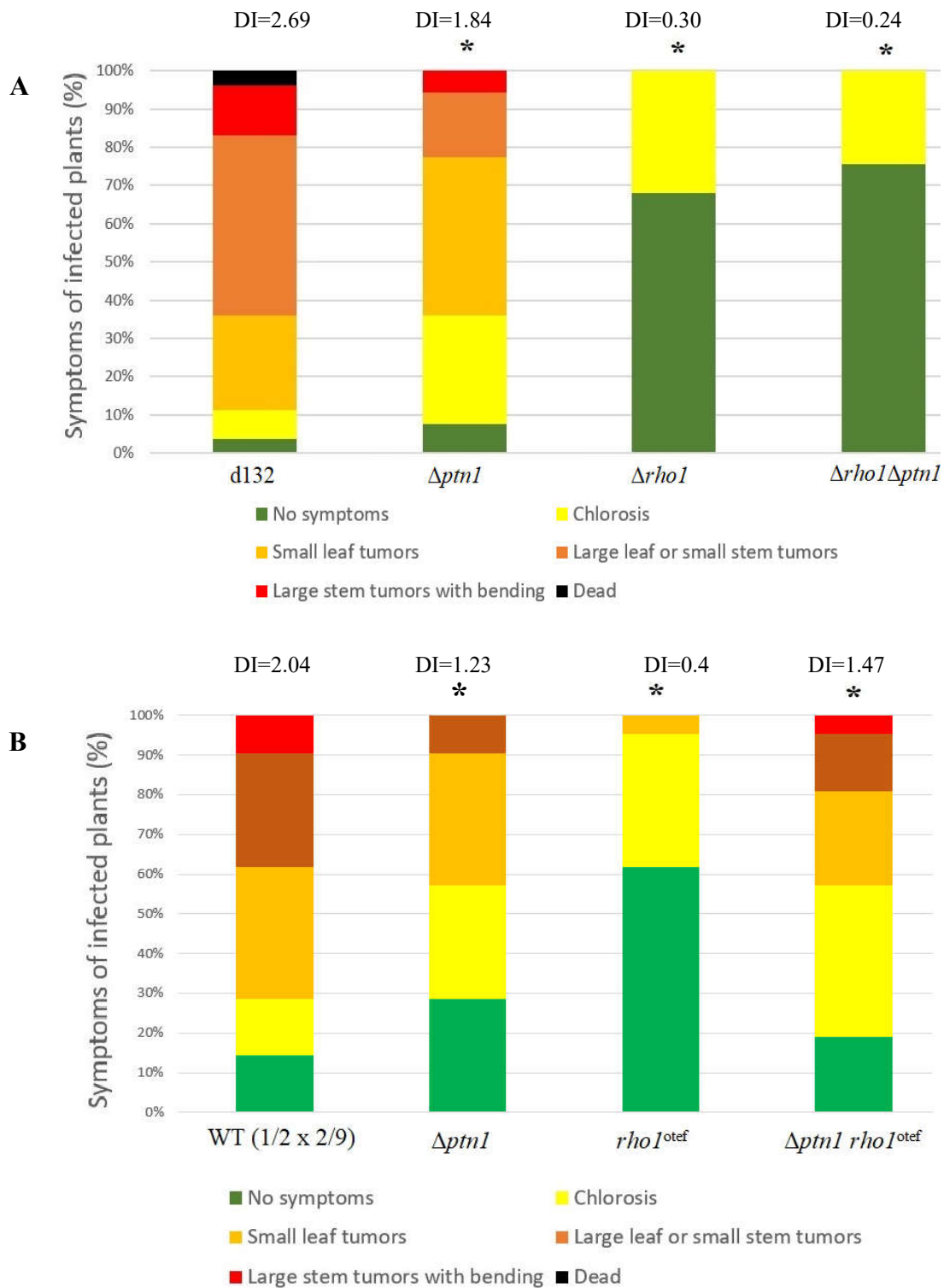
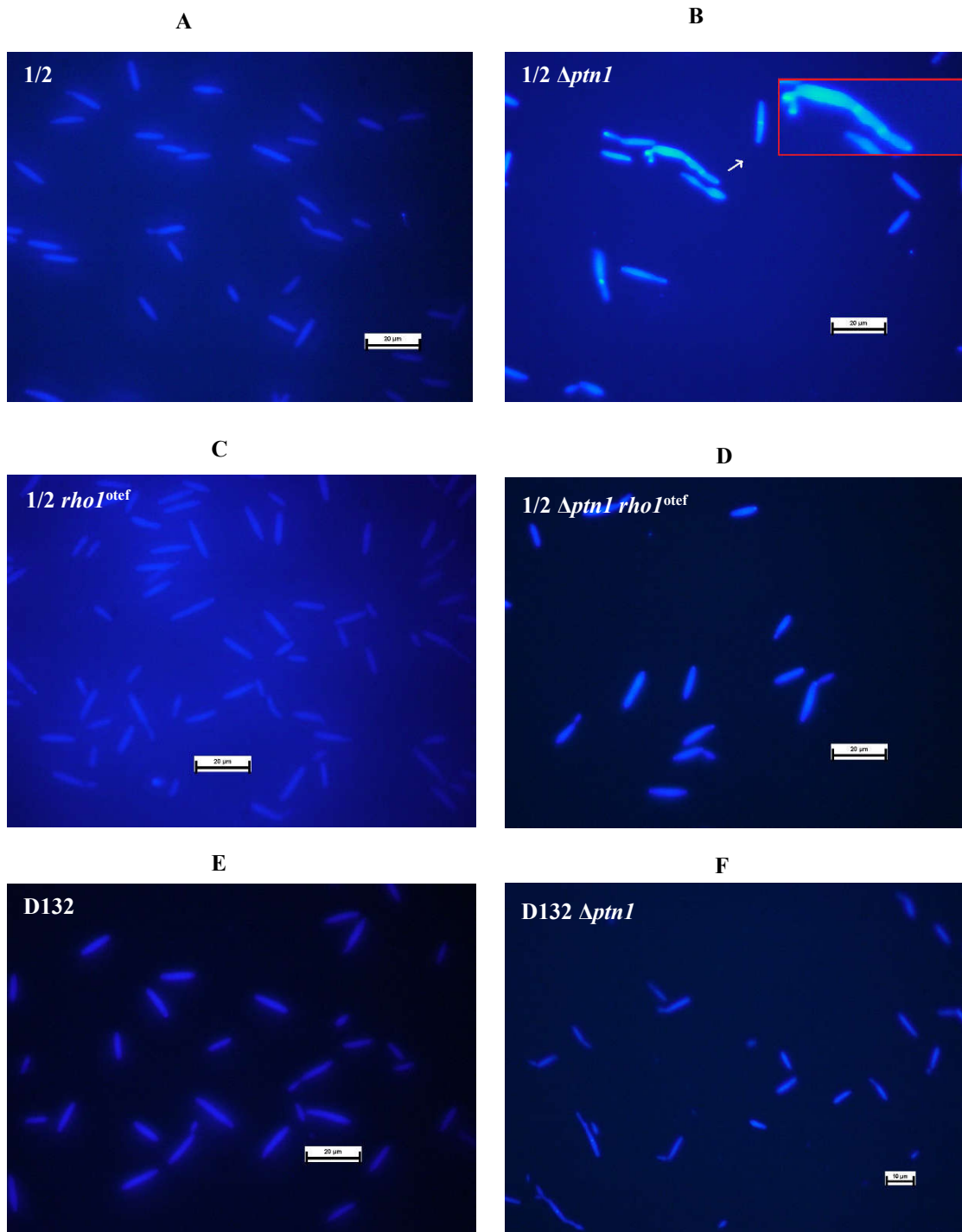


**Figure 3.8.** Testing for the virulence of *rho1* and *ptn1* mutant strains. Statistics were performed using Kruskal-Wallis test followed by multiple comparison post-hoc test. A p-value lower than 0.05 was considered to be significant. **A.** Strains where both *ptn1* and *pdcl* were deleted was compared with *ptn1* deletion, *pdcl* deletion and wild type strains.

The severity of infection of the double deletion strain (d132  $\Delta rho1 \Delta ptn1$ ) was not different from d132  $\Delta rho1$ , however, that of d132  $\Delta ptn1 \Delta rho1$  was significantly different from d132  $\Delta ptn1$  and wild type infection. **B.** Strains where *rho1* alone is overexpressed (*rho1*<sup>otef</sup>) and also strains with *rho1* overexpression in *ptn1* deletion background ( $\Delta ptn1$  *rho1*<sup>otef</sup>) were used. The effect of mutation on pathogenicity were compared between wild type crosses (WT (1/2 x 2/9)),  $\Delta ptn1$  and  $\Delta ptn1$  *rho1*<sup>otef</sup> strains, indicating a difference between strains in the order, *rho1*<sup>otef</sup> <  $\Delta ptn1$  *rho1*<sup>otef</sup> =  $\Delta ptn1$  < wildtype strains.  $\Delta ptn1$  *rho1*<sup>otef</sup> had significantly better infection rates than *rho1*<sup>otef</sup>; *rho1*<sup>otef</sup> showed significantly reduced virulence compared to wild type.

**Deletion of both *rho1* and *ptn1* did not significantly change the  $\Delta rho1$  cell morphology**

**phenotype.** The depletion of *rho1* was found to result in abnormal cell morphology (Pham et al., 2009). The abnormal cell morphology is characterized by more branching than the wild type cells. Here we explored the effect of *ptn1* deletion on the *rho1* deleted cells. The wild type and mutant cells were stained using calcofluor white stain, a  $\beta$ -glucan specific cell wall stain (Aimanianda et al., 2017). While the wild type d132 and d132  $\Delta ptn1$  cells appeared as characteristic elongated single cells, the d132  $\Delta rho1$  and d132  $\Delta rho1 \Delta ptn1$  cells showed a branched phenotype as observed in the case of d132  $\Delta pdc1 \Delta ptn1$  mutants. Unlike the *pdc1* deletion, the deletion of *ptn1* in *rho1* deletion strains did not appear to increase or decrease the severity of morphology defect shown by the d132  $\Delta rho1$  strain. Similarly, the deletion of *ptn1* in the haploid background had a minor effect on the morphology of the cells, leading to some cells appearing as multiseptated (see Figure 3.9 B). The overexpression of *rho1* did not appear to have an effect on the morphology, both in the case of *rho1*<sup>otef</sup> and  $\Delta ptn1$  *rho1*<sup>otef</sup> cells.



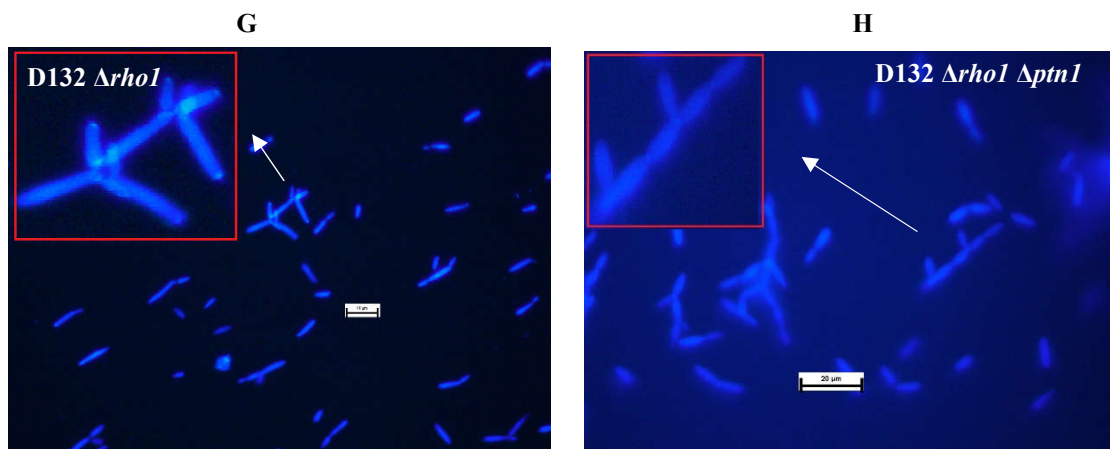


**Figure 3.9** Morphology of wild type and mutant *rho1* and *ptn1* strains. Deletion of *rho1* leads to an increase in aberrant morphology while *ptn1* deletion results in a minor defect in morphology; the *rho1 ptn1* double deletion mutant does not differ significantly from the *rho1* deletion mutant. The panels A, B, C, and D represents the comparison of the morphology of the haploid strains, wild type,  $\Delta pt n 1$ ,  $rho 1^{ote f}$  and  $\Delta pt n 1 rho 1^{ote f}$  strains. Panels E, F, G and H represent the diploid strains, wildtype d132, d132  $\Delta rho 1$ , d132  $\Delta pt n 1$ , d132  $\Delta rho 1 \Delta pt n 1$ . Size bar for A, B, C, D, E and H is 20  $\mu m$ ; size bar for F and G is 10  $\mu m$ .

**Effect on spore germination.** As our earlier experiments have shown that the deletion of *ptn1* results in reduced spore germination rate, the effect of the overexpression of *pdcl* or *rho1* in cells that lack a *ptn1* gene was examined. The tumors from plants infected with wild type and mutant strains were harvested and subjected to the extraction of teliospores and subsequent germination of the spores. The various treatment groups included tumors from plants infected with wild type,  $\Delta pt n 1$ ,  $pd c 1^{ote f}$ ,  $rho 1^{ote f}$ ,  $\Delta pt n 1 pd c 1^{ote f}$ , and  $\Delta pt n 1 rho 1^{ote f}$ . The spores were extracted from the tumors and counted using hemocytometer. Fewer number of spores were found in the tumors of  $\Delta pt n 1$  compared to wild type as expected; moreover,  $rho 1^{ote f}$  showed a substantial reduction in spore count while the other mutant strains had spore count more or less comparable to wild type levels.

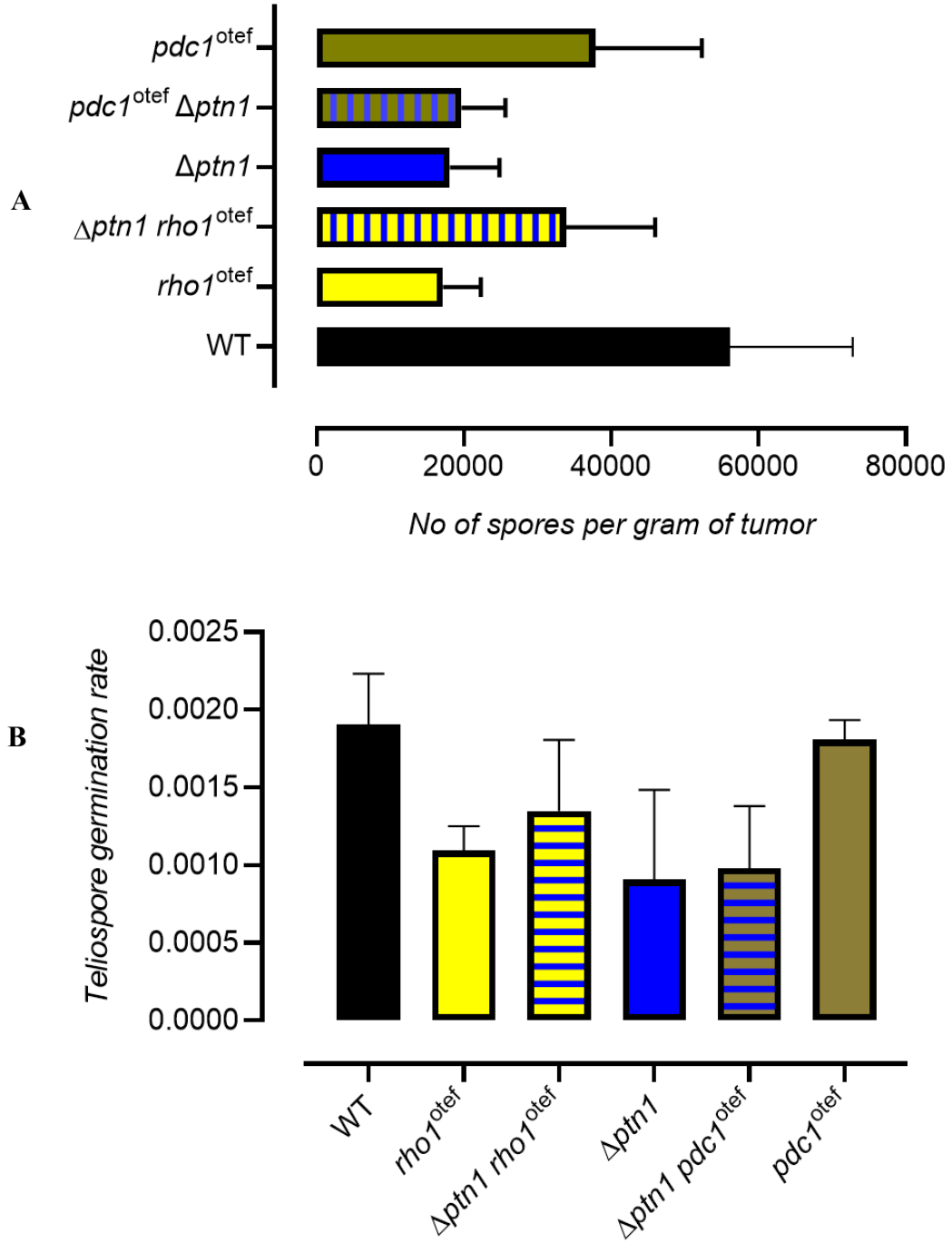


**Figure 3.10.** Spore count and teliospore germination rate. Spores were extracted from plant tumors produced from infection with different treatment groups (wild type,  $\Delta ptn1$ ,  $rho1^{otef}$ ,  $pdcl^{otef}$ ,  $\Delta ptn1 rho1^{otef}$ , and  $\Delta ptn1 pdcl^{otef}$ ). **A.** Spore count was obtained using a hemocytometer. Spore production from  $\Delta ptn1$  (p-value = 0.0663) and  $rho1^{otef}$  (p-value = 0.0580) was greatly reduced compared to wild type. **B.** Spore germination was calculated by counting the number of colonies germinated from spores plated on water agar plates incubated at 30 °C for 72 hours. Spore germination was reduced in  $\Delta ptn1$  treatment group



as expected (p-value = 0.0824); spore germination rate of  $\Delta ptn1 pdc1^{otef}$  treatment group showed a downward trend while others were more comparable to wild type levels.

The spore germination rate of  $\Delta ptn1$  was reduced as expected. Spores from  $rho1^{otef}$  treatment group displayed a lower germination rate than that of the wild type or  $pdc1^{otef}$  treatment groups. However, the difference was not found to be statistically significant in both cases. The results indicated that overexpressing  $rho1$  had a negative effect on spore formation but not on spore germination; overexpressing  $pdc1$  did not appear to have an effect on spore formation but, the spore germination showed a downward trend when overexpressed in  $\Delta ptn1$  background.

## DISCUSSION

Numerous studies conducted in mammalian systems and other model systems have established the interplay between 14-3-3 proteins, Rho GTPase, and PTEN proteins of the mTOR and associated signaling pathways. Here, we studied the epistatic interaction between the  $rho1$ ,  $pdc1$  and  $ptn1$  genes as their respective proteins are known to physically interact with each other in *U. maydis* (Pham et al., 2009). Previous experiments have demonstrated that the deletion of  $ptn1$  in the haploid background will cause defects in the mating process especially during the initial 24 hours. However, when  $pdc1$  was overexpressed in these strains, it resulted in further reduction in aerial hyphae formation compared to  $\Delta ptn1$  strains. It has been found previously that  $pdc1$  is not essential for aerial hyphal formation in *U. maydis* (Pham et al., 2009). However, we observed a reduction in aerial hyphae formation when  $pdc1$  was overexpressed along with the deletion of  $ptn1$ , exacerbating the  $\Delta ptn1$  phenotype, whereas the overexpression of  $pdc1$  alone did not alter

the wild type phenotype. It is possible that in the absence of *ptn1*, the overexpressed *pdcl* acts on alternate targets. An alternative explanation is that the overexpression of *pdcl* is unchecked in the absence of *ptn1*, indicating *ptn1* as a potential direct modulator of *pdcl*. This holds true in the case of most of the other phenotypes exhibited by the  $\Delta pt n 1$  *pdcl*<sup>otef</sup> strains. The  $\Delta pt n 1$  *pdcl*<sup>otef</sup> strains exhibited reduced stress tolerance ability than the  $\Delta pt n 1$  strains when spotted onto plates containing the cell wall antagonist, Congo red. The overexpression of *pdcl* in the *ptn1* deletion background also affected the growth of the fungus; the  $\Delta pt n 1$  *pdcl*<sup>otef</sup> strains showed reduced growth rates when compared to  $\Delta pt n 1$  strains. The growth defect was tested in both solid and liquid media with both exhibiting similar results. When plants were infected with these strains, the disease symptoms were reduced even compared to  $\Delta pt n 1$  infected plants. In *Paracoccidioides brasiliensis*, a human fungal pathogen, reduced gene expression of Pb14-3-3 led to a reduction in fungal virulence (Marcos et al., 2016). Similarly, in our study the *pdcl* deletion in the d132 strains reduced infection. Also, it has been demonstrated in *Funneliformis mosseae*, an arbuscular mycorrhizal fungi which forms a symbiotic relationship with its host plants, that 14-3-3 genes are highly induced during the early stages of the fungal-plant symbiotic interaction (Sun, Song, Xin, Xie, & Zhao, 2018). These data suggest the possibility of *pdcl* having a role in host interaction and pathogenesis. Also, the gene expression levels of 14-3-3 proteins of *F. mosseae* and *Rhizophagus irregularis* such as, Fm201 (*F. mosseae* 14-3-3 orthologue), Ri14-3-3, and RiBMH2 (*R. irregularis* 14-3-3 orthologues), are strongly induced in germinating spores (Sun et al., 2018). However, the overexpression of *pdcl* in *U. maydis* did not significantly alter the  $\Delta pt n 1$  spore germination profile, though a marginal improvement was observed. The effect of overexpression of *pdcl* alone was also tested

with various phenotypic assays to serve as a control. In *S. pombe*, the overexpression of *rad24* or *rad25* (14-3-3 orthologues) resulted in reduced mating and sporulation (Ozoe et al., 2002). However, in *U. maydis*, the overexpression of *pdcl* by itself did not appear to significantly alter most observed phenotypes. This confirms that the phenotypes that we observe in the  $\Delta ptn1$  *pdcl*<sup>otef</sup> strains are due to *pdcl* overexpression in conjunction with the absence of *ptn1*. Overall the overexpression of *pdcl* in  $\Delta ptn1$  did not rescue the phenotypes resulting from *ptn1* deletion, but rather, it aggravated the effects. The deletion of *pdcl* and *ptn1* resulted in a cumulative effect; the d132  $\Delta ptn1$   $\Delta pdcl$  strains were more stress sensitive and less virulent than the d132  $\Delta ptn1$  or d132  $\Delta pdcl$  strains. While the simultaneous deletion of *ptn1* and *pdcl* produced a combined phenotypic effect, the deletion of each of them by itself did not lead to significant stress phenotype in the diploid background. Studies conducted in the model plant, *Medicago truncatula*, found that 14-3-3 proteins are involved in stress response to salinity stress (Sun et al., 2018). The yeast ortholog of 14-3-3, *bmh1*, when deleted resulted in sensitivity to cell wall stress (Lottersberger et al., 2006). Thus, it is possible that *pdcl* is part of a pathway that is related to maintaining cell wall integrity to which *ptn1* is also a part.

The overexpression of *rho1* in  $\Delta ptn1$  strains did not yield any significant phenotype in the mating assay or Congo red stress test; the  $\Delta ptn1$  *rho1*<sup>otef</sup> strains showed phenotypes similar to  $\Delta ptn1$  strains. However, we know that both copies of *rho1* are required for production of aerial hyphae and plant infection (Pham & Perlin, 2010). The plants infected with *rho1* overexpression strains resulted in severe reduction in virulence. A recent study in *Epichloë festucae*, an endophytic fungus, demonstrated the role of small GTPase proteins (Cdc42 and RacA) in the regulation of *E. festucae* growth in planta, where the

mutation of these genes resulted in reduced plant infection (Kayano, Tanaka, & Takemoto, 2018). However, the plant infection assay indicated that the virulence of the  $\Delta ptn1$   $rho1^{otef}$  strains appeared to have marginally improved when compared to that of the  $\Delta ptn1$  strains, considering a slight increase in disease symptoms and a slightly greater number of spores. Also, the overexpression of  $rho1^{otef}$  in  $\Delta ptn1$  strains appears to have slightly improved the spore germination rate. The immunofluorescence experiments studying the localization of RhoA protein in the fungus, *Phycomyces blakesleeanus*, showed that it is expressed differentially during spore germination (Ramírez-Ramírez, García-Soto, González-Hernández, & Martínez-Cadena, 1999). In addition, the role of Rho-GTPases, AgRho1a and AgRho1b, in regulating spore length and spore wall integrity is demonstrated in the filamentous fungus *Ashbya gossypii* (Lickfeld & Schmitz, 2012). The double deletion strain, d132  $\Delta ptn1$   $\Delta rho1$ , showed phenotypes similar to those of d132  $\Delta rho1$ , i.e., the deletion of  $ptn1$  in  $rho1$  deleted strains did not significantly alter the d132  $\Delta rho1$  phenotype. The d132  $\Delta ptn1$   $\Delta rho1$  strains exhibited similar aerial hyphae, stress tolerance, and plant infection phenotypes as those of d132  $\Delta rho1$ . In general, this suggests that deletion of  $rho1$  is dominant or epistatic to that of  $ptn1$ , however, the overexpression of  $rho1$  only partially rescued the  $ptn1$  deletion phenotype. The importance of Rho GTPase in cell wall synthesis is established in *S. pombe* where it has been shown that the Rho1 and Rho2 are important for cell wall synthesis (Arellano, Coll, & Perez, 1999; Cabib, Drgonova, & Drgon, 1998) while Rho3 plays a substantial role in polarized cell growth (Nakano et al., 2002). Our results are consistent with this finding; however, it also indicates that the  $\Delta rho1$  phenotype is epistatic to  $\Delta ptn1$  phenotype.

Our recent plant infections, including those using wild type strains, were not as robust as the previous infections. The lower infection rate may be due to some unknown change in the growth conditions in the growth chamber or growing the strains in less optimal conditions before plant infection. Due to the lack of availability of a 28 ° C shaker lately, the fungal strains were shaken at room temperature conditions which might not be ideal for a robust plant infection. However, the fact that infection pattern of the different treatment groups followed the same trend as the past infections makes it reasonably reliable irrespective of the slightly lower infection rates.

The mutation in *rho1*, *pdcl* and *ptn1* appears to have an effect on the morphology of the fungal cells. Previous studies have shown that depletion of *rho1* and *pdcl* genes result in cellular morphological defects. Our experiments exploring the morphology of the mutant strains have confirmed that the overexpression of these genes in a *ptn1* deletion background is associated with morphological phenotypes. The  $\Delta ptn1 pdc1^{otef}$  strains showed an increase in branching of the cells, indicating that the overexpression of *pdcl* in the *ptn1* deletion background affects the cell separation process. 14-3-3 proteins in *Cryptococcus neoformans* are known to play a role in cell morphology since 14-3-3 mutant strains displayed enlarged cell size, and drastic changes in morphology (J. Li et al., 2016). Also, the 14-3-3 orthologue of *Aspergillus nidulans*, *artA*, is believed to play a role in the formation of septum during cytokinesis (Kraus, Hofmann, & Harris, 2002). Some of the  $\Delta ptn1$  cells exhibited an unusual morphology, characterized by long cells with cross walls, rather than the branched phenotype as seen in  $\Delta ptn1 pdc1^{otef}$ . The deletion of both *ptn1* and *pdcl* appear to have marginally worsened the d132  $\Delta pdcl$  phenotype; more of the d132  $\Delta pdcl \Delta ptn1$  cells appear to have branched morphology. In contrast, the d132  $\Delta rho1 \Delta ptn1$

cells showed the characteristic branched morphology seen in d132  $\Delta\rho h o 1$ , essentially indicating that the  $\Delta\rho h o 1 \Delta p t n 1$  double deletion follows the same trend across all phenotypes tested *i.e.*, cell wall stress, aerial hyphae formation and plant infection profile. This is consistent with the finding that the depletion of RhoA, RhoB and RhoC proteins in mammalian glioblastoma cells results in altered cellular morphology suggesting the role of such proteins in cell morphology and proliferation (Tseliou et al., 2016). However, our studies indicate that the overexpression of  $\rho h o 1$  by itself or in  $\Delta p t n 1$  strains did not have a significant effect on the morphology. Perhaps this is due to the fact that  $\rho h o 1$  used in overexpression here was not specifically in its activated form. We are currently conducting these studies using a mutant variant of Rho1 that is constitutively activated.

Several lines of evidence suggest a common role for PTEN, 14-3-3 and RhoA proteins in cytoskeletal organization. It has been demonstrated that these proteins are required for actin filament formation and microtubular organization (Brandwein & Wang, 2017; Krtková et al., 2017; Wittmann & Waterman-Storer, 2001). Our studies suggest the existence of an epistatic interaction between  $p t n 1$ ,  $p d c 1$  and  $\rho h o 1$  as evidenced by the phenotypic traits of the various mutant strains. The phenotypes indicate that these genes are involved in functions associated with cell wall stress tolerance, maintaining morphology and virulence. It is possible that they participate in the activation of signal transduction pathways related to cell wall integrity and cytoskeletal reorganizations.

## CHAPTER IV

### DELETION OF AGA1 OF *USTILAGO MAYDIS* LEADS TO MORPHOLOGICAL DEFECTS AND REDUCED STRESS TOLERANCE

#### SUMMARY

This project was initiated as a natural extension of the exploration of PTEN related pathways. However, it was later noticed that the gene has been explored in the SG200 strain background in a different lab, the results of which showed that *agal* is central to the formation of appressoria in *U. maydis*. *Agal* is a serine-threonine kinase belonging to the AGC kinase family. Here we confirm previously described phenotypes of *agal* using strains of the 1/2 and 2/9 haploid backgrounds. Also, we explored the effect of *agal* deletion on the morphology of the fungus, its ability to grow under low ammonium conditions, and to tolerate a variety of stress agents. Our study shows additional phenotypes indicating potential effect of gene disruption on cell wall and cell morphology. Furthermore, the deletion strains appeared to be sensitive to ionic stress, especially from LiCl.

#### INTRODUCTION

Among the various signaling pathways, the mTOR pathway is very significant one with an intricate network of kinases, phosphatases and other proteins that control various metabolic activities. mTOR (mammalian Target Of Rapamycin) is a protein kinase that regulates cell growth in response to nutrients, growth factors, and acts as a sensor of

nutrient availability in the cell (Tavares et al., 2015). One among the key actors of the mTOR pathway are the S6Ks (ribosomal protein kinase) which belongs to the AGC kinase family (Magnuson, Ekim, & Fingar, 2012). The consensus CAT domain is almost 90% identical among the Akt isoforms and also among the AGC kinase subfamilies such as PKC, PKA, SGK, and S6 (Kumar & Madison, 2005). One of the ways through which mTOR and PI3K exert control on cell growth is through the phosphorylation of S6K1 which in turn phosphorylates SKAR, a nuclear protein (Richardson et al., 2004). Studies have shown that S6K1 plays a role in neuronal growth and survival through the CRMP-2 protein expression which is controlled by the PI3K-mTOR-S6K signaling axis (Na et al., 2017). It has been shown that S6K(p70<sup>S6K</sup>) colocalizes with actin stress fibers in Swiss 3T3 fibroblasts cells (Leise A. Berven, Francis S. Willard, & Michael F. Crouch, 2004). Neoangiogenesis is a vital process which happens in response to adverse events such as pathogen attack or cancer where the formation of new blood vessels from existing ones ensures the supply of oxygen and nutrients thereby decreasing cell death (Zarrinpashneh et al., 2013). It has been shown that the activation of mTOR-S6K pathway plays a significant role in hepatocellular carcinoma progression by promoting neoangiogenesis in endothelial cells (W. Li, Tan, Zhang, Liang, & Brown, 2008). In *Saccharomyces cerevisiae* phosphorylation of Ypk2p (S6K1 orthologue) by Tor2p (mTORC1 orthologue) is required for actin organization and regulation of cell wall integrity. In *U. maydis*, studies conducted using SG200 strains have shown that *agal*, a potential *S6K1* orthologue, is required for actin-mediated endocytosis and in the maintenance of actin cytoskeleton (Berndt, Lanver, & Kahmann, 2010).



In the present study we confirm the role of *aga1* in mating and pathogenicity using strains from the 1/2 and 2/9 backgrounds while we also explore the role of this gene in stress tolerance and the effect of low ammonium on the growth of the deletion strains. The results indicate that the deletion of *aga1* alters the cellular morphology, and leads to reduced growth under low ammonium conditions. Furthermore, the study points out that *aga1* is vital for the cell to endure cell wall, osmotic and ionic stresses.

## MATERIALS AND METHODS

**Strains and growth conditions.** *Ustilago maydis* strains employed in this study are listed in Table 4.1. *Escherichia coli* strains DH5- $\alpha$  and TOP10 (Invitrogen/ Thermo Fisher) were used for all bacterial cloning and plasmid amplification reactions. *U. maydis* strains were grown in media and conditions as described in materials and methods of chapter II.

**Table 4.1. Strains used in this study.**

<b>List of strains</b>		
<i>Ustilago maydis</i> Strain	Genotype	References
1/2	<i>alb1</i>	(Gold et al., 1997)
2/9	<i>a2b2</i>	(Gold et al., 1997)
1/2 $\Delta$ <i>aga1</i>	<i>alb1 aga1::hyg<sup>R</sup></i>	This study
2/9 $\Delta$ <i>aga1</i>	<i>a2b2 aga1::hyg<sup>R</sup></i>	This study

**Genetic manipulation and vector construction.** The design of primers, PCR, vector construction, cloning reactions, deletion construction, and *U. maydis* transformations, were performed as described previously (Materials and Methods, Chapter II).

**Growth rate, cell wall stress tests, mating assays, and plant infection assays.** Growth rate measurements, cell wall stress tests, mating assays, and plant infection assays, were performed as described in Materials and Methods of Chapter II.

**Low ammonium studies using SLAD media.** *U. maydis* strains were grown at 27 °C in YEP (1% yeast extract, 2% peptone) supplemented with 2% sucrose or dextrose and SLAD (0.17% yeast nitrogen base without ammonium sulfate or amino acids [YNB] with 2% dextrose and 10 µM or 30 µM ammonium sulfate) (Lovely et al., 2011).

**Staining and microscopy.** *U. maydis* strains were stained with calcofluor white and subjected to microscopic analysis as described previously (Lovely et al., 2011; Pham et al., 2009).

## RESULTS

**The deficiency of *agal* results in some mating abnormalities, indicating potential defect in hyphal filament formation.** When two compatible haploid wild type cells are combined on charcoal-containing plates, it results in the formation of dikaryotic hyphae (Steinberg et al., 1998). Compatible strains of wildtype and *agal* deletion strains of *U. maydis* were spotted on activated charcoal plates to investigate the effect of *agal* gene deletion on the ability of the fungus to produce aerial hyphae representative of successful mating. The filamentous growth is indicated by the appearance of aerial hyphae giving a ‘white fuzzy’ appearance as can be seen in the case of the wildtype cross (1/2 x 2/9) (Figure 4.1). The deletion mutants of *agal* showed a drastic reduction in aerial hyphae indicating potential mating defects. When the mutant strain was mated with its corresponding

wildtype mating partner *i.e.*,  $1/2 \Delta agal \times 2/9$  and  $1/2 \times 2/9 \Delta agal$ , it did not show a substantial difference in white ‘fuzz’ phenotype.

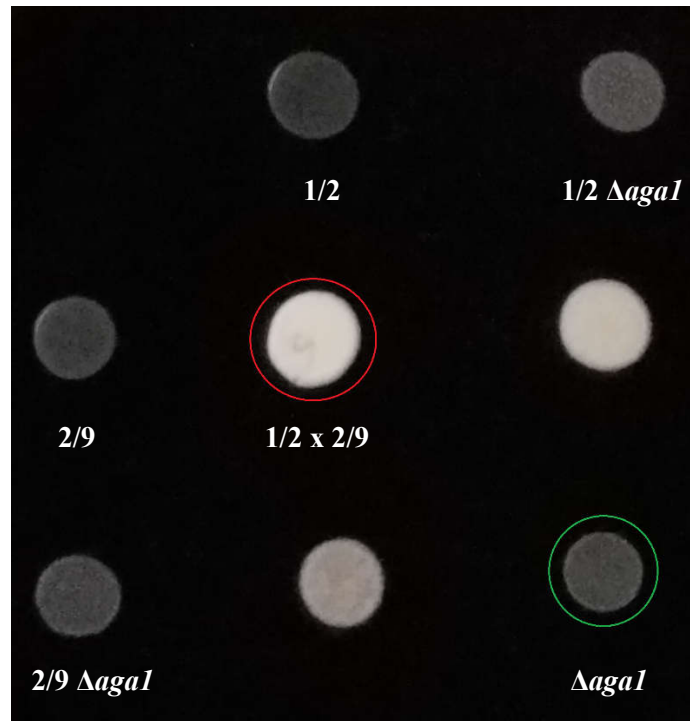


**Figure 4.1.** Charcoal assay showing defect in aerial hyphae formation 24 hours post-mating. These data show that only mutant x mutant results in a reduction in white ‘fuzz’ representative of the aerial hyphae.

**The *agal* gene is required for complete symptom development in plants.** The infection of *U. maydis* cause the plants to produce anthocyanin pigment and results in the formation of tumors that are filled with fungal hyphae that will ultimately differentiate into teliospores (Banuett & Herskowitz, 1996). The capability of  $\Delta agal$  strains to infect the plants were tested by injecting an inoculum containing opposite mating types of the fungus and comparing the wildtype treatment group ( $1/2 \times 2/9$ ) with the mutant treatment group ( $1/2 \Delta agal \times 2/9 \Delta agal$ ). The wild type treatment group plants were able to infect the plants and produce tumors and eventually teliospores while the mutant treatment group plants showed severely reduced plant infection symptoms.

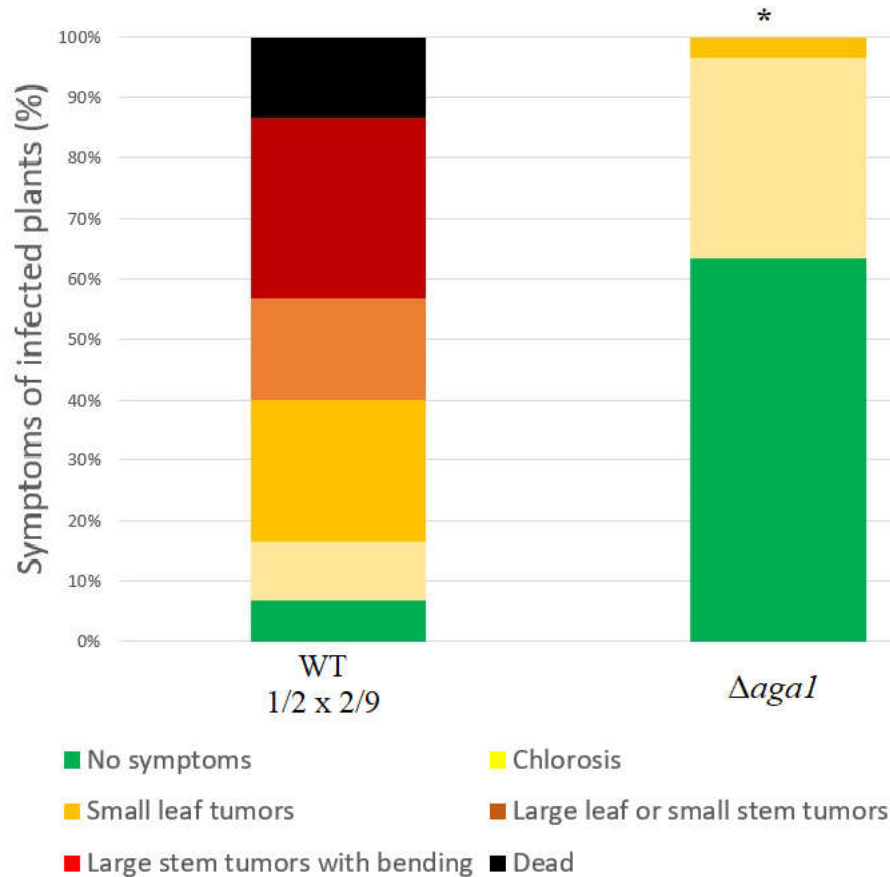


**Figure 4.2.** Virulence assay and analysis of symptoms in planta. Leaves of maize plants were inoculated with either with wildtype (1/2 x 2/9) or deletion strains (1/2  $\Deltaagal$  x 2/9  $\Deltaagal$ ). Plants were scored based on the disease score index; as shown in the graph, *agal* mutants exhibited drastically reduced symptoms.

The majority of plants (~60%) did not show any disease symptoms. Some (30%) showed chlorosis and just 3% produced very tiny leaf tumors (Figure 4.2). This is consistent with the studies conducted in SG200 strains where the fungus lacking a functional *agal* gene could not produce appressoria (Berndt et al., 2010) and hence were unable to enter the plant.

**The growth of *agal* deletion strain is considerably slower compared to the non-deletion strain.** We confirmed the effect of *agal* deletion on the growth of the fungus by plotting growth curves. The growth rate curve of wild type and *agal* deletion strains were

performed by determining the optical density (absorbance) at 600 nm at various time points. The results indicated that  $\Delta agal$  strains have a lower growth rate when compared to the wild type (Figure 4.3) and the difference was found to be statistically significant. This observation is consistent with the *S6K1* studies in other systems. The deletion of *dS6K*, orthologue of *S6K1*, in *Drosophila* caused an extreme delay in development and a severe reduction in body size (Montagne et al., 1999). Similarly, the deletion of *S6K1* in mouse had a significant effect on the size of the animal (Shima et al., 1998), whereas the overexpression of *S6K1* in cell culture increased the cell size (Fingar, Salama, Tsou, Harlow, & Blenis, 2002).

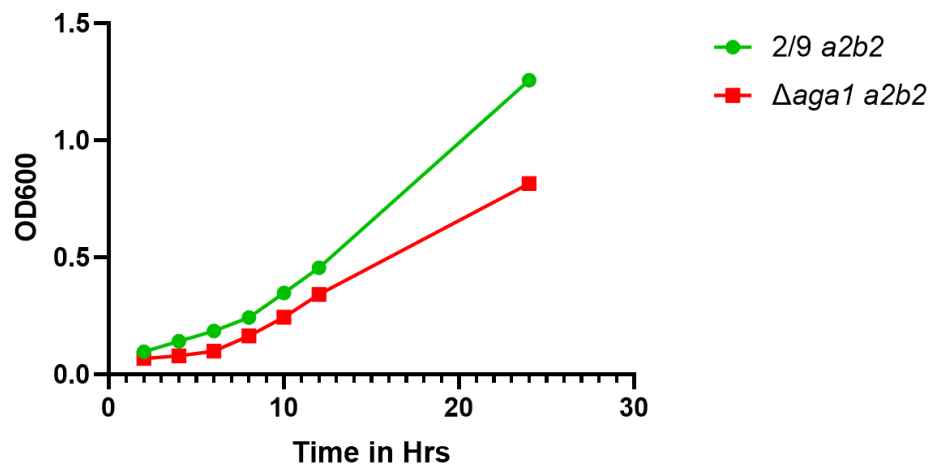


**Figure 4.3.** Assay comparing the growth of wildtype with  $\Delta agal$  strains. It appears that the deletion reduces the rate of growth.

**Deletion of *agal* results in an abnormal cell morphology.** The slow rate of growth for *agal* deletion mutants led us to investigate the effects of deletion on cell morphology. Cells, wildtype and *agal* deletion strains, grown overnight to an OD600 of 0.6- 0.8 were used for microscopic analysis. Light microscopy analysis revealed that a greater number of  $\Delta agal$  mutant cells appear as multi-septate filaments. Staining with calcofluor stain showed that the cell clusters having cells joined together without separating from the parent

cell, possibly contained only single cross wall separating compartments as described previously in a *rho1* study (Lovely et al., 2011; Pham et al., 2009) This observation further supports the idea that *agal* is required for normal cell growth and cell separation.

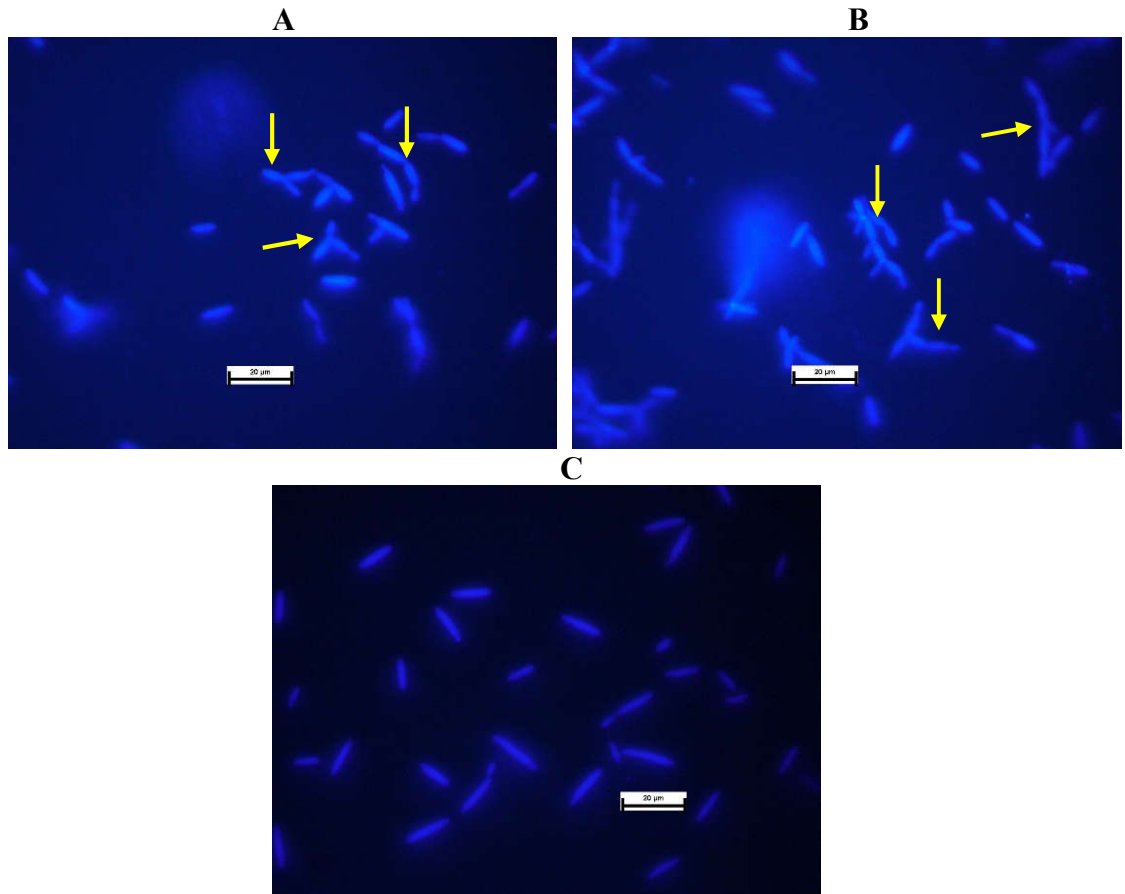


**Figure 4.4.** Defects in cell morphology as observed through calcofluor staining of fungal cells. The *agal* mutants exhibited cell separation defects. Top panel (A) and (B) shows *agal* mutants in 2/9 background and the bottom panel (C) shows wildtype 2/9 strain. The size bar represents 20 µm.

**Deletion of *agal* makes the fungus less tolerant to stressful conditions.** The ability of microorganisms to adjust to extreme conditions such as high temperature and changes in osmolarity is critical for survival. While sorbitol can stabilize proteins or cell membrane, it can be used to induce an osmotic stress on yeast mainly because it does not dissociate into ions in liquids and cannot be assimilated by yeast. Thus, it can be used as a stress agent

to study the effect of osmotic stress on yeast (Hirasawa et al., 2006; Salmerón-Santiago et al., 2011) or other fungi. The effect of the *aga1* deletion on the ability of the fungus to deal with osmotic stress was tested on YPS agar plates containing 1M NaCl or 1 M sorbitol for 24-48 hours and comparing the phenotypes with those of wildtype.

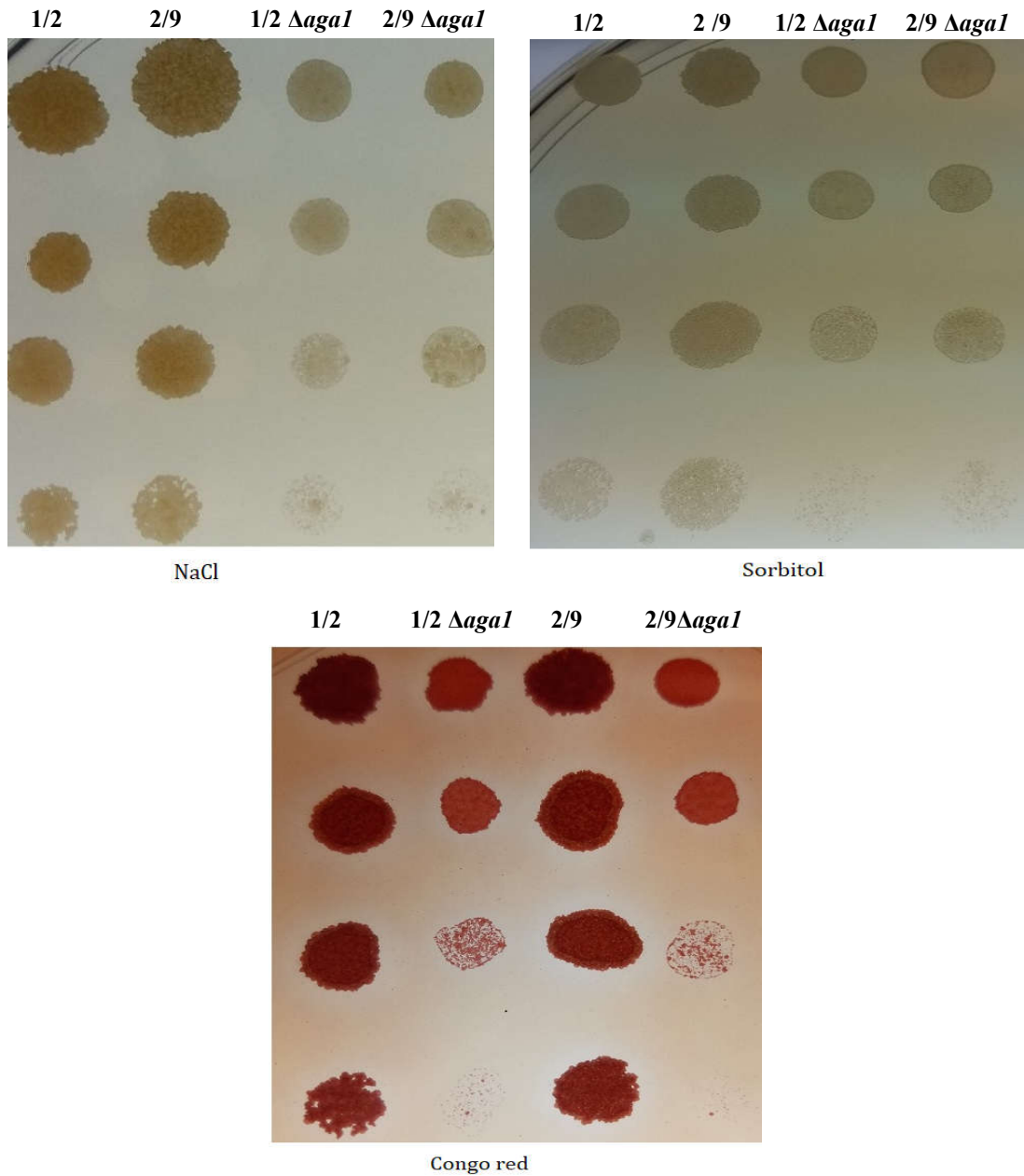


**Figure 4.5.** Osmotic and cell wall stress assays testing the effect of *aga1* deletion on stress tolerance. Top panel shows the growth of wildtype and *aga1* on 1M NaCl and sorbitol plates after serial dilution, full strength, 10<sup>-1</sup>, 10<sup>-2</sup>, and 10<sup>-3</sup> from top to bottom of each

plate. Bottom panel is the stress test with Congo red after serial dilution, full strength,  $10^{-1}$ ,  $10^{-2}$ , and  $10^{-3}$ .  $\Delta agal$  mutants have a lower stress tolerance to cell wall and osmotic stress agents

The *agal* deletion strains did not grow as much as the wildtype strains on either NaCl plates or on sorbitol plates (From Figure 4.5), indicating that the deletion had a deleterious effect on the ability of the fungus to cope with osmotic stress. Congo red is a cell wall stress agent that inhibits chitin microfibril assembly (Roncero & Duran, 1985). The  $\Delta agal$  mutants also showed increased sensitivity to Congo red, a cell wall antagonist. In *Candida albicans*, it has been observed that one of the ways through which the cells respond to wall stress is to strengthen the cell wall by increasing the chitin production (Heilmann et al., 2013; K. K. Lee et al., 2012). In *S. cerevisiae* thermal stress causes the activation of the cell wall integrity pathway (Levin, 2005). Studies of *U. maydis* SG200 strains indicate that *agal* is vital for cytoskeleton maintenance (Berndt et al., 2010). The sensitivity of  $\Delta agal$  strains to various stress agents demonstrates that this gene is important in the protection of the fungus to diverse and adverse environmental conditions.

**Effect of LiCl on *agal* deletion strains.** Lithium is widely used to treat bipolar disorder (Manji & Lenox, 2000). It alters several biochemical and molecular signal transduction cascades, hormonal and circadian regulation, ion transport, and gene expression (Machado-Vieira, Manji, & Zarate, 2009). Recent studies have shown that  $\text{Li}^+$  ions alter the mTOR dependent autophagy processes in mammalian systems (Motoi, Shimada, Ishiguro, & Hattori, 2014). As S6K1 is part of the mTOR pathway, we were curious to test the effect of lithium on cells lacking *agal*. Moreover, lithium also can act as a stress agent in fungi, for instance, lithium results in the suppression of hyphal outgrowth in *Candida albicans* (Martins et al., 2008). Serial dilution of wildtype and *agal* mutant strains overnight culture



were spotted on to YPS agar plates containing LiCl and allowed to grow for 24-48 hours. The growth of the *aga1* mutants was severely restricted when compared to that of wildtype. The ability of *aga1* cells to grow was further reduced with increase in concentration (5mM to 10mM) of LiCl (Figure 4.6).

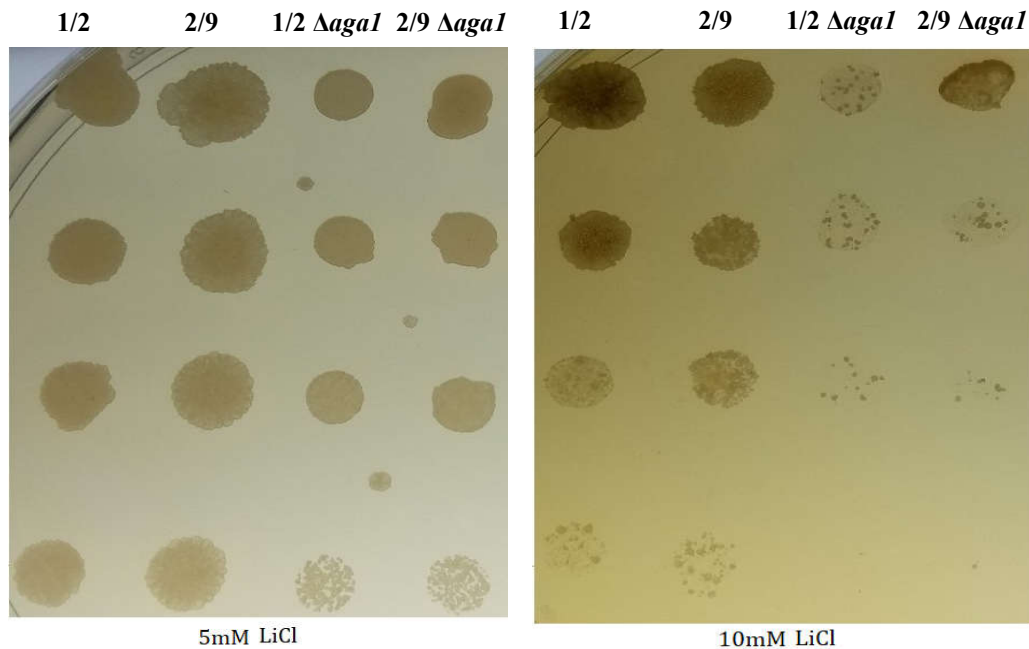


**Figure 4.6.** Testing the effect of LiCl on *U. maydis* strains. Wildtype and *aga1* strains of a1b1 and a2b2 mating background tested on YPS agar-LiCl plates by spotting after serial dilution, ordered (top to bottom) from full strength,  $10^{-1}$ ,  $10^{-2}$ , and  $10^{-3}$ . Results indicate a significant LiCl-sensitive phenotype

***aga1* deletion strains show less growth and filamentation in low ammonium**

**conditions.** Wildtype and *aga1* mutants were grown in SLAD media for 24-48 hours under low and high ammonium conditions and observed for colony morphology with light microscopy. Under high ammonium conditions the growth of *aga1* mutants did not show major differences from the wildtype while the growth of *aga1* mutants was considerably reduced under low ammonium conditions (Figure 4.7). In addition, it appears that *aga1* mutant colonies appear to be smaller and are relatively less dense compared to wildtype.

In *U. maydis*, low ammonium plays an indispensable role in regulating the dimorphic

switch in response to nutrient limitation, specifically nitrogen in the form of ammonium (Paul, Barati, Cooper, & Perlin, 2014). This indicates that *agal* may have a role in the growth of the fungus under low ammonium conditions and play a role in the filamentous response pathway in *U. maydis*.

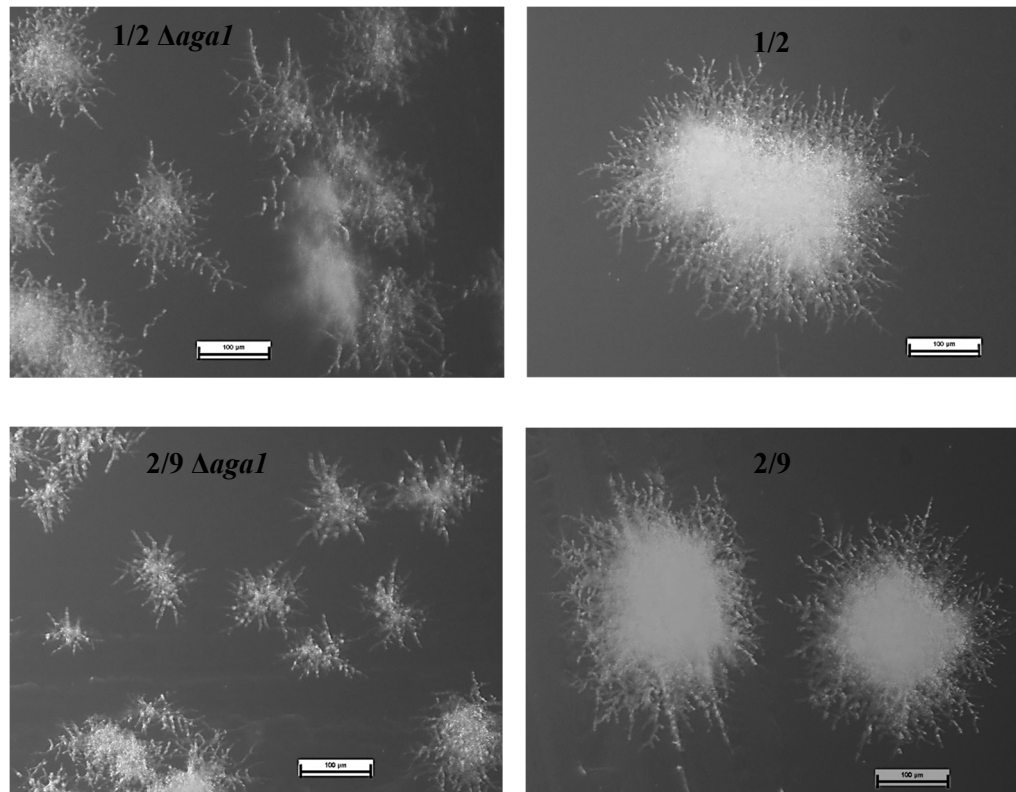


**Figure 4.7.** Effect of low ammonium (10  $\mu$ M) on *agal* mutants. Wild type and  $\Delta$ *agal* grown in low ammonium conditions. Wildtype colonies are bigger, and have a larger core filamentation area when compared to  $\Delta$ *agal* mutants. Scale bar is 100  $\mu$ m

## DISCUSSION

In our study we have observed that deletion of *agal* in the 1/2 and 2/9 background leads to reduced mating especially during the initial 24 hours when compared to the

corresponding mating of their wild type progenitors. However, when an *agal* mutant is crossed with the compatible wildtype strain, there was very limited alteration in the aerial hyphae production, thus showing that one wild type copy is sufficient to maintain nearly wild type phenotype. The cells lacking *agal* showed a defect in actin-mediated endocytosis. (Berndt et al., 2010). Also, actin-mediated endocytosis of Pra1 receptor is required for the a2 pheromone perception and cell fusion (Fuchs, Hause, Schuchardt, & Steinberg, 2006). This will possibly explain the reason for delayed mating reaction observed in *agal* mutants.

The plants infected with *agal* deletion strains showed highly reduced disease symptoms and did not produce tumors. This is consistent with the observation from studies in SG200 strains that *agal* deletion results in loss of pathogenicity. It has also been seen that cells lacking *agal* could not produce appressoria effectively (Berndt et al., 2010). For the successful invasion of the plants, the dikaryotic fungal hyphae should be able to produce the appressorium (Castanheira & Pérez-Martín, 2015).

When the actin structures were destructed with jasplakinolide in *S. cerevisiae*, it decreased the life span of strains deleted for *tor1* (orthologue of mTOR) or *sch9* (orthologue of *S6K*) genes, indicating the role of these genes in regulating actin dynamics (Y. Liu, Liu, Wu, Bi, & Meng, 2015). Studies conducted in Swiss 3T3 fibroblast cells provided evidence that the S6K pathway is important for signaling at two F-actin microdomains in cells and regulates cell migration. S6K1 (p70<sup>S6K</sup>) along with proteins such as AKT1 and PI3K (phosphoinositide 3-kinase) were found to be localized to the cytoskeletal structure called 'actin arc' located at the leading edge of migrating cells (L. A. Berven, F. S. Willard, & M. F. Crouch, 2004). This is consistent with the previous finding

that *agal* is required for the maintenance of actin cytoskeleton in *U. maydis*. This is probably a reason why we observed the abnormal cell morphology in the case of *agal* mutants. Furthermore, studies in yeast have shown that polarization of actin cytoskeleton leads to aberrant morphologies and that changes in morphology are coordinated with cell growth through the TORC1 pathway (Goranov et al., 2013).

The stress tests with cell-wall antagonists and osmotic stress agents such as NaCl and sorbitol indicated that  $\Delta$ *agal* strains were considerably more sensitive compared to wild type strains. Studies conducted in yeast have demonstrated that Sch9 (yeast S6K1 orthologue) affects the activity of the inositol phosphosphingolipid phospholipase C, *Isc1*, which is essential for producing ceramide from the hydrolysis of sphingolipids (Swinnen et al., 2014). It is also established that sphingolipids and their metabolites such as ceramides play a role in signaling cascades involving cell wall integrity and actin cytoskeleton organization, among others (Dickson, 2010). Hence it can be expected that *agal* may have a role in the regulation of stress tolerance and longevity of *U. maydis* cells.

Experiments with LiCl showed that  $\Delta$ *agal* mutants are more sensitive to Li<sup>+</sup> stress than the wild type counterparts. Studies conducted in *S. cerevisiae* have shown that overexpression of SIT4, serine/threonine protein phosphatase, increases Li<sup>+</sup> tolerance under specific nutrient conditions (Martins et al., 2008). It is possible that *agal* is the direct target of Li<sup>+</sup> or it is part of a pathway which is affected by Li<sup>+</sup>. Mouse model studies have demonstrated that GSK3 (glycogen synthase kinase 3), serine/threonine protein kinase, is an important physiological target of Li<sup>+</sup> ions (Stambolic, Ruel, & Woodgett, 1996). Furthermore it is also established that GSK-3 is a direct target of S6K1 (H. H. Zhang, Lipovsky, Dibble, Sahin, & Manning, 2006). GSK3 has many substrates that, when mis

regulated, could contribute to the location and unusual characteristics of many lesions due to tuberculosis sclerosis complex (a genetic disorder where benign tumors grow in many parts of the body) (H. H. Zhang et al., 2006).

Assuming *agal* is the orthologue of *S6K1* and hence a potential downstream effector of mTORC1, we tested for the effect of nitrogen conditions on growth of *U. maydis*. Also, it is widely known that TORC1 signaling is involved in nutrient sensing (Barbet et al., 1996; Stracka, Jozefczuk, Rudroff, Sauer, & Hall, 2014). Our study showed that *agal* mutants grew less and filamented less in low ammonium media. In muscle cells, the deletion of *S6K1* suppresses growth adaptations to nutrient availability (Aguilar et al., 2007; Ohanna et al., 2005). Similarly, the yeast equivalent of S6K1, Sch9, is required for nitrogen-induced activation of the fermentable-growth-medium-induced (FGM) pathway (Crauwels et al., 1997). Neurons are highly dependent on astrocyte (star-shaped glial cells in the central nervous system) survival during brain damage. The deletion of *S6K1* in astrocytes increased the reactive oxygen species in the cell and caused impairment in protein translation suggesting a S6K1 mediated functional pathway that senses nutrient and oxygen levels associated with neuronal survival (Pastor et al., 2009).

In our study we have observed a reduction in growth rate of the  $\Deltaagal$  mutants. This is consistent with the phenotype of  $\Deltaagal$  in the SG200 background (Berndt et al., 2010). Furthermore, mammalian studies of S6K1 showed that S6K1-deficiency resulted in smaller mice while not affecting the fertility or viability of the organism (Shima et al., 1998). This slow rate of growth in YPS media which is a rich medium could indicate that *Agal* may have a role in nutrient sensing or control of protein synthesis. This has been the case with *Ypk1* of yeast (*S. cerevisiae*), a serine threonine kinase that regulates protein

translation initiation in response to nutrient signals (Gelperin, Horton, DeChant, Hensold, & Lemmon, 2002).

In summary, our study reveals that *U. maydis agal* plays an important role in cell growth and is vital for the virulence of the fungus. The absence of *agal* gene in axenic haploid cultures leads to morphological defects and makes the fungus less adaptable to harsh environmental conditions. As the *agal* deletion results in a series of stress phenotypes, it would be worth to investigate the biochemical changes/events that happen in response to various stress conditions by analyzing the cell proteome.

## CHAPTER V

### DISCUSSION

PTEN signaling in mammalian systems is fairly well studied. The importance of PTEN protein for the proper functioning of various cellular activities and the observation that deficiency or mutation of PTEN can lead to devastating diseases as in the case for a variety of cancers and other metabolic disorders have led to the increased interest in PTEN research. However, as greater knowledge is acquired about PTEN, its diverse functions suggest that it is much more complex than initially thought. Researchers became interested in understanding the role of this conserved pathway in other eukaryotic systems. Studies have been conducted in *C. elegans* (Ogg & Ruvkun, 1998), *D. rerio* (Stumpf, Choorapoikayil, & den Hertog, 2015), *D. melanogaster* (Huang et al., 1999a), *E. colioides* (Luo et al., 2016), *S. cerevisiae* (Heymont et al., 2000), and *F. graminearum* (D. Zhang et al., 2010). The presence of an orthologue of the *PTEN* gene in *Ustilago maydis* prompted us to study the role of this gene in this fungal system. The availability of various functional and genetic tools in *U. maydis* makes it an ideal system for genetic experiments and signaling studies. This study has identified the presence of a *ptn1* orthologue in *Ustilago maydis*. I demonstrated that the lack of *ptn1* causes minor defects in the mating process or related functions normally seen in aerial hyphae production. The production of mating pheromone appears to be less in the 2/9  $\Delta$ *ptn1* strains as indicated by experiments with FBD tester strains. However, the gene expression studies aimed at exploring the

transcriptional profile of mating pathway targets did not provide conclusive evidence, except that *prf1* was upregulated in  $\Delta$ *ptn1* under low ammonium conditions, a condition during which filamentation occurs, similar to the mating conditions. The deletion of *ptn1* led to functional defects in the fungus with respect to its response to certain stress conditions and to complete its life cycle in the host plant. These  $\Delta$ *ptn1* strains were cell wall stress-sensitive and less virulent as indicated by the reduced size and number of galls. Microscopic analysis of the tumors from the  $\Delta$ *ptn1* treatment group revealed a reduced number of mature spores. This was further confirmed by counting the spores using a hemocytometer. Furthermore, the germination rate of the teliospores collected from plants infected with these mutant strains were low, indicating the potential role of *ptn1* in spore germination as well as development. This is consistent with the observation that 45 minutes after teliospores were induced to germinate, there is a burst of respiratory activity and there is an increase in *ptn1* expression (personal communication from Dr. Barry Saville, Trent University). The examination of the spore germination tube indicated no defect in the germ tube formation. The diploid strains in which one copy of *ptn1* was deleted showed reduced virulence, indicating haploinsufficiency for this gene. This is yet another example of such a phenomenon for *U. maydis* genes involved in signaling (Pham & Perlin, 2010). The effect of *ptn1* deletion on virulence was confirmed through alternate methods such as measuring the plant growth indicators *i.e.*, chlorophyll a/b ratio, plant height, number of leaves and dry biomass of the plant. The alternate methods showed that the  $\Delta$ *ptn1* infected plants are healthier compared to wild type infected plants. The complemented strains,  $\Delta$ *ptn1**c*, *i.e.*, strains made after inserting an active copy of *ptn1* into the  $\Delta$ *ptn1* strains, showed only partial complementation. Hence, new *ptn1* deletion strains were made using an alternate



deletion construct. The experiments using the newly made  $\Delta ptn1$  ( $\Delta ptn1J$  strains) strains were tested, and they confirmed the results from the original  $\Delta ptn1$  strains.

This is the first report of the presence and functional role of a PTEN orthologue in the basidiomycete fungi. The study indicates that *ptn1* plays a role in virulence and teliospore germination. This is consistent with the observations from *S. cerevisiae* (Heymont et al., 2000) and *F. graminearum* (D. Zhang et al., 2010), where the mutant strains showed defect in sporulation.

Studies have shown that the PTEN signaling has diverse implications. The PTEN protein has been found to interact with several other signaling molecules. In *U. maydis*, it has previously been shown that Rho1 and Pdc1 proteins physically interact with Ptn1 (Pham et al., 2009). Our experiments with the *rho1* deletion strain showed that they are stress sensitive while the *pdcl* and *ptn1* deletion strains in diploid background showed only a minor phenotype. The double deletion strains of *pdcl* and *ptn1* had defects in aerial hyphae production, were more sensitive to cell wall stress and were less virulent. Also, the overexpression of *pdcl* in the *ptn1* deletion background significantly reduced aerial hyphae formation, growth rate, virulence and made the strains more sensitive to cell wall stress. While the overexpression of *pdcl* in wildtype strains did not have a major effect, its overexpression in the *ptn1* deletion background exacerbated the  $\Delta ptn1$  phenotype, indicating a potential interaction between these proteins. Similarly, the *rho1* overexpression led to reduced plant virulence while its overexpression in the *ptn1* deletion background did not affect the virulence of the  $\Delta ptn1$  strains; in fact, these strains appeared to be marginally more virulent than the  $\Delta ptn1$  strains. In this aspect, the *ptn1* interaction with *rho1* is the opposite of its interaction with *pdcl*. This is similar to the observation

made in a previous study where Rho1 and Pdc1 were thought to have antagonistic functions towards Rac1 (Pham et al., 2009).

This study identified the presence of Ptn1 (PTEN orthologue) in *U. maydis* and the previous studies have shown that *U. maydis* contains counterparts of other mammalian proteins such as Pdc1 (14-3-3 orthologue), Aga1 (S6K1 orthologue), Rho1, Cdc42, and Rac1 (Rho/Rac family of GTPases), among others. The presence of these orthologues suggests possible conservation of the functions of these proteins; the studies in *U. maydis* and other non-mammalian systems support this to a great extent. In most species of fungi, the pathways such as MAPK and PKA are found to have vital importance in regulating physiology, development, mating, and stress responses. It is possible that the processes regulated by Rho1, Pdc1, Aga1 and Ptn1 have crosstalk with the components of the MAPK signaling pathway or the PKA pathway as they are present in *U. maydis* and evolutionarily conserved in eukaryotes. Studies of yeast 14-3-3 have shown that they interact with specific MEK (Mitogen-activated protein kinase) kinases (Fanger et al., 1998). Although we attempted to look at the effect of *ptn1* deletion on some of the mating pathway genes, which are connected to the aforementioned pathways, we could not find a meaningful connection at this point.

As shown in this study, gene deletion or disruption to manipulate the signaling pathways has resulted in revealing phenotypes; the phenotypic similarity between the mutants studied when taken together in the context of already existing literature suggest a possible common theme behind them, cytoskeletal rearrangements. Studies in fission yeast and *Fusarium oxysporum* have indicated that Rho1 may be involved in cell wall biosynthesis through regulating the activity of chitin synthase (Martinez-Rocha et al., 2008;

Santos, Gutierrez, Calonge, & Perez, 2003). Previous studies in *U. maydis* have demonstrated that Rho1 is required for cell polarity and cytokinesis. Also, chitinases are found to be required for cell separation in *U. maydis* (Langner et al., 2015). In our study the *pdcl*, *rho1*, *agal* and *ptn1* mutants show varying degrees of cell separation defects. Also, it has been demonstrated in *U. maydis* that septation of the dikaryotic hyphae is critical for appressoria formation and subsequent virulence (Freitag et al., 2011). This can be attributed as the potential reason for the varying degrees of reduction in virulence seen in our mutant strains considering that they suffer from cell separation defects. Furthermore, it has been demonstrated in *C. neoformans* that the virulence of the fungus is dependent on cell wall remodeling that it undergoes upon entering the host (Esher et al., 2018). The disruption of actin cytoskeleton in yeast led to the formation of an aberrant cell wall, indicating that the two processes are closely linked (Gabriel & Kopecka, 1995; Gabriel, Kopecka, & Svoboda, 1992; Takagi, Ishijima, Ochi, & Osumi, 2003). The localization of the cytosolic proteins to the cell membrane depends on their interactions with various proteins. For example, 14-3-3 proteins through its interaction with guanine nucleotide exchange factors (GEFs) have been shown to control the localization of Rho and Rac (Ngok, Geyer, Kourtidis, Storz, & Anastasiadis, 2013; Zenke et al., 2004). These interactions are found to be facilitating a broad range of cytoskeletal alterations that determine cell morphology (Zhai, Lin, Shamim, Schlaepfer, & Canete-Soler, 2001). In cultured podocytes (specialized kidney cells), the downregulation of PTEN caused actin cytoskeletal reorganization and this response was associated with unbalanced activation of small GTPases Rac1/Cdc42 and RhoA (Lin et al., 2015). Also, cardiac myocytes where

PTEN activity is inhibited, exhibited a reduction in actin dynamics (Jieli Li, Tanhehco, & Russell, 2014).

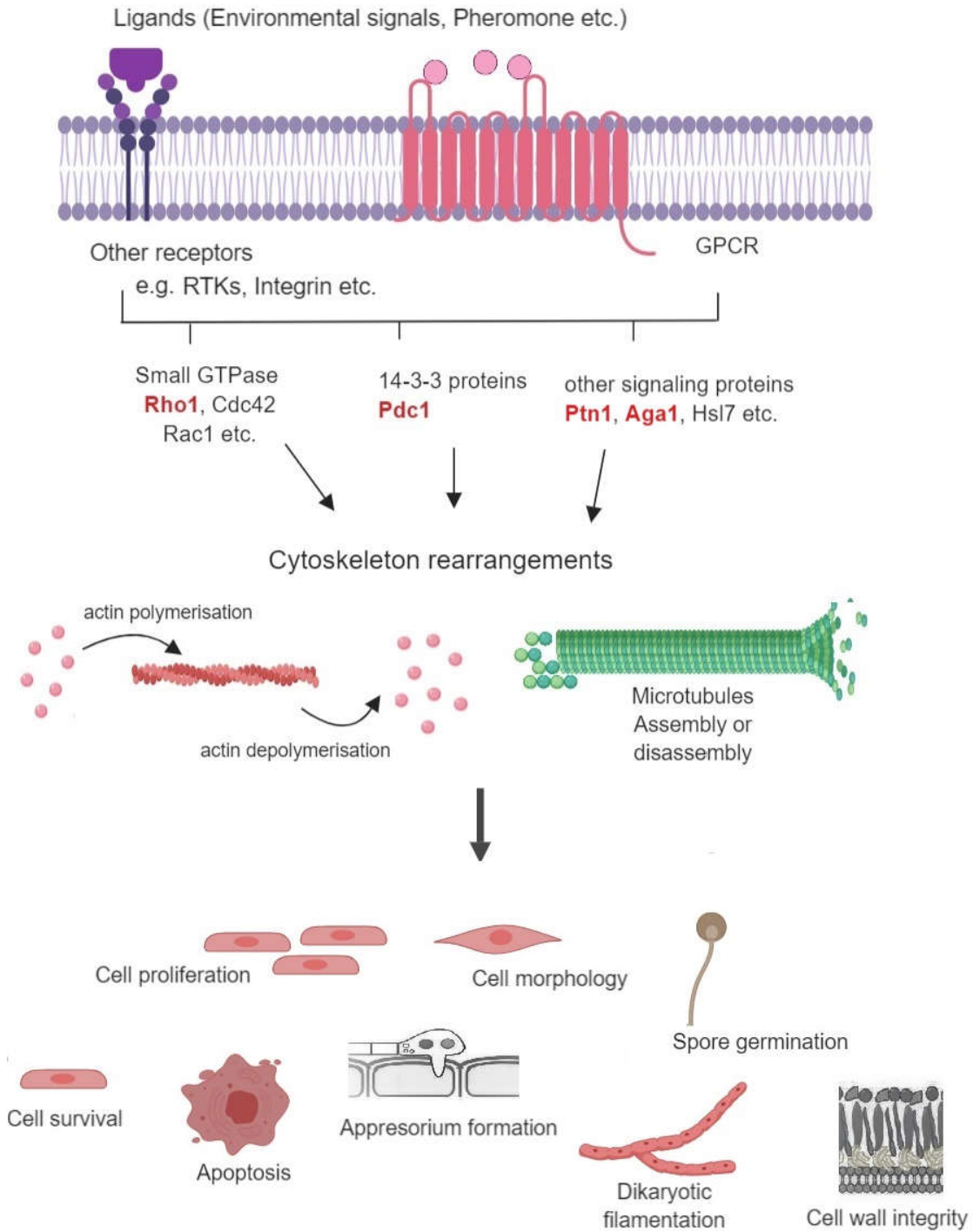


**Figure 5.1.** Possible mode of action of the signaling proteins.

Endocytosis is a vital process for eukaryotic cells in maintaining the composition of the plasma membrane, nutrient uptake and regulation of cell size. Several studies conducted in yeast have demonstrated that mutation in Rho GTPase proteins results in defects in endocytosis (Philip & Levin, 2001; D. C. Prosser, Drivas, Maldonado-Baez, & Wendland, 2011; Derek C. Prosser & Wendland, 2012). Our experiments with *agal* mutants have revealed defects in cell morphology and reduced cell wall integrity. This can be explained by the fact that Aga1 plays a role in endocytosis and in the maintenance of actin cytoskeleton as demonstrated in *U. maydis* (Berndt et al., 2010).

In *S. cerevisiae*, a cell wall sensor protein, Wsc1, is involved in the reorganization of actin cytoskeleton in response to osmotic shock, and the absence of this protein weakened cell wall integrity (Gualtieri, Ragni, Mizzi, Fascio, & Popolo, 2004). This underlines the role of actin cytoskeleton in stress response events. Studies conducted in *S. cerevisiae* have indicated that components of the spore wall are vital to ensure a protective shell around the spore. When a gene, *OSW3*, responsible for dityrosine layer of the yeast spore wall was mutated, it resulted in spores with permeable walls (Suda, Rodriguez, Coluccio, & Neiman, 2009). Furthermore, *TEP1* (*ptn1* orthologue) mutants in yeast had defects in the trafficking or deposition of dityrosine, a major component of yeast spore walls (Heymont et al., 2000). In addition, RhoA protein is found to be expressed differentially during spore germination of *P. blakesleeanus* (Ramírez-Ramírez et al., 1999). Another interesting piece of evidence is that in yeast, actin is essential for spore wall formation and dynamic organization of actin occurs during spore assembly (Taxis et al., 2006). All these studies point to the central idea that the transmission of signals to cytoskeleton and the subsequent reorganization results in a variety of cellular responses,

including cell survival, proliferation, motility, spore formation, cell wall synthesis, and stress responses, to name a few. This potential mode of action is visually depicted in Figure 5.1.

Over the past two decades, knowledge of the signaling pathways in fungal systems has greatly progressed. Despite these advances, our knowledge of the signaling mechanisms is far from complete and many important questions remain to be answered. We have shown that *ptn1* in *U. maydis* is active and plays a role in virulence and spore formation. Biochemical characterization of this protein would be worthwhile, *e.g.*, demonstrating its phosphatase activity, and elucidating its protein structure. It would be interesting to identify other interaction partners of Ptn1, as this would give more insight into the functions of Ptn1. Though it shows the presence of a class III PI3-Kinase domain, a preliminary investigation performed in our lab has revealed that *U. maydis* does not contain a class I PI3-Kinase which is one of the major components of the canonical PTEN-AKT-mTOR signaling. Still it is worth identifying other elements of the mTOR pathway in *U. maydis* as a possible future direction.

## REFERENCES

- Abramovitch, R. B., Yang, G., & Kronstad, J. W. (2002). The *ukb1* gene encodes a putative protein kinase required for bud site selection and pathogenicity in *Ustilago maydis*. *Fungal Genetics and Biology*, 37(1), 98-108.  
doi:[https://doi.org/10.1016/S1087-1845\(02\)00030-0](https://doi.org/10.1016/S1087-1845(02)00030-0)
- Aguilar, V., Alliouachene, S., Sotiropoulos, A., Sobering, A., Athea, Y., Djouadi, F., . . . Pende, M. (2007). S6 Kinase Deletion Suppresses Muscle Growth Adaptations to Nutrient Availability by Activating AMP Kinase. *Cell Metabolism*, 5(6), 476-487.  
doi:<https://doi.org/10.1016/j.cmet.2007.05.006>
- Aimanianda, V., Simenel, C., Garnaud, C., Clavaud, C., Tada, R., Barbin, L., . . . Latge, J. P. (2017). The Dual Activity Responsible for the Elongation and Branching of beta-(1,3)-Glucan in the Fungal Cell Wall. *MBio*, 8(3). doi:10.1128/mBio.00619-17
- Akhtar, T., Zia-Ur-Rehman, M., Naeem, A., Nawaz, R., Ali, S., Murtaza, G., . . . Rizwan, M. (2017). Photosynthesis and growth response of maize (*Zea mays* L.) hybrids exposed to cadmium stress. *Environ Sci Pollut Res Int*, 24(6), 5521-5529.  
doi:10.1007/s11356-016-8246-0
- Ali, I. U., Schriml, L. M., & Dean, M. (1999). Mutational spectra of PTEN/MMAC1 gene: a tumor suppressor with lipid phosphatase activity. *J Natl Cancer Inst*, 91(22), 1922-1932.
- Alimonti, A., Carracedo, A., Clohessy, J. G., Trotman, L. C., Nardella, C., Egia, A., . . . Pandolfi, P. P. (2010). Subtle variations in Pten dose determine cancer susceptibility. *Nat Genet*, 42(5), 454-458. doi:10.1038/ng.556
- Arellano, M., Coll, P. M., & Perez, P. (1999). RHO GTPases in the control of cell morphology, cell polarity, and actin localization in fission yeast. *Microsc Res Tech*, 47(1), 51-60. doi:10.1002/(sici)1097-0029(19991001)47:1<51::Aid-jemt5>3.0.Co;2-3
- Backman, S., Stambolic, V., & Mak, T. (2002). PTEN function in mammalian cell size regulation. *Curr Opin Neurobiol*, 12(5), 516-522.
- Bankoglu, E. E., Tschopp, O., Schmitt, J., Burkard, P., Jahn, D., Geier, A., & Stopper, H. (2016). Role of PTEN in Oxidative Stress and DNA Damage in the Liver of Whole-Body Pten Haplodeficient Mice. *PLoS One*, 11(11), e0166956.  
doi:10.1371/journal.pone.0166956
- Banuett, F., & Herskowitz, I. (1996). Discrete developmental stages during teliospore formation in the corn smut fungus, *Ustilago maydis*. *Development*, 122(10), 2965-2976.

- Barbet, N. C., Schneider, U., Helliwell, S. B., Stansfield, I., Tuite, M. F., & Hall, M. N. (1996). TOR controls translation initiation and early G1 progression in yeast. *Mol Biol Cell*, 7(1), 25-42.
- Basse, C. W., & Steinberg, G. (2004). *Ustilago maydis*, model system for analysis of the molecular basis of fungal pathogenicity. *Mol Plant Pathol*, 5(2), 83-92. doi:10.1111/j.1364-3703.2004.00210.x
- Berndt, P., Lanver, D., & Kahmann, R. (2010). The AGC Ser/Thr kinase Aga1 is essential for appressorium formation and maintenance of the actin cytoskeleton in the smut fungus *Ustilago maydis*. *Mol Microbiol*, 78(6), 1484-1499. doi:10.1111/j.1365-2958.2010.07422.x
- Berven, L. A., Willard, F. S., & Crouch, M. F. (2004). Role of the p70(S6K) pathway in regulating the actin cytoskeleton and cell migration. *Exp Cell Res*, 296(2), 183-195. doi:10.1016/j.yexcr.2003.12.032
- Berven, L. A., Willard, F. S., & Crouch, M. F. (2004). Role of the p70S6K pathway in regulating the actin cytoskeleton and cell migration. *Experimental Cell Research*, 296(2), 183-195. doi:<https://doi.org/10.1016/j.yexcr.2003.12.032>
- Bokoch, G. M. (2000). Regulation of cell function by rho family GTPases. *Immunologic Research*, 21(2), 139-148. doi:10.1385/IR:21:2-3:139
- Bolker, M. (2001). *Ustilago maydis*--a valuable model system for the study of fungal dimorphism and virulence. *Microbiology*, 147(Pt 6), 1395-1401. doi:10.1099/00221287-147-6-1395
- Bölker, M. (2001). *Ustilago maydis*--a valuable model system for the study of fungal dimorphism and virulence. *Microbiology*, 147(Pt 6), 1395-1401. doi:10.1099/00221287-147-6-1395
- Bolker, M., Urban, M., & Kahmann, R. (1992). The a mating type locus of *U. maydis* specifies cell signaling components. *Cell*, 68(3), 441-450.
- Bononi, A., & Pinton, P. (2015). Study of PTEN subcellular localization. *Methods (San Diego, Calif.)*, 77-78, 92-103. doi:10.1016/j.ymeth.2014.10.002
- Boyce, K. J., Chang, H., D'Souza, C. A., & Kronstad, J. W. (2005). An *Ustilago maydis* septin is required for filamentous growth in culture and for full symptom development on maize. *Eukaryot Cell*, 4(12), 2044-2056. doi:10.1128/EC.4.12.2044-2056.2005
- Brachmann, A., König, J., Julius, C., & Feldbrügge, M. (2004). A reverse genetic approach for generating gene replacement mutants in *Ustilago maydis*. *Mol Genet Genomics*, 272(2), 216-226. doi:10.1007/s00438-004-1047-z
- Brandwein, D., & Wang, Z. (2017). Interaction between Rho GTPases and 14-3-3 Proteins. *International Journal of Molecular Sciences*, 18(10), 2148. doi:10.3390/ijms18102148
- Brefort, T., Doehlemann, G., Mendoza-Mendoza, A., Reissmann, S., Djamei, A., & Kahmann, R. (2009). *Ustilago maydis* as a Pathogen. *Annu Rev Phytopathol*, 47, 423-445. doi:10.1146/annurev-phyto-080508-081923
- Briza, P., Winkler, G., Kalchhauser, H., & Breitenbach, M. (1986). Dityrosine is a prominent component of the yeast ascospore wall. A proof of its structure. *J Biol Chem*, 261(9), 4288-4294.



- Cabib, E., Drgonova, J., & Drgon, T. (1998). Role of small G proteins in yeast cell polarization and wall biosynthesis. *Annu Rev Biochem*, *67*, 307-333. doi:10.1146/annurev.biochem.67.1.307
- Cantley, L. C. (2002). The phosphoinositide 3-kinase pathway. *Science*, *296*(5573), 1655-1657. doi:10.1126/science.296.5573.1655
- Carnero, A., & Paramio, J. M. (2014). The PTEN/PI3K/AKT Pathway in vivo, Cancer Mouse Models. *Frontiers in Oncology*, *4*, 252-252. doi:10.3389/fonc.2014.00252
- Castanheira, S., & Pérez-Martín, J. (2015). Appressorium formation in the corn smut fungus *Ustilago maydis* requires a G2 cell cycle arrest. *Plant signaling & behavior*, *10*(4), e1001227-e1001227. doi:10.1080/15592324.2014.1001227
- Cervantes-Chávez, J. A., Ali, S., & Bakkeren, G. (2011). Response to environmental stresses, cell-wall integrity, and virulence are orchestrated through the calcineurin pathway in *Ustilago hordei*. *Molecular Plant-Microbe Interactions*, *24*(2), 219-232.
- Chalhoub, N., & Baker, S. J. (2009). PTEN and the PI3-kinase pathway in cancer. *Annu Rev Pathol*, *4*, 127-150. doi:10.1146/annurev.pathol.4.110807.092311
- Cheney, I. W., Johnson, D. E., Vaillancourt, M. T., Avanzini, J., Morimoto, A., Demers, G. W., . . . Bookstein, R. (1998). Suppression of tumorigenicity of glioblastoma cells by adenovirus-mediated MMAC1/PTEN gene transfer. *Cancer Res*, *58*(11), 2331-2334.
- Cherfils, J., & Zeghouf, M. (2013). Regulation of small GTPases by GEFs, GAPs, and GDIs. *Physiol Rev*, *93*(1), 269-309. doi:10.1152/physrev.00003.2012
- Chu, S., DeRisi, J., Eisen, M., Mulholland, J., Botstein, D., Brown, P. O., & Herskowitz, I. (1998). The transcriptional program of sporulation in budding yeast. *Science*, *282*(5389), 699-705.
- Comer, F. I., & Parent, C. A. (2002). PI 3-kinases and PTEN: how opposites chemoattract. *Cell*, *109*(5), 541-544.
- Conover, W. J. (1999). *Practical nonparametric statistics* (3rd ed. ed.). New York ; Chichester: John Wiley.
- Crauwels, M., Donaton, M. C., Pernambuco, M. B., Winderickx, J., de Winde, J. H., & Thevelein, J. M. (1997). The Sch9 protein kinase in the yeast *Saccharomyces cerevisiae* controls cAPK activity and is required for nitrogen activation of the fermentable-growth-medium-induced (FGM) pathway. *Microbiology*, *143* ( Pt 8), 2627-2637. doi:10.1099/00221287-143-8-2627
- Dickson, R. C. (2010). Roles for sphingolipids in *Saccharomyces cerevisiae*. *Adv Exp Med Biol*, *688*, 217-231.
- Doehlemann, G., Wahl, R., Horst, R. J., Voll, L. M., Usadel, B., Poree, F., . . . Kämper, J. (2008). Reprogramming a maize plant: transcriptional and metabolic changes induced by the fungal biotroph *Ustilago maydis*. *The Plant Journal*, *56*(2), 181-195. doi:10.1111/j.1365-313X.2008.03590.x
- Doyle, C. E., Kitty Cheung, H. Y., Spence, K. L., & Saville, B. J. (2016). Unh1, an *Ustilago maydis* Ndt80-like protein, controls completion of tumor maturation, teliospore development, and meiosis. *Fungal Genet Biol*, *94*, 54-68. doi:10.1016/j.fgb.2016.07.006

- Durrenberger, F., Laidlaw, R. D., & Kronstad, J. W. (2001). The *hgl1* gene is required for dimorphism and teliospore formation in the fungal pathogen *Ustilago maydis*. *Mol Microbiol*, *41*(2), 337-348.
- Durrenberger, F., Wong, K., & Kronstad, J. W. (1998). Identification of a cAMP-dependent protein kinase catalytic subunit required for virulence and morphogenesis in *Ustilago maydis*. *Proc Natl Acad Sci U S A*, *95*(10), 5684-5689.
- Eng, C. (2003). PTEN: one gene, many syndromes. *Hum Mutat*, *22*(3), 183-198. doi:10.1002/humu.10257
- Esher, S. K., Ost, K. S., Kohlbrenner, M. A., Pianalto, K. M., Telzrow, C. L., Campuzano, A., . . . Alspaugh, J. A. (2018). Defects in intracellular trafficking of fungal cell wall synthases lead to aberrant host immune recognition. *PLOS Pathogens*, *14*(6), e1007126. doi:10.1371/journal.ppat.1007126
- Fanger, G. R., Widmann, C., Porter, A. C., Sather, S., Johnson, G. L., & Vaillancourt, R. R. (1998). 14-3-3 proteins interact with specific MEK kinases. *J Biol Chem*, *273*(6), 3476-3483.
- Feldbrugge, M., Kamper, J., Steinberg, G., & Kahmann, R. (2004). Regulation of mating and pathogenic development in *Ustilago maydis*. *Curr Opin Microbiol*, *7*(6), 666-672. doi:10.1016/j.mib.2004.10.006
- Fingar, D. C., Salama, S., Tsou, C., Harlow, E., & Blenis, J. (2002). Mammalian cell size is controlled by mTOR and its downstream targets S6K1 and 4EBP1/eIF4E. *Genes Dev*, *16*(12), 1472-1487. doi:10.1101/gad.995802
- Flor-Parra, I., Castillo-Lluva, S., & Pérez-Martín, J. (2007). Polar growth in the infectious hyphae of the phytopathogen *ustilago maydis* depends on a virulence-specific cyclin. *The Plant cell*, *19*(10), 3280-3296. doi:10.1105/tpc.107.052738
- Flor-Parra, I., Vranes, M., Kamper, J., & Perez-Martin, J. (2006). Biz1, a zinc finger protein required for plant invasion by *Ustilago maydis*, regulates the levels of a mitotic cyclin. *Plant Cell*, *18*(9), 2369-2387. doi:10.1105/tpc.106.042754
- Freitag, J., Lanver, D., Böhmer, C., Schink, K. O., Bölker, M., & Sandrock, B. (2011). Septation of Infectious Hyphae Is Critical for Appressoria Formation and Virulence in the Smut Fungus *Ustilago Maydis*. *PLOS Pathogens*, *7*(5), e1002044. doi:10.1371/journal.ppat.1002044
- Fuchs, U., Hause, G., Schuchardt, I., & Steinberg, G. (2006). Endocytosis is essential for pathogenic development in the corn smut fungus *Ustilago maydis*. *Plant Cell*, *18*(8), 2066-2081. doi:10.1105/tpc.105.039388
- Funayama-Noguchi, S., & Terashima, I. (2006). Effects of Eupatorium yellow vein virus infection on photosynthetic rate, chlorophyll content and chloroplast structure in leaves of *Eupatorium makinoi* during leaf development %J Functional Plant Biology. *33*(2), 165-175. doi:<https://doi.org/10.1071/FP05172>
- Gabriel, M., & Kopecka, M. (1995). Disruption of the actin cytoskeleton in budding yeast results in formation of an aberrant cell wall. *Microbiology*, *141* ( Pt 4), 891-899. doi:10.1099/13500872-141-4-891
- Gabriel, M., Kopecka, M., & Svoboda, A. (1992). Structural rearrangement of the actin cytoskeleton in regenerating protoplasts of budding yeasts. *Journal of General Microbiology*, *138*(10), 2229-2234. doi:10.1099/00221287-138-10-2229
- García-Pedrajas, M. D., Baeza-Montañez, L., & Gold, S. E. (2010). Regulation of *Ustilago maydis* dimorphism, sporulation, and pathogenic development by a

- transcription factor with a highly conserved APSES domain. *Mol Plant Microbe Interact*, 23(2), 211-222. doi:10.1094/MPMI-23-2-0211
- Garcia-Pedrajas, M. D., Nadal, M., Kapa, L. B., Perlin, M. H., Andrews, D. L., & Gold, S. E. (2008). DelsGate, a robust and rapid gene deletion construction method. *Fungal Genet Biol*, 45(4), 379-388. doi:10.1016/j.fgb.2007.11.001
- Gelperin, D., Horton, L., DeChant, A., Hensold, J., & Lemmon, S. K. (2002). Loss of ypk1 function causes rapamycin sensitivity, inhibition of translation initiation and synthetic lethality in 14-3-3-deficient yeast. *Genetics*, 161(4), 1453-1464.
- Gil, E. B., Malone Link, E., Liu, L. X., Johnson, C. D., & Lees, J. A. (1999). Regulation of the insulin-like developmental pathway of *Caenorhabditis elegans* by a homolog of the PTEN tumor suppressor gene. *Proceedings of the National Academy of Sciences of the United States of America*, 96(6), 2925-2930.
- Goberdhan, D. C., Paricio, N., Goodman, E. C., Mlodzik, M., & Wilson, C. (1999). *Drosophila* tumor suppressor PTEN controls cell size and number by antagonizing the Chico/PI3-kinase signaling pathway. *Genes Dev*, 13(24), 3244-3258.
- Gold, S. E., Brogdon, S. M., Mayorga, M. E., & Kronstad, J. W. (1997). The *Ustilago maydis* regulatory subunit of a cAMP-dependent protein kinase is required for gall formation in maize. *Plant Cell*, 9(9), 1585-1594. doi:10.1105/tpc.9.9.1585
- Gomez-Suarez, M., Gutierrez-Martinez, I. Z., Hernandez-Trejo, J. A., Hernandez-Ruiz, M., Suarez-Perez, D., Candelario, A., . . . Nava, P. (2016). 14-3-3 Proteins regulate Akt Thr308 phosphorylation in intestinal epithelial cells. *Cell Death Differ*, 23(6), 1060-1072. doi:10.1038/cdd.2015.163
- Goranov, A. I., Gulati, A., Dephoure, N., Takahara, T., Maeda, T., Gygi, S. P., . . . Amon, A. (2013). Changes in cell morphology are coordinated with cell growth through the TORC1 pathway. *Current biology : CB*, 23(14), 1269-1279. doi:10.1016/j.cub.2013.05.035
- Gualtieri, T., Ragni, E., Mizzi, L., Fascio, U., & Popolo, L. (2004). The cell wall sensor Wsc1p is involved in reorganization of actin cytoskeleton in response to hypo-osmotic shock in *Saccharomyces cerevisiae*. *Yeast*, 21(13), 1107-1120. doi:10.1002/yea.1155
- Guevara-Lara, F., Valverde, M. E., & Paredes-López, O. (2000). Is pathogenicity of *Ustilago maydis* (huitlacoche) strains on maize related to in vitro production of indole-3-acetic acid? *World Journal of Microbiology and Biotechnology*, 16(5), 481-490. doi:10.1023/A:1008906013524
- Gupta, R., Ting, J. T. L., Sokolov, L. N., Johnson, S. A., & Luan, S. (2002). A tumor suppressor homolog, AtPTEN1, is essential for pollen development in *Arabidopsis*. *The Plant cell*, 14(10), 2495-2507. doi:10.1105/tpc.005702
- Harrison, N., Cavinder, B., Townsend, J. P., & Trail, F. (2013). Optimized primers and other critical conditions for efficient fusion PCR to generate knockout vectors in filamentous fungi. *Fungal Genetics Reports*, 60(1), 1-10. doi:10.4148/1941-4765.1006
- Heilmann, C. J., Sorgo, A. G., Mohammadi, S., Sosinska, G. J., de Koster, C. G., Brul, S., . . . Klis, F. M. (2013). Surface stress induces a conserved cell wall stress response in the pathogenic fungus *Candida albicans*. *Eukaryotic cell*, 12(2), 254-264. doi:10.1128/EC.00278-12

- Heymont, J., Berenfeld, L., Collins, J., Kaganovich, A., Maynes, B., Moulin, A., . . . Engebrecht, J. (2000). TEP1, the yeast homolog of the human tumor suppressor gene PTEN/MMAC1/TEP1, is linked to the phosphatidylinositol pathway and plays a role in the developmental process of sporulation. *Proc Natl Acad Sci U S A*, *97*(23), 12672-12677. doi:10.1073/pnas.97.23.12672
- Hippenstiel, S., Schmeck, B., N'Guessan, P. D., Seybold, J., Krüll, M., Preissner, K., . . . Suttorp, N. (2002). Rho protein inactivation induced apoptosis of cultured human endothelial cells. *American Journal of Physiology-Lung Cellular and Molecular Physiology*, *283*(4), L830-L838. doi:10.1152/ajplung.00467.2001
- Hirasawa, T., Ashitani, K., Yoshikawa, K., Nagahisa, K., Furusawa, C., Katakura, Y., . . . Shioya, S. (2006). Comparison of transcriptional responses to osmotic stresses induced by NaCl and sorbitol additions in *Saccharomyces cerevisiae* using DNA microarray. *Journal of Bioscience and Bioengineering*, *102*(6), 568-571. doi:<https://doi.org/10.1263/jbb.102.568>
- Hiscox, J. D., & Israelstam, G. F. (1979). A method for the extraction of chlorophyll from leaf tissue without maceration. *Canadian Journal of Botany*, *57*(12), 1332-1334. doi:10.1139/b79-163
- Ho, E. C. H., Cahill, M. J., & Saville, B. J. (2007). Gene discovery and transcript analyses in the corn smut pathogen *Ustilago maydis*: expressed sequence tag and genome sequence comparison. *BMC Genomics*, *8*, 334-334. doi:10.1186/1471-2164-8-334
- Holliday, R. (1974). *Ustilago maydis*. In R. C. King (Ed.), *Bacteria, Bacteriophages, and Fungi: Volume 1* (pp. 575-595). Boston, MA: Springer US.
- Horst, R. J., Engelsdorf, T., Sonnewald, U., & Voll, L. M. (2008). Infection of maize leaves with *Ustilago maydis* prevents establishment of C4 photosynthesis. *J Plant Physiol*, *165*(1), 19-28. doi:10.1016/j.jplph.2007.05.008
- Huang, H., Potter, C. J., Tao, W., Li, D. M., Brogiolo, W., Hafen, E., . . . Xu, T. (1999a). PTEN affects cell size, cell proliferation and apoptosis during *Drosophila* eye development. *Development*, *126*(23), 5365-5372.
- Huang, H., Potter, C. J., Tao, W., Li, D. M., Brogiolo, W., Hafen, E., . . . Xu, T. (1999b). PTEN affects cell size, cell proliferation and apoptosis during *Drosophila* eye development. *Development*, *126*(23), 5365.
- Jones, D. H., Ley, S., & Aitken, A. (1995). Isoforms of 14-3-3 protein can form homo- and heterodimers in vivo and in vitro: implications for function as adapter proteins. *FEBS Lett*, *368*(1), 55-58.
- Justiniano, S. E., Mathew, A., Mitra, S., Manivannan, S. N., & Simcox, A. (2012). Loss of the tumor suppressor Pten promotes proliferation of *Drosophila melanogaster* cells in vitro and gives rise to continuous cell lines. *PLoS One*, *7*(2), e31417. doi:10.1371/journal.pone.0031417
- Kaffarnik, F., Muller, P., Leibundgut, M., Kahmann, R., & Feldbrugge, M. (2003). PKA and MAPK phosphorylation of Prf1 allows promoter discrimination in *Ustilago maydis*. *EMBO J*, *22*(21), 5817-5826. doi:10.1093/emboj/cdg554
- Kahmann, R., Romeis, T., Bölker, M., & Kämper, J. (1995). Control of mating and development in *Ustilago maydis*. *Current Opinion in Genetics & Development*, *5*(5), 559-564. doi:[https://doi.org/10.1016/0959-437X\(95\)80023-9](https://doi.org/10.1016/0959-437X(95)80023-9)

- Kamper, J. (2004). A PCR-based system for highly efficient generation of gene replacement mutants in *Ustilago maydis*. *Mol Genet Genomics*, 271(1), 103-110. doi:10.1007/s00438-003-0962-8
- Kamper, J., Kahmann, R., Bolker, M., Ma, L. J., Brefort, T., Saville, B. J., . . . Birren, B. W. (2006). Insights from the genome of the biotrophic fungal plant pathogen *Ustilago maydis*. *Nature*, 444(7115), 97-101. doi:10.1038/nature05248
- Kayano, Y., Tanaka, A., & Takemoto, D. (2018). Two closely related Rho GTPases, Cdc42 and RacA, of the endophytic fungus *Epichloë festucae* have contrasting roles for ROS production and symbiotic infection synchronized with the host plant. *PLOS Pathogens*, 14(1), e1006840. doi:10.1371/journal.ppat.1006840
- Kitagishi, Y., Kobayashi, M., Kikuta, K., & Matsuda, S. (2012). Roles of PI3K/AKT/GSK3/mTOR Pathway in Cell Signaling of Mental Illnesses. *Depression research and treatment*, 2012, 752563-752563. doi:10.1155/2012/752563
- Klose, J., de Sa, M. M., & Kronstad, J. W. (2004). Lipid-induced filamentous growth in *Ustilago maydis*. *Mol Microbiol*, 52(3), 823-835. doi:10.1111/j.1365-2958.2004.04019.x
- Klosterman, S. J., Perlin, M. H., Garcia-Pedrajas, M., Covert, S. F., & Gold, S. E. (2007). Genetics of morphogenesis and pathogenic development of *Ustilago maydis*. *Adv Genet*, 57, 1-47. doi:10.1016/S0065-2660(06)57001-4
- Klosterman, S. J., Perlin, M. H., Garcia-Pedrajas, M., Covert, S. F., & Gold, S. E. (2007). Genetics of Morphogenesis and Pathogenic Development of *Ustilago maydis*. In *Advances in Genetics* (Vol. 57, pp. 1-47): Academic Press.
- Kraus, P. R., Hofmann, A. F., & Harris, S. D. (2002). Characterization of the *Aspergillus nidulans* 14-3-3 homologue, ArtA. *FEMS Microbiol Lett*, 210(1), 61-66. doi:10.1111/j.1574-6968.2002.tb11160.x
- Kretschmer, M., Lambie, S., Croll, D., & Kronstad, J. W. (2018). Acetate provokes mitochondrial stress and cell death in *Ustilago maydis*. *Mol Microbiol*, 107(4), 488-507. doi:10.1111/mmi.13894
- Kronstad, J. W., & Leong, S. A. (1989a). Isolation of two alleles of the b locus of *Ustilago maydis*. *Proceedings of the National Academy of Sciences*, 86(3), 978.
- Kronstad, J. W., & Leong, S. A. (1989b). Isolation of two alleles of the b locus of *Ustilago maydis*. *Proc Natl Acad Sci U S A*, 86(3), 978-982.
- Krtková, J., Xu, J., Lalle, M., Steele-Ogus, M., Alas, G. C. M., Sept, D., & Paredez, A. R. (2017). 14-3-3 Regulates Actin Filament Formation in the Deep-Branching Eukaryote *Giardia lamblia*. *mSphere*, 2(5), e00248-00217. doi:10.1128/mSphere.00248-17
- Krüger, J., Loubradou, G., Wanner, G., Regenfelder, E., Feldbrügge, M., & Kahmann, R. (2000). Activation of the cAMP Pathway in *Ustilago maydis* Reduces Fungal Proliferation and Teliospore Formation in Plant Tumors. *Molecular Plant-Microbe Interactions*, 13(10), 1034-1040. doi:10.1094/MPMI.2000.13.10.1034
- Kumar, C. C., & Madison, V. (2005). AKT crystal structure and AKT-specific inhibitors. *Oncogene*, 24(50), 7493-7501. doi:10.1038/sj.onc.1209087
- Langner, T., Ozturk, M., Hartmann, S., Cord-Landwehr, S., Moerschbacher, B., Walton, J. D., & Gohre, V. (2015). Chitinases Are Essential for Cell Separation in *Ustilago maydis*. *Eukaryot Cell*, 14(9), 846-857. doi:10.1128/ec.00022-15

- Lee, K. K., Maccallum, D. M., Jacobsen, M. D., Walker, L. A., Odds, F. C., Gow, N. A., & Munro, C. A. (2012). Elevated cell wall chitin in *Candida albicans* confers echinocandin resistance in vivo. *Antimicrob Agents Chemother*, *56*(1), 208-217. doi:10.1128/aac.00683-11
- Lee, N., D'Souza, C. A., & Kronstad, J. W. (2003). Of smuts, blasts, mildews, and blights: cAMP signaling in phytopathogenic fungi. *Annu Rev Phytopathol*, *41*, 399-427. doi:10.1146/annurev.phyto.41.052002.095728
- Leslie, N. R., & Downes, C. P. (2004). PTEN function: how normal cells control it and tumour cells lose it. *The Biochemical journal*, *382*(Pt 1), 1-11. doi:10.1042/BJ20040825
- Levin, D. E. (2005). Cell wall integrity signaling in *Saccharomyces cerevisiae*. *Microbiol Mol Biol Rev*, *69*(2), 262-291. doi:10.1128/membr.69.2.262-291.2005
- Lewandowski, T. J., Dunfield, K. E., & Antunes, P. M. (2013). Isolate Identity Determines Plant Tolerance to Pathogen Attack in Assembled Mycorrhizal Communities. *PLoS One*, *8*(4), e61329. doi:10.1371/journal.pone.0061329
- Li, J., Chang, Y. C., Wu, C. H., Liu, J., Kwon-Chung, K. J., Huang, S. H., . . . Jong, A. (2016). The 14-3-3 Gene Function of *Cryptococcus neoformans* Is Required for its Growth and Virulence. *J Microbiol Biotechnol*, *26*(5), 918-927. doi:10.4014/jmb.1508.08051
- Li, J., Tanhehco, E. J., & Russell, B. (2014). Actin dynamics is rapidly regulated by the PTEN and PIP2 signaling pathways leading to myocyte hypertrophy. *American journal of physiology. Heart and circulatory physiology*, *307*(11), H1618-H1625. doi:10.1152/ajpheart.00393.2014
- Li, J., Yen, C., Liaw, D., Podsypanina, K., Bose, S., Wang, S. I., . . . Parsons, R. (1997). <em>PTEN</em>, a Putative Protein Tyrosine Phosphatase Gene Mutated in Human Brain, Breast, and Prostate Cancer. *Science*, *275*(5308), 1943.
- Li, W., Tan, D., Zhang, Z., Liang, J. J., & Brown, R. E. (2008). Activation of Akt-mTOR-p70S6K pathway in angiogenesis in hepatocellular carcinoma. *Oncol Rep*, *20*(4), 713-719.
- Li, Z., Dong, X., Wang, Z., Liu, W., Deng, N., Ding, Y., . . . Wu, D. (2005). Regulation of PTEN by Rho small GTPases. *Nat Cell Biol*, *7*(4), 399-404. doi:10.1038/ncb1236
- Li, Z., Hannigan, M., Mo, Z., Liu, B., Lu, W., Wu, Y., . . . Wu, D. (2003). Directional sensing requires G beta gamma-mediated PAK1 and PIX alpha-dependent activation of Cdc42. *Cell*, *114*(2), 215-227.
- Lickfeld, M., & Schmitz, H. P. (2012). A network involving Rho-type GTPases, a paxillin and a formin homologue regulates spore length and spore wall integrity in the filamentous fungus *Ashbya gossypii*. *Mol Microbiol*, *85*(3), 574-593. doi:10.1111/j.1365-2958.2012.08128.x
- Lin, J., Shi, Y., Peng, H., Shen, X., Thomas, S., Wang, Y., . . . Xu, J. (2015). Loss of PTEN promotes podocyte cytoskeletal rearrangement, aggravating diabetic nephropathy. *The Journal of pathology*, *236*(1), 30-40. doi:10.1002/path.4508
- Liu, J., & Chin-Sang, I. D. (2015). *C. elegans* as a model to study PTEN's regulation and function. *Methods*, *77-78*, 180-190. doi:<https://doi.org/10.1016/j.ymeth.2014.12.009>



- Liu, Y., Liu, N., Wu, D., Bi, Q., & Meng, S. (2015). The longevity of *tor1Δ*, *sch9Δ*, and *ras2Δ* mutants depends on actin dynamics in *Saccharomyces cerevisiae*. *Cell & Bioscience*, 5(1), 18. doi:10.1186/s13578-015-0008-z
- Lobato, A. K. S., Gonçalves-Vidigal, M. C., Vidigal Filho, P. S., Andrade, C. A. B., Kvitschal, M. V., & Bonato, C. M. (2010). Relationships between leaf pigments and photosynthesis in common bean plants infected by anthracnose. *New Zealand Journal of Crop and Horticultural Science*, 38(1), 29-37. doi:10.1080/01140671003619308
- Lottersberger, F., Panza, A., Lucchini, G., Piatti, S., & Longhese, M. P. (2006). The *Saccharomyces cerevisiae* 14-3-3 proteins are required for the G1/S transition, actin cytoskeleton organization and cell wall integrity. *Genetics*, 173(2), 661-675. doi:10.1534/genetics.106.058172
- Lovely, C. B., Aulakh, K. B., & Perlin, M. H. (2011). Role of Hsl7 in morphology and pathogenicity and its interaction with other signaling components in the plant pathogen *Ustilago maydis*. *Eukaryot Cell*, 10(7), 869-883. doi:10.1128/EC.00237-10
- Luo, S.-W., Wang, W.-N., Xie, R.-C., Xie, F.-X., Kong, J.-R., Xiao, Y.-C., . . . Wang, C. (2016). Molecular cloning and characterization of PTEN in the orange-spotted grouper (*Epinephelus coioides*). *Fish Shellfish Immunol*, 58, 686-700. doi:<https://doi.org/10.1016/j.fsi.2016.10.007>
- Ma, J., Jaraba, J., Kirkpatrick, T. L., & Rothrock, C. S. (2013). Effects of *Meloidogyne incognita* and *Thielaviopsis basicola* on Cotton Growth and Root Morphology. *Phytopathology*, 104(5), 507-512. doi:10.1094/PHYTO-06-12-0120-R
- Machado-Vieira, R., Manji, H. K., & Zarate, C. A., Jr. (2009). The role of lithium in the treatment of bipolar disorder: convergent evidence for neurotrophic effects as a unifying hypothesis. *Bipolar disorders*, 11 Suppl 2(Suppl 2), 92-109. doi:10.1111/j.1399-5618.2009.00714.x
- Maehama, T., & Dixon, J. E. (1998). The tumor suppressor, PTEN/MMAC1, dephosphorylates the lipid second messenger, phosphatidylinositol 3,4,5-trisphosphate. *J Biol Chem*, 273(22), 13375-13378.
- Magnuson, B., Ekim, B., & Fingar, D. C. (2012). Regulation and function of ribosomal protein S6 kinase (S6K) within mTOR signalling networks. *Biochem J*, 441(1), 1-21. doi:10.1042/bj20110892
- Mahlert, M., Leveleki, L., Hlubek, A., Sandrock, B., & Bolker, M. (2006). Rac1 and Cdc42 regulate hyphal growth and cytokinesis in the dimorphic fungus *Ustilago maydis*. *Mol Microbiol*, 59(2), 567-578. doi:10.1111/j.1365-2958.2005.04952.x
- Manji, H. K., & Lenox, R. H. (2000). Signaling: cellular insights into the pathophysiology of bipolar disorder. *Biol Psychiatry*, 48(6), 518-530.
- Manolopoulou, E., Varzakas, T., & Petsalaki, A. (2016). Chlorophyll Determination in Green Pepper Using two Different Extraction Methods. *Current Research in Nutrition and Food Science Journal*, 4(Special Issue Carotenoids March 2016), 52-60.
- Marcos, C. M., Silva Jde, F., Oliveira, H. C., Assato, P. A., Singulani Jde, L., Lopez, A. M., . . . Fusco-Almeida, A. M. (2016). Decreased expression of 14-3-3 in *Paracoccidioides brasiliensis* confirms its involvement in fungal pathogenesis. *Virulence*, 7(2), 72-84. doi:10.1080/21505594.2015.1122166

- Martinez-Rocha, A. L., Roncero, M. I., Lopez-Ramirez, A., Marine, M., Guarro, J., Martinez-Cadena, G., & Di Pietro, A. (2008). Rho1 has distinct functions in morphogenesis, cell wall biosynthesis and virulence of *Fusarium oxysporum*. *Cell Microbiol*, *10*(6), 1339-1351. doi:10.1111/j.1462-5822.2008.01130.x
- Martins, L. F., Montero-Lomeli, M., Masuda, C. A., Fortes, F. S. A., Previato, J. O., & Mendonça-Previato, L. (2008). Lithium-mediated suppression of morphogenesis and growth in *Candida albicans*. *FEMS Yeast Research*, *8*(4), 615-621. doi:10.1111/j.1567-1364.2008.00376.x
- Mattison, C. P., Spencer, S. S., Kresge, K. A., Lee, J., & Ota, I. M. (1999). Differential regulation of the cell wall integrity mitogen-activated protein kinase pathway in budding yeast by the protein tyrosine phosphatases Ptp2 and Ptp3. *Molecular and cellular biology*, *19*(11), 7651-7660.
- Meili, R., Sasaki, A. T., & Firtel, R. A. (2005). Rho Rocks PTEN. *Nat Cell Biol*, *7*(4), 334-335. doi:10.1038/ncb0405-334
- Mihaylova, V. T., Borland, C. Z., Manjarrez, L., Stern, M. J., & Sun, H. (1999). The PTEN tumor suppressor homolog in *Caenorhabditis elegans* regulates longevity and dauer formation in an insulin receptor-like signaling pathway. *Proceedings of the National Academy of Sciences of the United States of America*, *96*(13), 7427-7432.
- Mitra, P., Zhang, Y., Rameh, L. E., Ivshina, M. P., McCollum, D., Nunnari, J. J., . . . Ross, A. H. (2004). A novel phosphatidylinositol(3,4,5)P3 pathway in fission yeast. *The Journal of cell biology*, *166*(2), 205-211. doi:10.1083/jcb.200404150
- Molina, J. R., & Adjei, A. A. (2006). The Ras/Raf/MAPK Pathway. *Journal of Thoracic Oncology*, *1*(1), 7-9. doi:10.1016/S1556-0864(15)31506-9
- Montagne, J., Stewart, M. J., Stocker, H., Hafen, E., Kozma, S. C., & Thomas, G. (1999). *Drosophila* S6 kinase: a regulator of cell size. *Science*, *285*(5436), 2126-2129.
- Moretti, M., Wang, L., Grognet, P., Lanver, D., Link, H., & Kahmann, R. (2017). Three regulators of G protein signaling differentially affect mating, morphology and virulence in the smut fungus *Ustilago maydis*. *Mol Microbiol*, *105*(6), 901-921. doi:10.1111/mmi.13745
- Morrison, E. N., Emery, R. J., & Saville, B. J. (2015). Phytohormone Involvement in the *Ustilago maydis*- *Zea mays* Pathosystem: Relationships between Abscisic Acid and Cytokinin Levels and Strain Virulence in Infected Cob Tissue. *PLoS One*, *10*(6), e0130945. doi:10.1371/journal.pone.0130945
- Motoi, Y., Shimada, K., Ishiguro, K., & Hattori, N. (2014). Lithium and autophagy. *ACS chemical neuroscience*, *5*(6), 434-442. doi:10.1021/cn500056q
- Moulton, J. E. (1942). Extraction of Auxin from Maize, from Smut Tumors of Maize, and from *Ustilago zeae*. *Botanical Gazette*, *103*(4), 725-739. doi:10.1086/335090
- Muller, P., Aichinger, C., Feldbrugge, M., & Kahmann, R. (1999). The MAP kinase kpp2 regulates mating and pathogenic development in *Ustilago maydis*. *Mol Microbiol*, *34*(5), 1007-1017.
- Muller, P., Katzenberger, J. D., Loubradou, G., & Kahmann, R. (2003). Guanyl nucleotide exchange factor Sql2 and Ras2 regulate filamentous growth in *Ustilago maydis*. *Eukaryot Cell*, *2*(3), 609-617.
- Müller, P., Weinzierl, G., Brachmann, A., Feldbrügge, M., & Kahmann, R. (2003). Mating and pathogenic development of the Smut fungus *Ustilago maydis* are



- regulated by one mitogen-activated protein kinase cascade. *Eukaryotic cell*, 2(6), 1187-1199. doi:10.1128/EC.2.6.1187-1199.2003
- Muslin, A. J., Tanner, J. W., Allen, P. M., & Shaw, A. S. (1996). Interaction of 14-3-3 with signaling proteins is mediated by the recognition of phosphoserine. *Cell*, 84(6), 889-897.
- Na, E. J., Nam, H. Y., Park, J., Chung, M. A., Woo, H. A., & Kim, H.-J. (2017). PI3K-mTOR-S6K Signaling Mediates Neuronal Viability via Collapsin Response Mediator Protein-2 Expression. *Frontiers in molecular neuroscience*, 10, 288-288. doi:10.3389/fnmol.2017.00288
- Nadal, M., Garcia-Pedrajas, M. D., & Gold, S. E. (2008). Dimorphism in fungal plant pathogens. *FEMS Microbiol Lett*, 284(2), 127-134. doi:10.1111/j.1574-6968.2008.01173.x
- Nakano, K., Imai, J., Arai, R., Toh, E. A., Matsui, Y., & Mabuchi, I. (2002). The small GTPase Rho3 and the diaphanous/formin For3 function in polarized cell growth in fission yeast. *J Cell Sci*, 115(Pt 23), 4629-4639.
- Ngok, S. P., Geyer, R., Kourtidis, A., Storz, P., & Anastasiadis, P. Z. (2013). Phosphorylation-mediated 14-3-3 protein binding regulates the function of the rho-specific guanine nucleotide exchange factor (RhoGEF) Syx. *J Biol Chem*, 288(9), 6640-6650. doi:10.1074/jbc.M112.432682
- Ogg, S., & Ruvkun, G. (1998). The *C. elegans* PTEN homolog, DAF-18, acts in the insulin receptor-like metabolic signaling pathway. *Mol Cell*, 2(6), 887-893.
- Ohanna, M., Sobering, A. K., Lapointe, T., Lorenzo, L., Praud, C., Petroulakis, E., . . . Pende, M. (2005). Atrophy of S6K1(-/-) skeletal muscle cells reveals distinct mTOR effectors for cell cycle and size control. *Nat Cell Biol*, 7(3), 286-294. doi:10.1038/ncb1231
- Ozoe, F., Kurokawa, R., Kobayashi, Y., Jeong, H. T., Tanaka, K., Sen, K., . . . Kawamukai, M. (2002). The 14-3-3 proteins Rad24 and Rad25 negatively regulate Byr2 by affecting its localization in *Schizosaccharomyces pombe*. *Mol Cell Biol*, 22(20), 7105-7119.
- Pastor, M. D., Garcia-Yebenes, I., Fradejas, N., Perez-Ortiz, J. M., Mora-Lee, S., Tranque, P., . . . Calvo, S. (2009). mTOR/S6 kinase pathway contributes to astrocyte survival during ischemia. *J Biol Chem*, 284(33), 22067-22078. doi:10.1074/jbc.M109.033100
- Paul, J. A., Barati, M. T., Cooper, M., & Perlin, M. H. (2014). Physical and genetic interaction between ammonium transporters and the signaling protein Rho1 in the plant pathogen *Ustilago maydis*. *Eukaryotic cell*, 13(10), 1328-1336. doi:10.1128/EC.00150-14
- Paul, J. A., Wallen, R. M., Zhao, C., Shi, T., & Perlin, M. H. (2018). Coordinate regulation of *Ustilago maydis* ammonium transporters and genes involved in mating and pathogenicity. *Fungal Biology*, 122(7), 639-650. doi:<https://doi.org/10.1016/j.funbio.2018.03.011>
- Pavlovic, D., Nikolic, B., Djurovic, S., Waisi, H., Andjelkovic, A., & Marisavljevic, D. (2014). Chlorophyll as a measure of plant health: Agroecological aspects. *Pesticidi i fitomedicina*, 29(1), 21-34. doi:10.2298/pif1401021p
- Pennington, K. L., Chan, T. Y., Torres, M. P., & Andersen, J. L. (2018). The dynamic and stress-adaptive signaling hub of 14-3-3: emerging mechanisms of regulation

- and context-dependent protein–protein interactions. *Oncogene*, 37(42), 5587-5604. doi:10.1038/s41388-018-0348-3
- Perez-Nadales, E., Nogueira, M. F., Baldin, C., Castanheira, S., El Ghalid, M., Grund, E., . . . Wendland, J. (2014). Fungal model systems and the elucidation of pathogenicity determinants. *Fungal Genet Biol*, 70, 42-67. doi:10.1016/j.fgb.2014.06.011
- Pham, C. D., & Perlin, M. H. (2010). Possible additional roles in mating for *Ustilago maydis* Rho1 and 14-3-3 homologues. *Commun Integr Biol*, 3(1), 57-59.
- Pham, C. D., Yu, Z., Ben Lovely, C., Agarwal, C., Myers, D. A., Paul, J. A., . . . Perlin, M. H. (2012). Haplo-insufficiency for different genes differentially reduces pathogenicity and virulence in a fungal phytopathogen. *Fungal Genet Biol*, 49(1), 21-29. doi:10.1016/j.fgb.2011.11.007
- Pham, C. D., Yu, Z., Sandrock, B., Bölker, M., Gold, S. E., & Perlin, M. H. (2009). *Ustilago maydis* Rho1 and 14-3-3 homologues participate in pathways controlling cell separation and cell polarity. *Eukaryot Cell*, 8(7), 977-989. doi:10.1128/EC.00009-09
- Philip, B., & Levin, D. E. (2001). Wsc1 and Mid2 are cell surface sensors for cell wall integrity signaling that act through Rom2, a guanine nucleotide exchange factor for Rho1. *Mol Cell Biol*, 21(1), 271-280. doi:10.1128/mcb.21.1.271-280.2001
- Prosser, D. C., Drivas, T. G., Maldonado-Baez, L., & Wendland, B. (2011). Existence of a novel clathrin-independent endocytic pathway in yeast that depends on Rho1 and formin. *J Cell Biol*, 195(4), 657-671. doi:10.1083/jcb.201104045
- Prosser, D. C., & Wendland, B. (2012). Conserved roles for yeast Rho1 and mammalian RhoA GTPases in clathrin-independent endocytosis. *Small GTPases*, 3(4), 229-235. doi:10.4161/sgtp.21631
- Quadbeck-Seeger, C., Wanner, G., Huber, S., Kahmann, R., & Kamper, J. (2000). A protein with similarity to the human retinoblastoma binding protein 2 acts specifically as a repressor for genes regulated by the b mating type locus in *Ustilago maydis*. *Mol Microbiol*, 38(1), 154-166.
- Ramírez-Ramírez, N., García-Soto, J., González-Hernández, A., & Martínez-Cadena, G. (1999). The small GTP-binding protein Rho is expressed differentially during spore germination of *Phycomyces blakesleeanus*. *Microbiology*, 145 ( Pt 5), 1097-1104. doi:10.1099/13500872-145-5-1097
- Redkar, A., Hoser, R., Schilling, L., Zechmann, B., Krzymowska, M., Walbot, V., & Doehle, G. (2015). A Secreted Effector Protein of *Ustilago maydis* Guides Maize Leaf Cells to Form Tumors. *Plant Cell*, 27(4), 1332-1351. doi:10.1105/tpc.114.131086
- Reichmann, M., Jammischek, A., Weinzierl, G., Ladendorf, O., Huber, S., Kahmann, R., & Kamper, J. (2002). The histone deacetylase Hda1 from *Ustilago maydis* is essential for teliospore development. *Mol Microbiol*, 46(4), 1169-1182.
- Richardson, C. J., Bröenstrup, M., Fingar, D. C., Jülich, K., Ballif, B. A., Gygi, S., & Blenis, J. (2004). SKAR Is a Specific Target of S6 Kinase 1 in Cell Growth Control. *Current Biology*, 14(17), 1540-1549. doi:<https://doi.org/10.1016/j.cub.2004.08.061>

- Roncero, C., & Duran, A. (1985). Effect of Calcofluor white and Congo red on fungal cell wall morphogenesis: in vivo activation of chitin polymerization. *J Bacteriol*, *163*(3), 1180-1185.
- Roncero, C., & Durán, A. (1985). Effect of Calcofluor white and Congo red on fungal cell wall morphogenesis: in vivo activation of chitin polymerization. *J Bacteriol*, *163*(3), 1180-1185.
- Ruiz-Herrera, J., León-Ramírez, C., Cabrera-Ponce, J. L., Martínez-Espinoza, A. D., & Herrera-Estrella, L. (1999). Completion of the sexual cycle and demonstration of genetic recombination in *Ustilago maydis* in vitro. *Molecular and General Genetics MGG*, *262*(3), 468-472. doi:10.1007/s004380051107
- Ruiz-Herrera, J., Leon, C. G., Guevara-Olvera, L., & Carabez-Trejo, A. (1995). Yeast-mycelial dimorphism of haploid and diploid strains of *Ustilago maydis*. *Microbiology*, *141*(3), 695-703. doi:10.1099/13500872-141-3-695
- Salmena, L., Carracedo, A., & Pandolfi, P. P. (2008). Tenets of PTEN Tumor Suppression. *Cell*, *133*(3), 403-414. doi:<https://doi.org/10.1016/j.cell.2008.04.013>
- Salmerón-Santiago, K. G., Pardo, J. P., Flores-Herrera, O., Mendoza-Hernández, G., Miranda-Arango, M., & Guerra-Sánchez, G. (2011). Response to osmotic stress and temperature of the fungus *Ustilago maydis*. *Archives of Microbiology*, *193*(10), 701. doi:10.1007/s00203-011-0706-9
- Santos, B., Gutierrez, J., Calonge, T. M., & Perez, P. (2003). Novel Rho GTPase involved in cytokinesis and cell wall integrity in the fission yeast *Schizosaccharomyces pombe*. *Eukaryot Cell*, *2*(3), 521-533.
- Sassone-Corsi, P. (2012). The cyclic AMP pathway. *Cold Spring Harb Perspect Biol*, *4*(12). doi:10.1101/cshperspect.a011148
- Saville, B. J., Donaldson, M. E., & Doyle, C. E. (2012). Investigating Host Induced Meiosis in a Fungal Plant Pathogen. In *Meiosis - Molecular Mechanisms and Cytogenetic Diversity*: InTech.
- Scanga, S. E., Ruel, L., Binari, R. C., Snow, B., Stambolic, V., Bouchard, D., . . . Manoukian, A. S. (2000). The conserved PI3'K/PTEN/Akt signaling pathway regulates both cell size and survival in *Drosophila*. *Oncogene*, *19*(35), 3971-3977. doi:10.1038/sj.onc.1203739
- Scarpari, L. M., Meinhardt, L. W., Mazzafera, P., Pomella, A. W., Schiavinato, M. A., Cascardo, J. C., & Pereira, G. A. (2005). Biochemical changes during the development of witches' broom: the most important disease of cocoa in Brazil caused by *Crinipellis pernicios*a. *J Exp Bot*, *56*(413), 865-877. doi:10.1093/jxb/eri079
- Schirawski, J., Bohnert, H. U., Steinberg, G., Snetselaar, K., Adamikowa, L., & Kahmann, R. (2005). Endoplasmic reticulum glucosidase II is required for pathogenicity of *Ustilago maydis*. *Plant Cell*, *17*(12), 3532-3543. doi:10.1105/tpc.105.036285
- Schulz, B., Banuett, F., Dahl, M., Schlesinger, R., Schafer, W., Martin, T., . . . Kahmann, R. (1990). The b alleles of *U. maydis*, whose combinations program pathogenic development, code for polypeptides containing a homeodomain-related motif. *Cell*, *60*(2), 295-306.
- Sharma, L., & Marques, G. (2018). *Fusarium*, an Entomopathogen-A Myth or Reality? *Pathogens (Basel, Switzerland)*, *7*(4), 93. doi:10.3390/pathogens7040093

- Shima, H., Pende, M., Chen, Y., Fumagalli, S., Thomas, G., & Kozma, S. C. (1998). Disruption of the p70(s6k)/p85(s6k) gene reveals a small mouse phenotype and a new functional S6 kinase. *EMBO J*, *17*(22), 6649-6659. doi:10.1093/emboj/17.22.6649
- Shimada, T., Fournier, A. E., & Yamagata, K. (2013). Neuroprotective function of 14-3-3 proteins in neurodegeneration. *BioMed research international*, *2013*, 564534-564534. doi:10.1155/2013/564534
- Shulewitz, M. J., Inouye, C. J., & Thorner, J. (1999). Hsl7 localizes to a septin ring and serves as an adapter in a regulatory pathway that relieves tyrosine phosphorylation of Cdc28 protein kinase in *Saccharomyces cerevisiae*. *Mol Cell Biol*, *19*(10), 7123-7137.
- Sinha, D., Wang, Z., Ruchalski, K. L., Levine, J. S., Krishnan, S., Lieberthal, W., . . . Borkan, S. C. (2005). Lithium activates the Wnt and phosphatidylinositol 3-kinase Akt signaling pathways to promote cell survival in the absence of soluble survival factors. *Am J Physiol Renal Physiol*, *288*(4), F703-713. doi:10.1152/ajprenal.00189.2004
- Slone, S. R., Lavalley, N., McFerrin, M., Wang, B., & Yacoubian, T. A. (2015). Increased 14-3-3 phosphorylation observed in Parkinson's disease reduces neuroprotective potential of 14-3-3 proteins. *Neurobiology of disease*, *79*, 1-13. doi:10.1016/j.nbd.2015.02.032
- Smith, D. G., Garcia-Pedrajas, M. D., Gold, S. E., & Perlin, M. H. (2003). Isolation and characterization from pathogenic fungi of genes encoding ammonium permeases and their roles in dimorphism. *Mol Microbiol*, *50*(1), 259-275.
- Smith, D. G., Garcia-Pedrajas, M. D., Hong, W., Yu, Z., Gold, S. E., & Perlin, M. H. (2004). An ste20 homologue in *Ustilago maydis* plays a role in mating and pathogenicity. *Eukaryot Cell*, *3*(1), 180-189.
- Snetselaar, K. M., Bolker, M., & Kahmann, R. (1996). *Ustilago maydis* Mating Hyphae Orient Their Growth toward Pheromone Sources. *Fungal Genet Biol*, *20*(4), 299-312.
- Solari, F., Bourbon-Piffaut, A., Masse, I., Payrastra, B., Chan, A. M. L., & Billaud, M. (2005). The human tumour suppressor PTEN regulates longevity and dauer formation in *Caenorhabditis elegans*. *Oncogene*, *24*, 20. doi:10.1038/sj.onc.1207978
- Song, M. S., Salmena, L., & Pandolfi, P. P. (2012). The functions and regulation of the PTEN tumour suppressor. *Nature reviews. Molecular cell biology*, *13*(5), 283-296. doi:10.1038/nrm3330
- Stambolic, V., Ruel, L., & Woodgett, J. R. (1996). Lithium inhibits glycogen synthase kinase-3 activity and mimics wingless signalling in intact cells. *Curr Biol*, *6*(12), 1664-1668.
- Steck, P. A., Pershouse, M. A., Jasser, S. A., Yung, W. K. A., Lin, H., Ligon, A. H., . . . Tavtigian, S. V. (1997). Identification of a candidate tumour suppressor gene, MMAC1, at chromosome 10q23.3 that is mutated in multiple advanced cancers. *Nature Genetics*, *15*, 356. doi:10.1038/ng0497-356
- Steinberg, G., & Perez-Martin, J. (2008). *Ustilago maydis*, a new fungal model system for cell biology. *Trends Cell Biol*, *18*(2), 61-67. doi:10.1016/j.tcb.2007.11.008

- Steinberg, G., Schliwa, M., Lehmler, C., Bolker, M., Kahmann, R., & McIntosh, J. R. (1998). Kinesin from the plant pathogenic fungus *Ustilago maydis* is involved in vacuole formation and cytoplasmic migration. *J Cell Sci*, *111* ( Pt 15), 2235-2246.
- Stracka, D., Jozefczuk, S., Rudroff, F., Sauer, U., & Hall, M. N. (2014). Nitrogen source activates TOR (target of rapamycin) complex 1 via glutamine and independently of Gtr/Rag proteins. *J Biol Chem*, *289*(36), 25010-25020. doi:10.1074/jbc.M114.574335
- Stumpf, M., Choorapoikayil, S., & den Hertog, J. (2015). Pten function in zebrafish: anything but a fish story. *Methods*, *77-78*, 191-196. doi:10.1016/j.ymeth.2014.11.002
- Suda, Y., Rodriguez, R. K., Coluccio, A. E., & Neiman, A. M. (2009). A Screen for Spore Wall Permeability Mutants Identifies a Secreted Protease Required for Proper Spore Wall Assembly. *PLoS One*, *4*(9), e7184. doi:10.1371/journal.pone.0007184
- Sun, Z., Song, J., Xin, X. a., Xie, X., & Zhao, B. (2018). Arbuscular Mycorrhizal Fungal 14-3-3 Proteins Are Involved in Arbuscule Formation and Responses to Abiotic Stresses During AM Symbiosis. *Frontiers in microbiology*, *9*, 91-91. doi:10.3389/fmicb.2018.00091
- Swinnen, E., Wilms, T., Idkowiak-Baldys, J., Smets, B., De Snijder, P., Accardo, S., . . . Winderickx, J. (2014). The protein kinase Sch9 is a key regulator of sphingolipid metabolism in *Saccharomyces cerevisiae*. *Mol Biol Cell*, *25*(1), 196-211. doi:10.1091/mbc.E13-06-0340
- Takagi, T., Ishijima, S. A., Ochi, H., & Osumi, M. (2003). Ultrastructure and behavior of actin cytoskeleton during cell wall formation in the fission yeast *Schizosaccharomyces pombe*. *J Electron Microsc (Tokyo)*, *52*(2), 161-174.
- Tamguney, T., & Stokoe, D. (2007). New insights into PTEN. *J Cell Sci*, *120*(Pt 23), 4071-4079. doi:10.1242/jcs.015230
- Tavares, M. R., Pavan, I. C. B., Amaral, C. L., Meneguello, L., Luchessi, A. D., & Simabuco, F. M. (2015). The S6K protein family in health and disease. *Life Sciences*, *131*, 1-10. doi:<https://doi.org/10.1016/j.lfs.2015.03.001>
- Taxis, C., Maeder, C., Reber, S., Rathfelder, N., Miura, K., Greger, K., . . . Knop, M. (2006). Dynamic organization of the actin cytoskeleton during meiosis and spore formation in budding yeast. *Traffic*, *7*(12), 1628-1642. doi:10.1111/j.1600-0854.2006.00496.x
- Tollot, M., Assmann, D., Becker, C., Altmüller, J., Dutheil, J. Y., Wegner, C. E., & Kahmann, R. (2016). The WOPR Protein Ros1 Is a Master Regulator of Sporogenesis and Late Effector Gene Expression in the Maize Pathogen *Ustilago maydis*. *PLoS Pathog*, *12*(6), e1005697. doi:10.1371/journal.ppat.1005697
- Torró, I., Bretó, P., & García-Yzaguirre, A. (2016). The influence of plant spacing in the early stages of selection of rice (*Oryza sativa* L.) varieties. *Spanish Journal of Agricultural Research*, *14*(2), e0704. doi:10.5424/sjar/2016142-8130
- Tseliou, M., Al-Qahtani, A., Alarifi, S., Alkahtani, S. H., Stournaras, C., & Sourvinos, G. (2016). The Role of RhoA, RhoB and RhoC GTPases in Cell Morphology, Proliferation and Migration in Human Cytomegalovirus (HCMV) Infected Glioblastoma Cells. *Cellular Physiology and Biochemistry*, *38*(1), 94-109. doi:10.1159/000438612

- van Heusden, G. P., Griffiths, D. J., Ford, J. C., Chin, A. W. T. F., Schrader, P. A., Carr, A. M., & Steensma, H. Y. (1995). The 14-3-3 proteins encoded by the BMH1 and BMH2 genes are essential in the yeast *Saccharomyces cerevisiae* and can be replaced by a plant homologue. *Eur J Biochem*, 229(1), 45-53.
- Vazquez, F., & Devreotes, P. (2006). Regulation of PTEN function as a PIP3 gatekeeper through membrane interaction. *Cell Cycle*, 5(14), 1523-1527. doi:10.4161/cc.5.14.3005
- Vollmeister, E., Schipper, K., Baumann, S., Haag, C., Pohlmann, T., Stock, J., & Feldbrugge, M. (2012). Fungal development of the plant pathogen *Ustilago maydis*. *FEMS Microbiol Rev*, 36(1), 59-77. doi:10.1111/j.1574-6976.2011.00296.x
- Wang, P., Zhou, Z., Hu, A., Ponte de Albuquerque, C., Zhou, Y., Hong, L., . . . Fu, X.-D. (2014). Both Decreased and Increased SRPK1 Levels Promote Cancer by Interfering with PHLPP-Mediated Dephosphorylation of Akt. *Molecular Cell*, 54(3), 378-391. doi:10.1016/j.molcel.2014.03.007
- Weinzierl, G., Leveleki, L., Hassel, A., Kost, G., Wanner, G., & Bolker, M. (2002). Regulation of cell separation in the dimorphic fungus *Ustilago maydis*. *Mol Microbiol*, 45(1), 219-231.
- Wennerberg, K., Rossman, K. L., & Der, C. J. (2005). The Ras superfamily at a glance. *Journal of Cell Science*, 118(5), 843. doi:10.1242/jcs.01660
- Wittmann, T., & Waterman-Storer, C. M. (2001). Cell motility: can Rho GTPases and microtubules point the way? *J Cell Sci*, 114(Pt 21), 3795-3803.
- Yamochi, W., Tanaka, K., Nonaka, H., Maeda, A., Musha, T., & Takai, Y. (1994). Growth site localization of Rho1 small GTP-binding protein and its involvement in bud formation in *Saccharomyces cerevisiae*. *J Cell Biol*, 125(5), 1077-1093.
- Yan, K., Gao, L.-N., Cui, Y.-L., Zhang, Y., & Zhou, X. (2016). The cyclic AMP signaling pathway: Exploring targets for successful drug discovery (Review). *Molecular medicine reports*, 13(5), 3715-3723. doi:10.3892/mmr.2016.5005
- Yu, J. S. L., & Cui, W. (2016). Proliferation, survival and metabolism: the role of PI3K/AKT/mTOR signalling in pluripotency and cell fate determination. *Development*, 143(17), 3050. doi:10.1242/dev.137075
- Zarrinpashneh, E., Poggioli, T., Sarathchandra, P., Lexow, J., Monassier, L., Terracciano, C., . . . Santini, M. P. (2013). Ablation of SGK1 Impairs Endothelial Cell Migration and Tube Formation Leading to Decreased Neo-Angiogenesis Following Myocardial Infarction. *PLoS One*, 8(11), e80268. doi:10.1371/journal.pone.0080268
- Zenke, F. T., Krendel, M., DerMardirossian, C., King, C. C., Bohl, B. P., & Bokoch, G. M. (2004). p21-activated kinase 1 phosphorylates and regulates 14-3-3 binding to GEF-H1, a microtubule-localized Rho exchange factor. *J Biol Chem*, 279(18), 18392-18400. doi:10.1074/jbc.M400084200
- Zhai, J., Lin, H., Shamim, M., Schlaepfer, W. W., & Canete-Soler, R. (2001). Identification of a novel interaction of 14-3-3 with p190RhoGEF. *J Biol Chem*, 276(44), 41318-41324. doi:10.1074/jbc.M107709200
- Zhang, D., Fan, F., Yang, J., Wang, X., Qiu, D., & Jiang, L. (2010). FgTep1p is linked to the phosphatidylinositol-3 kinase signalling pathway and plays a role in the

- virulence of *Fusarium graminearum* on wheat. *Molecular Plant Pathology*, 11(4), 495-502. doi:10.1111/j.1364-3703.2010.00626.x
- Zhang, H. H., Lipovsky, A. I., Dibble, C. C., Sahin, M., & Manning, B. D. (2006). S6K1 regulates GSK3 under conditions of mTOR-dependent feedback inhibition of Akt. *Molecular Cell*, 24(2), 185-197. doi:10.1016/j.molcel.2006.09.019
- Zhang, W., & Liu, H. T. (2002). MAPK signal pathways in the regulation of cell proliferation in mammalian cells. *Cell Res*, 12(1), 9-18. doi:10.1038/sj.cr.7290105
- Zhang, Y., Li, S., Zhou, L. Z., Fox, E., Pao, J., Sun, W., . . . McCormick, S. (2011). Overexpression of *Arabidopsis thaliana* PTEN caused accumulation of autophagic bodies in pollen tubes by disrupting phosphatidylinositol 3-phosphate dynamics. *Plant J*, 68(6), 1081-1092. doi:10.1111/j.1365-313X.2011.04761.x

## CURRICULUM VITAE

Name: Lalu M K Vijaykrishnapillai

Address: 1500 S 5<sup>th</sup> Street, Apt#102  
Louisville, KY  
USA 40208

### Education

2019 PhD Cellular, Molecular, and Developmental Biology  
University of Louisville

2005 Master of Science in Biotechnology  
Bangalore University

2003 Bachelor of Science in Biotechnology  
University of Kerala

### Awards and fellowships

2019 Doctoral dissertation completion award  
University of Louisville

2018 GSC travel award  
University of Louisville

2018 GNAS research fund award  
University of Louisville

2017 GNAS research fund award  
University of Louisville

2017 Intramural Research Grant  
College of Arts and Sciences, University of Louisville

2016 Graduate teaching assistantship  
Department of biology, University of Louisville



- 2015 Graduate teaching assistantship  
Department of biology, University of Louisville
- 2014 University fellowship  
University of Louisville
- 2008 Best Performer Award  
Centre for clinical excellence, CTS

Teaching experience:

- 2018 (Fall) Teaching Assistant for Genetics BIOL331
- 2017 (Summer) Teaching Assistant for Microbiology (BIOL257 and BIOL258)
- 2017 (Spring) Teaching Assistant for Genetics BIOL331
- 2016 (Summer) Teaching Assistant for Microbiology (BIOL257 and BIOL258)
- 2016 (Spring, Fall) Teaching Assistant for Genetics BIOL331
- 2015 (Fall) Teaching Assistant for Genetics BIOL331

Work experience

- 2006-08, 2010-14 Clinical research professional  
  
Worked with biopharmaceutical research organizations (in the life science division of Contract Research Organizations such as Accenture, CTS, Novartis in India, France and UK). Major duties involved clinical protocol review and design for drug testing.

Publications

- L M.K. Vijayakrishnapillai and M H. Perlin. Potential interactions of *ptn1* with signaling components *rho1* and *pdc1* in *U maydis*. (*Manuscript under preparation*)
- L M.K. Vijayakrishnapillai, M. Groeschen, John S. Desmarais, and M. H. Perlin. Deletion of *ptn1*, a *PTEN/TEP1* Orthologue, in *Ustilago maydis* Reduces Pathogenicity and Teliospore Development. *J Fungi* 2018 (*Journal Article*)

## Presentations

L M.K. Vijayakrishnapillai, M. Groeschen, John S. Desmarais, and M. H. Perlin. The role of *PTEN* ortholog of *Ustilago maydis* in controlling mating, plant infection, teliospore spore formation and germination. International Gordon Research Conference on Cellular and Molecular Fungal Biology 2018, Holderness, NH (*Poster presentation*)

L M.K. Vijayakrishnapillai, M. Groeschen, John S. Desmarais, P. Parikh and M H. Perlin. Role of *Ustilago maydis PTEN* in mating, and virulence. GSRRC 2018, Louisville, KY (*Poster presentation*)

L M.K. Vijayakrishnapillai and M.H Perlin. Examining the role of *PTEN* gene of *Ustilago maydis* in pathogenicity and spore germination. Kentucky Academy of Science Annual Meeting 2016, Louisville, KY (*Oral Presentation*)

Attended the 14th annual UT-KBRIN bioinformatics summit 2015, Buchanan, TN

## Community service

- |      |  |
|------|--|
| 2019 | Judge in Cell and Molecular biology<br>Dupont Manual Regional Science Fair, Louisville, KY |
| 2018 | Judge in Cell and Molecular biology<br>Dupont Manual Regional Science Fair, Louisville, KY |